In Vivo Visualization of CaMKII Activity in Ocular Dominance Plasticity

By

Show Ming Kwok

B.S., Biology (2003)
Massachusetts Institute of Technology

SUBMITTED TO THE DEPARTMENT OF BRAIN AND COGNITIVE SCIENCES IN PARTIAL FULFILLMENT OF THE REQUIREMENTS FOR THE DEGREE OF

DOCTOR OF PHILOSOPHY IN NEUROSCIENCE
AT THE
MASSACHUSETTS INSTITUTE OF TECHNOLOGY

JUNE 2009

Signature of Author ……..……..
Department of Brain and Cognitive Sciences
May 15, 2009

Certified by …….…….....
Yasunori Hayashi, M.D., Ph.D.
Assistant Professor of Neurobiology
Thesis Supervisor

Accepted by……...
Earl Miller, Ph.D.
Picower Professor of Neuroscience
Chairman, Department Committee for Graduate Students

In vivo Visualization of CaMKII Activity in Ocular Dominance Plasticity

By

Show Ming Kwok

Submitted to the Department of Brain and Cognitive Sciences
On May 15, 2009 in Partial Fulfillment of the Requirements
for the Degree of Doctor of Philosophy in Neuroscience

Abstract

Alterations in sensory experience can persistently modify the responses of cortical neurons. Ocular dominance (OD) plasticity, a process in which alternation of visual input induces a shift in cortical responsiveness, is an extensively studied model of such experience-dependent plasticity. However, the synaptic mechanisms underlying OD plasticity are not well understood. Recent studies revealed that both Hebbian and homeostatic mechanisms play a role in OD plasticity. Therefore, we were interested in monitoring the process of rapid plasticity at individual synapses *in vivo* to gain insight into the interplay of these two mechanisms. Ca^{2+}/calmodulin dependent protein kinase II (CaMKII) is a major component of the postsynaptic density. Activation of CaMKII is necessary and sufficient for LTP induction, is required for OD plasticity, and its expression pattern coincides with the site of rapid plasticity in the supragranular layers II/III of the visual cortex. Moreover, CaMKII can convert transient Ca^{2+} influx into a prolonged biochemical process via autophosphorylation that renders CaMKII activity Ca^{2+} independent. Hence, CaMKII is well suited as a reporter of synaptic activity.

We previously engineered a probe, Camui, which utilizes the optical phenomenon of fluorescence resonance energy transfer (FRET), to monitor CaMKII activation. This thesis embodies the work done to improve Camui to be a better tool for *in vivo* reporting of CaMKII activity, as well as the use of this improved probe for *in vivo* detection of CaMKIIα activity in single spines before and after 4 hrs of monocular deprivation (MD) in the ferret visual cortex. We found that after only 4 hrs of MD, the overall CaMKIIα activity in spines, and adjacent dendritic regions, of neurons in the deprived eye domain increased significantly. This increase was also seen in the binocular eye domain. In the open eye domain, however, this overall increase in CaMKIIα activity was absent. These observations were specific to MD as control experiments did not show such changes. Moreover, detailed analysis revealed that spines that were eliminated after 4 hrs of MD had a low level of basal CaMKIIα activity. Our results lend support to the model that both Hebbian, as well as homeostatic compensatory mechanism can subserve OD plasticity.

Thesis Supervisor: Yasunori Hayashi, M.D., Ph.D.
Title: Assistant Professor of Neurobiology

Acknowledgments

Professional

Throughout my educational journey, I was lucky enough to meet many great mentors who inspired, encouraged, and helped me reach my goals. First of all, I have to thank Yasunori Hayashi, my thesis advisor. When I attended his talk during the IAP of my sophomore year, the course of my career path was changed. As a graduate student in his lab, I always admired his dedication to do good science. As a result of his infectious enthusiasm, I was constantly motivated to do my best and overcome all the problems that layed between me and the true answers. He supported me, guided me, and troubleshot with me throughout different phases of the project. I appreciate how much he has taught me. I would also like to thank all the members of my thesis committee for their insightful suggestions: Mriganka Sur, Morgan Sheng, Carlos Lois, and John Lisman. I am amazed that I never found it difficult to squeeze an appointment into their schedules to ask for advice. They were superbly responsive and helpful.

The completion of this project would have been impossible without my collaborator, Amanda Mower. I thank you, Amanda. The days and nights that we spent in the dark imaging room together allowed us to exchange scientific ideas, share life stories, and build our friendship. Our mutually inspired dedication is what carried us through the difficult times when nothing seemed to be working. I wish to thank Hongbo Yu, Ania Majewska, Kenichi Okamoto, and Claudia Lee for their useful opinions and generous help. My special thanks also go to Rachael Neve and Ki Ann Goosens for their time in teaching me how to package herpes simplex virus and for their career advice.

The Hayashi Lab members have made my time here enjoyable and memorable: Mariko Hayashi, Kenichi Okamoto, Kenny Futai, Jiro Kasahara, Keizo Takao, Miquel Bosch, and Radhakrishnan Narayanan served as a scientific encyclopedia and provided valuable input that I much needed.

I thank our beloved academic administrators, Denise Heintze and her assistant Brandy Baker for their care and help on countless occasions throughout my graduate student life. My thanks also goes to JC Howard, the ex-Hayashi Lab administrative assistant, who took good care of my orders and supported all of us.

Personal

Many classmates and friends formed a strong support network that kept me on track. I thank Lena Khibnik for everything from science discussion to daily life counseling, and from being just a classmate to having invited me to visit her family. She will be a true and caring friend for a long time to come. Many thanks to Srinivas Turaga for all the discussions, sharing and encouragement; my experience at BCS would be very different without him. I thank Chung Tin for his technical and emotional support and for being a friend who is always ready to help. I cannot thank Rob Morrison enough for offering his helping hand at times that I needed it the most. My girl friends, Naomi

Muroga, Margaret Lau, Grace Zheng, Jane Zhang, Lisa Hsu, and Vivian Ma all deserve my thanks. They kept me company when I needed good conversation, comfort and guidance.

I would also like to extend my thanks to my parents, my brother, my in-laws, as well as my aunts and uncles. Their unconditional love and sacrifices have driven me to pursue my dreams. My belated second uncle; I have done what I have promised you! Finally, I have to thank my husband, Kayi Lee for his humorous remarks that give me so much joy everyday, for his programming skills that significantly sped up the data analysis process, for his opinions when I am confused and for his courage to marry me.

Table of Contents

CHAPTER 1:

Introduction and background

1.1. Ocular dominance plasticity

The most fascinating aspect of the brain lies in its ability to adapt to the ever changing environment. To fulfill such a dynamic and demanding task, neurons have to change the way they communicate with other neurons. During development and throughout life, the synaptic connectivity and circuitry that subserves brain function is constantly modified and refined in an activity-dependent manner. Since the pioneering work of David Hubel and Tornsten Wiesel in the early 1960's [1], a model system for studying the role of sensory experience in the shaping of cortical neural circuits has been the mammalian visual cortex. Among the various forms of visual cortical plasticity, the best characterized is ocular dominance (OD) plasticity, a process in which alteration of visual input shifts cortical responsiveness [1-7].

Working with cat primary visual cortex, Wiesel and Hubel first studied the effects of alteration in visual experience using extracellular single unit recording [1]. They recorded each neuron's response to stimulation of the contralateral and ipsilateral eye and qualitatively categorized the OD of these neurons. In control kittens, an equal response to stimulation of both eyes, with a slight bias towards the contralateral eye was found. However, they discovered that monocular deprivation (MD), either by monocular lid closure or use of a translucent eye cover for more than 2 months before eye-opening, resulted in a dramatic shift in responsiveness of cortical neurons to the non-deprived eye, whereas the response to the deprived eye was lost. Studies that followed demonstrated that this form of plasticity is found in various species including macaque monkeys, ferrets, rats and mice [8-16] and is probably common among the mammalian visual system.

In their subsequent studies, Wiesel and Hubel investigated the effect of binocular deprivation (BD) for a similar period of time[17]. Given the observed effect of MD on the responsiveness of the visual cortex, they expected a complete loss of responsiveness of cortical cells to the stimulation of either eye following BD. Surprisingly, they found that BD had little effect on the distribution of OD, although the kittens grew up blind. From these results, they concluded that the two converging ocular pathways were acting in a competitive fashion for control over a postsynaptic neuron, so that a reduction in drive in one set of synapses permitted another set to strengthen at the first set's expense. The presence or absence of activity is not the determinant of the OD formation. These groundbreaking discoveries led many researchers to find the potential mechanisms underlying OD plasticity. In the past four decades, neuroscientists have looked for the critical period, cortical laminar differences, morphological substrates, synaptic mechanisms and molecular basis of OD plasticity in various species, which we will discuss below.

1.1.1. Critical period for OD plasticity

The most dramatic effects of MD on OD plasticity occur in a restricted period during the early stages of animal development. This period of development was termed the "critical period". In Wiesel and Hubel's initial study of the effect of MD in cat visual cortex, they found that OD plasticity occurred only in very young kittens [1]. A detectable decline in the effect of MD on cortical plasticity was seen in older animals (2 months of age) with a nearly complete lack of effect observed in adults. A later study by the same group in which MD was performed on progressively older cats carefully narrowed down this vulnerable period to be between the start of the fourth and eighth

week of life [18]. Behavioral, physiological and morphological assessment showed that cats were no longer sensitive to long period of MD by three months of age. In ferrets, another animal species often used in vision studies including the one to be discussed here, the critical period peaks around postnatal day 42 (P42) [11]. Susceptibility to MD drops to about half that seen at the peak by ages P50 to P65, with a loss of effects occurring when MD begins after P100. Thus, like cats, ferrets have a well-defined critical period in which visual manipulations can dramatically alter cortical responses. Other studies showed that critical periods are a common phenomenon across different species including monkeys [9, 19], mice [15], and rats [14].

1.1.2. Interlaminar differences in OD plasticity within the visual cortex

In the mammalian visual system, the flow of visual information starts from the retina of the eyes. It is then relayed by the optic nerve to the lateral geniculate nucleus (LGN) of the thalamus. Geniculocortical axons then send visual information to the cortex, which is comprised of six layers. These axons terminate primarily in layer IV, with a lesser extent in layer VI and lower layer III [20-22]. Layer IV feeds forward the information to layer II/III, which in turn sends projections to layer V, and then to VI. Overall, it is suggested that the principle vertical flow of information through the cortical layers goes from layer IV to II/III to V to VI [23, 24]. Therefore, it was thought that the remodeling of synaptic connections following physiological changes occurred in the same order [9, 25-27]. However, recent indirect evidence in cats and ferrets hinted at the possibility that reorganization of the supragranular layers (layer II/III) precedes that of the geniculocortical afferents in layer IV [28-30]. These results suggested an alternative view that reorganization takes place at a higher stage of cortical processing in the

extragranular layers (layers other than IV) which might instruct the plastic changes in layer IV.

To test these seemingly contrasting hypotheses, Trachtenberg *et al*. performed experiments in kittens and specifically looked at laminar disparities [31]. They first used optical imaging (OI) to map cortical representations of the two eyes in normal kittens and in kittens that had received only 24 hrs of MD. The OD maps were used to accurately target microelectrode penetrations to regions of greatest plasticity and single unit recordings were then performed in four cortical layers (II/III, IV, V, VI). They found a clear OD shift favoring the non-deprived eye in the extragranular layers, but not in the input layer (IV). These results support the second view whereby the extragranular layers act in a permissive and instructive way to promote changes in the input layer and subcortical sites.

However, a recent study in mice provided counter evidence to this view [32]. Liu *et al*. examined the laminar difference in OD plasticity in young mice also after only 24 hrs of MD. They placed recording electrodes into the binocular region of mouse visual cortex and performed single unit recordings. They found that brief MD induced an OD shift in neurons of both layer II/III and IV. Interestingly, after cannabinoid receptor antagonist application, the same period of MD prevented the OD shift in layer II/III neurons while the shift in layer IV was preserved. Data shown in this study, therefore, argued strongly against the views that extragranular layers instruct changes in the input layer. Instead, these layers function in parallel but employ different plasticity mechanisms.

The reported laminar differences in these two studies might be due to anatomical and mechanistic differences between the two animal species used. Anatomically, it has been demonstrated that there are more LGN projections to layer II/III in mice than in cats [27, 33, 34]. Moreover, 24 hrs of MD might have a saturating effect on plasticity mechanisms in mice while this length of MD in cats may still allow interlaminar differences to be captured. Therefore, a shorter period of MD, on the order of hours, might be necessary to capture these interlaminar differences in mice. Nonetheless, it seems that fast changes in response to the deprived eye occur in cortical layer II/III. Thus, it is reasonable to focus on layer II/III for studying rapid molecular processes underlying OD plasticity.

Another study by Desai *et al*. investigating homeostatic scaling, a non-Hebbian form of synaptic plasticity that stabilizes firing rates by changing the synaptic strengths when perturbations occur in a system, found that layer differences exist for homeostatic scaling in rat visual cortex [35]. After two days of MD in P21 rats, layer IV miniature excitatory postsynaptic current (mEPSC) amplitude did not change. However, the same manipulation caused an increase in average mEPSC amplitude in layer II/III. These results showed that the critical period for mEPSC scaling occurs later in layer II/III than in layer IV. Therefore, layer II/III and layer IV not only differ in plasticity mechanisms, but also in the timing of the closing of the critical period.

1.1.3. Structural substrates of ocular dominance plasticity

1.1.3.1. Presynaptic reorganization

Whether the functional shift in OD measured by extracellular recording stems from a significant change in retinal output remains controversial [36, 37]. However, it is generally accepted that neurons in the dorsal LGN have normal response properties following MD, and little atrophy is observed in the deprived eye input [38-43]. Numerous transneuronal labeling studies point to changes at the level of geniculocortical axons being the structural substrate of OD plasticity. Following physiological changes after prolonged MD, there is a marked shrinkage of deprived-eye columns and an expansion of those from the normal eye [9, 27, 44]. Detailed analysis of the ultrastructure of axonal arbors showed that MD caused an expansion of the non-deprived axonal arbor and a reduction in deprived arbors [8, 45-47]. Zooming in further, Friedlander *et al*. observed that non-deprived axons contact proportionally more dendritic shafts than deprived boutons and form more synapses per bouton than deprived axons. In contrast, the boutons of deprived axons are smaller, have fewer mitochondria and occasionally make no synaptic contacts.

1.1.3.2. Postsynaptic reorganization

The information relayed by LGN axons is received small protrusions along the dendritic shafts of the cortical neurons, called spines. Just as presynaptic (LGN axons) changes are evident as mentioned above, postsynaptic changes found at the level of individual cortical neuron synapses further strengthen the idea that functional changes are supported by structural modifications [48-51]. Spines receive the majority of excitatory

synaptic contacts in the mammalian brain [52], and are the functional partner of presynaptic axon terminals. They act as biochemical compartments isolating influx of Ca^{2+} to individual synapses [53-55]. Spines are dynamic structures in that they can change their shape, disappear and appear [49, 55-58]. In addition, spine dynamics are developmentally and activity-dependently regulated [51, 56, 59-67]. Together, these dendritic spine properties empower spines to serve as the postsynaptic structural correlate of OD plasticity.

Majewska and Sur, have shown that spine motility of layer V neurons is upregulated during the critical period within the binocular region of mouse visual cortex, although the structural classification of protrusions remains unchanged [49]. More interestingly, they found that 8 days BD significantly increases spine motility by 60% during the critical period but not before or after. At odds with these results, Konur and Yuste showed that in acute slice, dark rearing and enucleation at P13 caused a decrease in spine motility of layer II/III neurons [48]. The difference might lie in the type of the dendrites analyzed, i.e. basal vs. apical, in the duration of deprivation, or the layer of origin of the cells. In a subsequent study, Oray *et al*. performed *in vivo* imaging of dendritic spines after MD, a deprivation paradigm that is more relevant to issues of synaptic competition than BD [51]. After 2-3 days of MD, they again found a significant increase in spine motility by about 35%. A report by Mataga *et al*. took the idea of spine dynamics underlying OD plasticity one step further [50]. They examined fixed dendrites from visual cortex that underwent 4 days of MD and saw a 20-40% decrease in spine density. Therefore, changes in visual experience lead to an imbalance between the inputs from two eyes and this imbalance causes an increase in spine motility. This rise in spine

motility might be followed by a loss of spines. However, direct evidence establishing such a link between the two observed events is missing.

1.1.4. Synaptic mechanisms of OD plasticity

Two questions of extraordinary interest are: (i) how are cortical synapses modified in the face of experience? (ii) how can these changes be reasonably explained? To state the challenge more clearly and specifically, scientists have to provide synaptic mechanisms to explain the bidirectional plastic consequences of MD: the depression of the deprived eye response followed by the potentiation of the open eye response. Many researchers' quests for the answers have yielded fruitful results in the past decade and many of the experiments that offered important insights were guided by the conceptual framework of the Bienenstock Cooper Munro (BCM) theory [68-70].

1.1.4.1. BCM theory

BCM theory is an extension of the Hebbian learning rule which states that the selective strengthening of synapses between two simultaneously active neurons results in learning [71]. The most essential concept of the BCM theory is the introduction of a critical value, termed the "modification threshold" (θ_m) that allows both potentiation and depression to take place. Consider a single neuron receiving excitatory inputs, such as visual stimuli, at its synapses. If the total postsynaptic response to depolarization of the active synapse exceeds θ_m, these active synapses will be potentiated (increase in synaptic efficacy) by the mechanism of long-term potentiation (LTP). The potentiation of only the active synapse is said to be homosynaptic. In the opposite scenario, if the total postsynaptic response is between zero and θ_m, the active synapses will be depressed

(decrease in synaptic efficacy) via the mechanism of homosynaptic long-term depression (LTD). This theory is further strengthened by the incorporation of the idea that the value of θ_m itself can also vary by feedback mechanisms. Bienenstock *et al*. showed that if the value of θ_m was allowed to slide as a nonlinear function of the average integrated postsynaptic activity, then the neuron would come to an equilibrium state in an input environment regardless of the initial state. This initial state would be a problem if the value of θ_m were not allowed to vary. For example, consider a case where input drives the total postsynaptic response below θ_m; all the active synapses are depressed and this neuron would gradually decrease its ability to respond to any given set of stimuli and eventually stop responding altogether. A similar situation in the opposite direction would produce a saturating potentiation that diminishes a neuron's capability to respond. Thus, a sliding θ_m value ensures that a neuron will operate within a functional range [69]. All three components in the BCM theory: homosynaptic LTD, changing the θ_m value, and homosynaptic LTP, have found their support in the experimental data from hippocampus [72-77], somatosensory cortex [78], and the visual cortex [77, 79-81], which we will focus next.

1.1.4.2. Supporting evidence of BCM theory in visual cortex

First, Artola *et al*. [79] intracellularly recorded layer II/III neurons in slices of the rat visual cortex after stimulation of underlying white matter or layer II. LTD in active synapses was obtained if postsynaptic depolarization by high-frequency tetanus was moderate, whereas LTP was induced if the level of postsynaptic activation was higher [69, 79]. Kirkwood *et al*. [77] measured field potentials in layer III neurons of rat visual cortical slices evoked by layer IV stimulation. They demonstrated similar results: low

frequency stimulation produced LTD and high frequency stimulation induced LTP. Taken together, the visual cortex is shown to be equipped with the capability of homosynaptic LTD and LTP mechanisms.

Second, if MD actually induces LTD, Heynen *et al*. hypothesized that MD should mimic LTD and occlude the subsequent expression of LTD [13]. They induced a significant depression of VEP amplitudes recorded from the cortical region A17 by applying low frequency stimulation (LFS) to the LGN *in vivo*. The same observation was made when they MD rats for 24 hrs. Hence MD mimics LTD. Next, they prepared A17 cortical slices from the ipsilateral and contralateral hemispheres of animals that had gone under 24 hrs of MD *in vivo*. They recorded field potentials in layer III neurons after LTD induction protocol in layer IV of these slices. It was found that LTD of field potentials was greatly diminished in the contralateral hemisphere when compared with the ipsilateral hemisphere despite no interhemispheric asymmetry in LTD response. This result confirmed that MD occluded subsequent LTD expression. They found molecular signatures of LTD, such as phosphorylation status and surface expression of α-amino-3-hydroxy-5-methyl-4-isoxazolepropionic acid receptor (AMPAR) found in hippocampus and also in the visual cortex after MD. Their results showed that indeed MD induced an AMPAR molecular signature typical of LTD. Hence, this study provided evidence that MD induces LTD in visual cortex. Another study from the same group also showed that LTD is occluded in layer IV and layer II/III of mouse visual cortex by previous MD [82].

Another candidate mechanism underlying deprivation induced loss of responsiveness is potentiation of inhibition [83]. In rat visual cortical slices, lid suture from P21 to P24 caused an increase in the inhibitory tone by strengthening excitatory

connections onto fast-spiking interneurons and a potentiation of inhibition from interneurons onto star pyramidal neurons in layer IV. This enhanced inhibition feedback was mediated via a new form of LTP of inhibition and is occluded by previous visual deprivation.

Data has emerged to support the idea that glutamate receptor N-methyl-D-aspartate receptor (NMDAR) dependent processes mediate open eye response potentiation [84]. VEPs were chronically recorded in area 17 of adult mice. Five days of MD induced an increase in VEP amplitude in the visual cortex ipsilateral to the open eye. This increase was persistent and remained after opening the sutured eye. They further investigated whether the cortex or thalamus was the origin of this open eye response potentiation by using cortical NMDAR subunit 1 (NR1) knockout mice. These mice demonstrated a lack of open eye potentiation after MD. The authors concluded that this potentiation was of cortical origin and that they were observing a process of experience- and NMDAR-dependent LTP in the visual cortex. Another study used theta burst stimulation of the dorsal LGN induced LTP of field potentials evoked in primary visual cortex of adult rats *in vivo* [80]. After LTP induction, cortical responses to full-field flash and grating stimuli were enhanced. In NMDAR subunit 2A (NR2A)-knock out mice, brief MD that normally causes deprived eye depression induced potentiation of the open eye [85]. These results pointed to an important role for NMDAR-dependent LTP in OD plasticity.

Third, not only is the modification threshold, θ_m, an adjustable value, but it has a theoretical requirement which states that the value must reflect the history of a neuron's postsynaptic activity. Kirkwood *et al*. provided support for this requirement by

comparing the frequency-response function in the visual cortex of dark reared rats with that in normally reared rats. As a result they found that LTP is enhanced in the visual cortex of dark reared rats and that LTD is decreased. Furthermore, these effects could be reversed by two days of light exposure. Thus, a variable synaptic modification threshold that allows synaptic weights in a network to achieve a stable equilibrium indeed exists [69, 81].

Finally, recent studies pinpointed that temporal changes that occur as a consequence of MD occur in two distinct phases. In the binocular region of mouse visual cortex, Frenkel and Bear performed chronic recording of visually evoked potentials (VEPs) before and after MD of the same awake alert animal with varying MD periods [16]. They found that three days of MD leads to a strong decrease in the ratio of contralateral eye VEP amplitude to ipsilateral eye VEP amplitude due to the weakening response of the deprived eye. After three days of MD, the non-deprived eye response was not affected. However, longer periods of MD (seven days) led to a significant potentiation of the non-deprived eye. The delay in open eye response shift was thought to be the time needed for θ_m to slide. These two phases were also reported in cats by Mioche and Singer [86]. Similar observations were reported in another study using two-photon calcium imaging in the visual cortex of mice where short MD durations decreased deprived-eye responses in neurons with binocular input and longer MD strengthened open-eye responses [87].

Combining the theoretical assumptions and experimental data, Frenkel and Bear proposed a model of synaptic mechanisms underlying OD plasticity. The three step model proposes: 1) deprived eye responses depress via homosynaptic LTD, 2) that the

modification threshold, which decides if input activity is potentiating or depressing, is lowered in response to decreased cortical activity following MD, thus favoring potentiation, and 3) that non-deprived eye responses potentiate via homosynaptic LTP as a result of the lowered threshold for synaptic potentiation [16, 88].

1.1.4.3. Other theories for mechanisms of OD plasticity

In recent years, a number of studies have point to a role for homeostatic mechanism in mediating OD plasticity. Homeostasis is a form of synaptic plasticity that acts to stabilize the activity of a neuron or neuronal circuit in the face of perturbations, such as developmental changes in cell size or in synapse number or strength, that alter excitability [89]. This was first described by Turrigiano *et al*. in dissociated rat cortical cultured neurons that are chronically blocked by tetrodotoxin (TTX) [90]. In response to decreased activity, the amplitude of miniature excitatory postsynaptic currents (mEPSC) is increased, whereas increased activity has an opposite effect. This increase is a global multiplicative scaling up of synaptic weight in all synapses of a neuron. Similar effects are also seen in the visual cortex after monocular inactivation by TTX or dark rearing [35, 91]. In both studies, an increase in mEPSC amplitude recorded from layerII/III neurons in young rats was observed. Such mechanism can potentially explain the strengthening of non-deprived eye responses after MD manipulation [92].

1.1.5. Molecular basis of OD plasticity

A large body of the literature has emerged to demonstrate the important molecular pathways underlying this form of cortical plasticity [88, 93-95]. Understanding the molecular basis of OD plasticity will shed light onto the mechanisms of learning and

memory, as OD plasticity is the most common memory correlate in the brain. Here, I will discuss the key molecules involved in OD plasticity that are most relevant to the studies included in this thesis.

1.1.5.1. Excitatory and inhibitory transmission

First, the key mediators of OD plasticity are excitatory neurotransmitter receptors. Two excitatory glutamate receptors, NMDARs and AMPARs are critically involved in the process of OD plasticity. Similar to classic hippocampal LTP and LTD, visual cortical LTP and LTD recorded from layer II/III in slices has been shown to depend on the activation of NMDAR [77]. Moreover, a study in adult mouse visual cortex showed that the OD shift that occurs via potentiation of synaptic responses depends on NMDAR activation [84]. Studies in rat visual cortex have also shown that visual experience triggers rapid insertion of new NMDARs at synapses. These new receptors have a higher proportion of NR2A subunits, which have faster channel kinetics than receptor containing NMDAR subunit 2B (NR2B) [96]. Moreover, dark rearing and visual experience have opposite effects on the NR2A/2B ratio: visual experience increases this ratio while dark rearing decreases this ratio. These findings point to a role of NMDARs in the maintenance of synaptic strength in cortical plasticity [97, 98]. A recent report demonstrating that MD, which normally induces depression of deprived eye response, failed to exhibit such depression in NR2A-knockout mice and instead led to a precocious potentiation of the non-deprived eye, providing evidence that decreased a NR2A/2B ratio is permissive for compensatory potentiation of non-deprived inputs [85]. In an effort to connect the effects of MD with the mechanisms of LTD in the visual cortex, Heynen *et al.* discovered that, as in the hippocampal LTD, AMPARs play an important role [13]. MD

of in rat mimics LTD in terms of depressed synaptic transmission in the corresponding contralateral cortical hemisphere, decreased phosphorylation of glutamate AMPA receptor subunit 1 (GluR1) subunit Serine 845, increased phosphorylation of glutamate AMPA receptor subunit 2 (GluR2) Serine880 and decreased surface expression of GluR1 and GluR2. Moreover, the changes induced by MD occlude subsequent LTD at synapses ex vivo, indicative of common mechanisms. Therefore, MD induces LTD in visual cortex. Another study in mouse visual cortex showed that LTD induced by low-frequency synaptic stimulation is mediated by clathrin-dependent AMPAR endocytosis in layer IV but not in layer II/III, pointing to the important role of synaptic AMPAR expression reduction in cortical LTD [82].

In addition to excitatory transmission, inhibitory transmission also plays a critical role. Inhibitory transmission relies on the neurotransmitter γ-aminobutyric acid (GABA) and its receptor, GABAR. In cat visual cortex, infusion of a GABAR agonist, diazepam, and an inverse agonist, β-carboline methyl 6,7-dimethoxy-4-ethyl-β-carboline-3-carboxylate (DMCM), led to a respective expansion and shrinkage of OD columns, the architectural hallmark of the mammalian visual cortex [99]. Infusion of an agonist of GABAR subtype A ($GABA_AR$) led to a shift of responses to the deprived eye after MD instead of the usual shift to the non-deprived eye [100]. Fagiolini *et al.* studied several "knock-in" mutations of $GABA_AR$ α subunits that render individual $GABA_ARs$ insensitive to diazepam [101]. They found that α1, not the α2 or α3 subunit containing $GABA_ARs$ specifically drive visual cortical plasticity during pre-critical period MD in α1 mutant mice. Among different GABA-synthesizing enzymes, glutamic acid decarboxylase 65 (GAD65) is found primarily in the synaptic terminal [102]. It is

localized to vesicles and serves as reservoir of inactive GAD that can be recruited more GABA synthesis is needed [103, 104]. when It is therefore speculated to be specialized for responses to rapid changes in demand at the synaptic terminal during heightened neuronal activity [105]. Mutant mice lacking GAD65 showed a severe disruption of OD plasticity in that MD induced OD shift was completely absent. Infusion of diazepam restored plasticity to these GAD65 knockout mice *in vivo*. Taken together, the intricate interplay of excitatory and inhibitory systems is essential for OD plasticity.

1.1.5.2. Intracellular signaling molecules

Activation of NMDARs leads to an influx of Ca^{2+}, which triggers the activation of several key kinases and phosphatases. Overwhelming data has identified three kinases that are necessary for the shift in OD caused by MD: cAMP-dependent protein kinase (PKA), Ca^{2+}/calmodulin-dependent protein kinase II (CaMKII), and extracellular-signal-regulated kinase (ERK). Blockade of PKA inhibits the OD shift [106]. CaMKIIα knockout mice develop normal visual cortical responses but have a significantly diminished OD shift [107]. Mice with CaMKIIα-T286A mutation, which abolishes Ca^{2+}-independent autonomous activity, were used to study the role of autophosphorylation in short-term and long-term OD plasticity [108, 109]. These mice showed impairments in short-term OD plasticity following 4 days of MD but long-term OD plasticity was not impaired, as longer periods (17 ± 6 days) of MD induced synaptic changes in these mice. Inhibitors of the ERK pathway suppress the induction of two forms of LTP: theta burst stimulation (TBS) of layer IV induced LTP and TBS induced white matter (WM) LTP (only present during the critical period), in rat cortical slices. Intracortical administration of inhibitors of the ERK pathway to MD rats prevents the shift in OD plasticity towards

the non-deprived eye [110]. It is surprising that these kinases, which control different pathways, all lead to impairment of the OD shift after MD. This indicates that perhaps a significant overlap between these pathways and they converge on a common downstream target that may mediate these effects.

The Ca^{2+}/calmodulin-activated protein phosphatase, calcineurin (CN), has also been shown to be a molecular constraint on OD plasticity [111] either by directly dephosphorylating its substrate or via the activation of downstream protein phosphates 1 (PP1) [112]. These two phosphatases dephosphorylate specific sites on NMDARs [113] and AMPARs [114]. Moreover, inhibition of CN blocks induction of LTD in rat visual cortex [115] and enhances the induction of LTP [116]. Also, it can antagonize the effects of PKA and CaMKII [111]. In a tetracycline-controlled transactivator (tTA) system, mutant mice expressing an active form of CN can be reversibly and transiently turned on by removing tetracycline. A transient increase in CN activity led to an impaired OD shift following MD which was reversible. Therefore, this study provided strong evidence that CN functions as a negative regulator of cortical plasticity.

1.1.5.3. Transcription factors

An important effecter downstream of these kinases and phosphatases is the nuclear transcription factor cAMP/Ca^{2+} response element-binding protein (CREB) [117, 118]. CREB is a nuclear protein that modulates the transcription of any gene with a consensus cAMP responsive element (CRE) in its promoter. Most Ca^{2+}-induced genes in the nervous system are regulated by CREB [119]. Its activation is controlled by phosphorylation at serine 133 [120]. PKA, ERK, CaMKIV and CaMKII are known activators of CREB [119-121], although it is controversial whether CaMKII is

translocated to the nucleus [122, 123]. CaMKIV is thought to be a more important member of the CaMK family in phosphorylating nuclear CREB. PP1, which is activated by CN, directly dephosphorylates CREB [124]. Upon activation of CREB, an array of immediate early gene transcripts that are essential for establishment and maintenance of plastic changes are produced [118]. Recent studies have also shown that CREB is activated in mouse visual cortex after MD [125]. In addition, a virally introduced dominant negative form of CREB, with a mutation that impedes phosphorylation at serine (Ser) 133, and hence its activation, blocked the loss of deprived eye responses following MD [12]. Interestingly, the loss of OD plasticity was restored when viral expression of the dominant negative mutant subsided. Thus, these results strongly support the essential role of CREB in OD plasticity. In short, the aforementioned kinases, phosphatases and transcription factor provide a complex but critical link between extracellular signals and the molecular events necessary for OD plasticity to occur.

1.1.5.4. Other important molecules

Other molecules such as cannabinoid receptors [32], extracellular matrix (ECM) degrading protein, tissue plasminogen activator (tPA) [50, 51], components of ECM such as chondroitin-sulfate peoteoglycans (CSPGs) [126], neuromodulators such as acetylcholine, serotonin and noradrenaline [127, 128], transcription modulator histone deacetylases (HDAC) [129], growth factors such as brain-derived neurotrophic factor BDNF and insulin-like growth factor 1 (IGF1) [130, 131], and tumor necrosis factor α [132] are all reported to be important in OD plasticity. However, they are not discussed in detail in this thesis. In sum, a large number of molecules are discovered to play a role in OD plasticity. Some of them appear to be cortical layer specific and age specific.

Considering the complexity of the process of OD plasticity, it is not surprising that as our understanding deepens and broadens, more molecules within existing classes as well as new categories of molecules will be found to participate in OD plasticity. One important consideration in studying these molecules is to differentiate key mediators from modulators in order to gain true insights into the mechanism of OD plasticity.

1.2. Ca^{2+}/calmodulin dependent protein Kinase II

Many of the studies above related to OD plasticity designed their experiments using the MD paradigm on the order of day(s) to months, with a few exceptions [13, 25, 86]. However, many molecular events underlying OD plasticity take place on a short time scale of minutes to hours before physiological and structural changes are apparent and detectable. For example, changes in phosphorylation at Ser84 of GluR1 and Ser880 of GluR2 are apparent after only 6 hrs of MD [13]. Hence, there is a gap in our understanding of molecular mechanisms at the very early phase of OD plasticity that warrants more careful investigation. Moreover, the induction pf plasticity at a synaptic level *in vivo* has been inferred but not directly shown. For example, which signaling pathway underlies the increase in spine motility and the decrease in spine density described in section 1.1.3.2.? To answer such questions would require a novel detection method of synaptic activity. For these reasons, we want to base our study on a molecular marker that is essential for the rapid induction of synaptic plasticity and at the same time, whose activation profile has a long enough window for detection.

1.2.1. Global and subcellular localization of CaMKII

CaMKII is a member of the Ser/threonine protein kinase family and is activated by Ca^{2+}/calmodulin (CaM) binding [133]. It is ubiquitously expressed but highly enriched in the brain [134, 135]. It constitutes about 1-2% of the total protein in the brain, with the hippocampus having the highest concentration followed by the cerebral cortex [135]. In the primary visual cortex, CaMKIIα has a distinct laminar distribution profile. In both monkey and mouse visual cortex, the highest expression level of CaMKII resides in supragranular layer II/III, is less concentrated in layer IV, I and VI and is absent in layer I [108, 136, 137]. Incidentally, the highest level of phosphorylated CaMKII is also seen in layer II/III of mouse visual cortex [108]. This expression pattern is interesting, as it overlaps with the locus of fast OD plasticity (please see session 1.1.2.), implying a possible role for CaMKII in fast OD plasticity processes. CaMKII is a soluble protein present throughout the neuron [138, 139] and is also localized in particular subcellular compartments through interactions with multiple proteins. CaMKII is enriched at the synapse, both presynaptically and postsynaptically, and is the main protein of the cytoplasmic side of the postsynaptic density (PSD) [140, 141], located a mean distance of 25 nm from the cleft. In electron microscopic tomograms, CaMKII can be visualized directly, appearing as tower-like structures protruding from the thick of the PSD [142]. Indeed, the association of CaMKII with the PSD correlates with the synaptic strength and size of individual spines [143]. CaMKII's strategic localization in the PSD denotes its critical involvement in the regulation of excitatory synaptic transmission.

1.2.2. Regulation of CaMKII activity

1.2.2.1. Structure of CaMKII

CaMKII has four domains: a catalytic domain, an autoinhibitory/regulatory domain, a variable domain and an association domain [144, 145]. Through the C-terminus of the association domain, CaMKII forms an oligomer comprised of two hexameric rings stacked on top of each other [146-150]. It has recently be shown that the transition between the paired and unpaired dimers formed between two subunits, one from each stacked ring, is important in regulating its activation [151]. In addition, these dodecameric holoenzymes can interact with each other and form a tertiary structure [152]. Combine, these unique structural properties confer a complex regulatory dynamic upon CaMKII, which will be described next.

1.2.2.2. Regulation of CaMKII activity

In the basal state, CaMKII is kept inactive due to the intrasubunit steric block of the substrate-binding site (S site) in the kinase domain by a pseudosubstrate region within the autoinhibitory domain [144]. Binding of CaM to the regulatory domain adjacent to the autoinhibitory domain alters its conformation and disrupts its inhibitory interaction at the S site. This disruption releases the kinase domain, which contains the ATP and substrate binding sites, from the block and allows it to rapidly autophosphorylate threonine 286 (T286), as well as other substrates [153-156]. CaMKII autophosphorylation at T286 prevents the autoinhibitory domain from binding with the T site of the catalytic domain and from blocking the kinase activity, thereby allowing the kinase to retain substantial activity even in the absence of Ca^{2+}. In addition,

autophosphorylation at T286 also decreases the dissociation of bound Ca^{2+}/CaM by several orders of magnitude, thereby prolonging its activation [157]. This autophosphorylation occurs by an intersubunit reaction only when two Ca^{2+}/CaM molecules bind to two proximal CaMKII subunits in the holoenzyme, which means a high Ca^{2+} signal is required for this process to occur [156, 158]. It has also been shown that the extent of CaMKII autonomy is dependent on of the frequency of Ca^{2+} oscillations [159]. Once one subunit within the ring is autophosphorylated, subsequent phosphorylation on the neighboring subunits will be easier because only one Ca^{2+}/CaM is required [160]. This leads to functional cooperativity. Thus, unless phosphatase activity is higher than kinase activity, this holoenzyme remains active for a prolonged period of time, significantly outlasting that of the Ca^{2+} spike.

A second way to obtain CaMKII autonomous activity is through its interaction with NMDARs located in the PSD [161-164]. Activation increases the association of CaMKIIα and β with the cytoplasmic C-terminal tail of NR2B, regardless of the autophosphorylation state, while autophosphorylation following activation enhances the binding of CaMKII to NR1. This autonomy is achieved by anchoring the kinase to a sequence on the tail of NR2B, which mimics the autoinhibitory domain that interacts with the T site of the catalytic domain [162]. Hence, if a subunit in the ring is bound to the NMDAR, a low level Ca^{2+} signal can trigger autonomy in a neighboring subunit.

The inactivation mechanism of CaMKII is also complex. There are two protein phosphatases (PP), PP1 and PP2A that can dephosphorylate CaMKII under different conditions. PP2A activation is dependent on Ca^{2+} entry through NMDARs upon LTD induction [165]. The PP2A holoenzyme has autocatalytic dephosphorylation properties

that mirror the autonomy of CaMKII [166]. It is shown that PP2A and CaMKII can negatively regulate each other [167]. PP2A can only dephosphorylate CaMKII in the cytoplasm but not in the PSD where dephosphorylation is executed exclusively by PP1 [168, 169]. The balance of the kinase/phosphatase system depends on the substrate concentration, activity level and their catalytic kinetics. This interplay between PP1/PP2A and CaMKII forms the basis of the theoretic framework of CaMKII as a memory switch [144, 170].

Besides regulatory mechanism of posttranslational modification, protein translation is also one way that neurons have evolved to control the function of CaMKII at the synapse. Whereas most dendritic proteins are transported from the soma, CaMKII mRNA is transported to dendrites [171]. Studies using targeted deletion of the 3'UTR of CaMKIIα, which inhibits CaMKIIα mRNA translocation to dendrites, showed a marked reduction in PSD associated CaMKIIα protein and instability of L-LTP and memory [172]. Neuronal depolarization recruits CaMKIIα mRNA into granular structures that are targeted to dendritic processes [173]. Furthermore, the translation of CaMKII is also regulated by activity. Tetanic stimulation led to an increase in accumulation of CaMKII via protein synthesis, which is indicative of the rapid local protein translational capacity of dendrites [174, 175]. Controlling the initiation factors enhance cap-dependent mRNA initiation by phosphorylation, such as eIF4E, is also one way to regulate protein synthesis [176].

In summary, regulation of CaMKII is multifaceted and dynamic. Such tight and complex control over the activity of a protein signifies its importance in multiple functions.

1.2.3. The role of CaMKII in hippocampal subdivision *cornu ammonis* 1 (CA1) LTP

In 1949, Donald Hebb proposed that the selective strengthening of the synapses between two simultaneously active neuron results in learning [71]. The first experiment that demonstrated this Hebbian learning rule was carried out by Bliss and Lømo in 1993 in the synapses between the entering entorhinal perforant path fibers and the hippocampal dentate granule cells, where a brief train of high frequency stimulation led to a persistent strengthening of synaptic transmission [177]. LTP has since been seen in multiple pathways within the hippocampus, with CA1 being the most intensively studied region, as well as in other regions of the brain such as visual cortex [77, 79, 178-181].

In the basal state, most excitatory postsynaptic current is mediated by AMPARs, which are not Ca^{2+} permeable [182, 183]. The LTP induction protocol that releases presynaptic glutamate and removes the Mg^{2+} block from the ion channel of NMDARs, causes an influx of Ca^{2+} through these channels [179-181]. Ca^{2+} binds to an adaptor protein, CAM, and they in turn activate CaMKII amongst numerous other proteins [184]. Activated CaMKII is involved in different phases of LTP.

1.2.3.1 Requirement of CaMKII in LTP induction

Activity of CaMKII is necessary and sufficient for LTP induction. The core process of LTP induction depends on CaMKII activity, as blocking CaMKII abolishes LTP induced by both tetanic stimulation and pairing protocols [184-187]. Hippocampal LTP magnitude was also found to be decreased in CaMKIIα knockout mice [188, 189]. To demonstrate a requirement for CaMKIIα autonomous activity in LTP induction,

mutant mice with the single amino acid mutation of threonine 286 (T286) to alanine (A), a mutation that renders T286 autophosphorylation deficient were generated [190]. LTP in these mice was largely abolished, with small amounts of residual LTP that could be attributed to other kinases such as CaMKIIβ, PKC and PKA also shown to be important for LTP [186, 191, 192]. In addition, expression of a constitutively active form of CaMKIIα in CA1 increases synaptic transmission and prevents further LTP [193, 194]. In sum, these studies demonstrated that LTP induction is largely dependent on the activity of CaMKIIα.

1.2.3.2. CaMKII is involved in LTP expression and maintenance

There are several CaMKII-dependent mechanisms by which observed increase in AMPAR function can be accounted for. The intracellular carboxyl tail of AMPAR subunit GluR1 is phosphorylated at Ser831 by CaMKII and NMDAR activation after LTP induction [195-198]. Phosphorylation at this site increases the single channel conductance [195, 197]. Moreover, increasing the number of AMPARs on the postsynapse is another way of increasing AMPAR function [199]. Indeed, CaMKII activity drives AMPARs to the synapse increasing surface expression of AMPARs, which contribute to the enhanced AMPA receptor-mediated transmission observed during LTP [200, 201]. The insertion of AMPARs is not dependent on Ser831 phosphorylation but is dependent on the interaction of this site with the PDZ domain [202]. In addition, as mentioned in section 1.2.2.2., CaMKII can be translocated into the PSD and bind to NMDARs in an activity regulated manner. This bound CaMKII can structurally organize AMPAR-binding proteins into the PSD by forming a complex with actin filaments, protein 4.1 and synapse-associated protein 97 ,and therefore recruit more AMPARs [203].

Given the prolonged activation of CaMKII after Ca^{2+} returns to basal levels, it has been speculated that it plays a role in the maintenance of. Evidence in support of this idea shows that AMPAR GluR1 is phosphorylated by CaMKII for one hour upon LTP induction [204], while the late phase of LTP is blocked by the synergistic effect of PKC and CaMKII inhibitory peptides [205]. However, most other studies that inhibited CaMKII activity showed that maintenance of LTP occurs independent of the activation of CaMKII [144].

1.2.4. Involvement of CaMKII in LTD

Although overwhelming evidence points to a role for CaMKII in LTP induction, it is worth noting that its role in LTD has also been studied. Stevens *et al*. showed, in hippocampal slice preparations from mutant mice that lack CaMKIIα, that LTD was markedly diminished [206]. Another study examined the effect of CaMKIIα on LTP after the single amino acid mutation of T286 to aspartate (D), a mutation that mimics autophosphorylation. In hippocampal slices from these mice, LTP was normal but a systematic shift in favor of LTD at medium to low frequencies stimulation was observed. The authors concluded that the study provided support for CaMKII's role in the induction of LTD. They further proposed two interesting mechanisms that could potentially account for their observations [207]. First, it is known that CaMKII autophosphorylation results in a more than 100-fold increase in its binding affinity for Ca^{2+}/CaM (see section 1.2.2.2.) [157]. This trapping mechanism can serve as a regulatable Ca^{2+}/CaM sink and effectively reduce the availability of Ca^{2+}/CaM in the PSD. Hence, the same size Ca^{2+} signal in an environment with a higher level of autophosphorylated CaMKII will have less available Ca^{2+}/CaM, which in turn shifts the system in favor of LTD. Second, CaMKII activation

could be the rate limiting step leading to LTD production along with other protein phosphatases (move citation here). While these theories are possible explanations of the results of this study, more direct evidence is required to prove a requirement for CaMKII in LTD.

1.2.5 Involvement of CaMKII in activity-dependent synaptic homeostasis

In addition to the role of CaMKII in LTP and LTD, a recent study by Thiagarajan *et al.* examined the activity-dependence of the relative level of CaMKII isoforms in hippocampal neurons and revealed that regulation of CaMKII holoenzyme subunit composition may be important for synaptic homeostasis [208]. When they reduced the neuronal activity by TTX bath application, it was found that CaMKIIα level decreased while CaMKIIβ level increased. An opposite effect was observed when they increased the neuronal activity by bicucculine application. Furthermore, electrophysiological data confirmed that CaMKIIα transfected cells had a significantly larger mean synaptic charge in mEPSCs but a decreased synaptic charge was seen in CaMKIIβ-infected cells. These isoform-specific effects are important because they can provide a mechanism for cells to tune their input.

It is known that CaMKIIα and CaMKIIβ have different sensitivities to Ca^{2+} since the half-maximal autophosphorylation is reached at 130 nM calmodulin for CaMKIIα but at 15 nM calmodulin for CaMKIIβ [209]. By regulating the ratio of CaMKIIα to CaMKIIβ, neurons can change their response to the subsequent rise in Ca^{2+}/camodulin as the sensitivity is no longer the same. Consider a situation where activity is increased. The CaMKIIα to CaMKIIβ ratio will increase and this leads to a lowered Ca^{2+}/camodulin

sensitivity of CaMKII. As a result, an increase in activity is counterbalanced by a decrease in Ca^{2+}/camodulin sensitivity in a homeostatic manner. Therefore, these data support the involvement of CaMKII in homeostatic mechanisms.

Furthermore, they showed that at least some aspects of adaptation to inactivity depend on the activity of CaMKII. NBQX treatment that blocked AMPA receptor transmission increased both the frequency and amplitude of mEPSCs but decreased the decay time of mEPSCs when compared with control cells. However, these effects were prevented by the concomitant application of KN-93, a calmodulin kinase inhibitor. Indeed, the effect of NBQX on mEPSCs frequency was reversed after addition of KN-93 such that NBQX led to a decrease in mEPSCs frequency. KN-92, an inactive analog of KN-93, failed to abolish these effects. These observations point to the involvement of CaMKII in activity-dependent homeostasis.

1.2.6. Design of a FRET probe (Camui) for the detection of CaMKIIα activation

Despite the well-established role of CaMKII in LTP, data on the spatial and temporal patterns of CaMKII activation *in vivo* is largely absent. Genetically manipulated CaMKII mice provide a powerful tool for *in vivo* functional and behavioral studies but real time observation of wild type CaMKII function during OD plasticity has not been possible. For these reasons, as part of a previous study in the lab [210], a probe (Camui) was engineered to optically monitor CaMKIIα activity by employing the principle of fluorescence resonance energy transfer (FRET) [211]. FRET is an optical phenomenon that depends on the distance and angle of two fluorophores (Figure 1). When two fluorophores are in close vicinity (~10 Å), the emission energy from one fluorophore

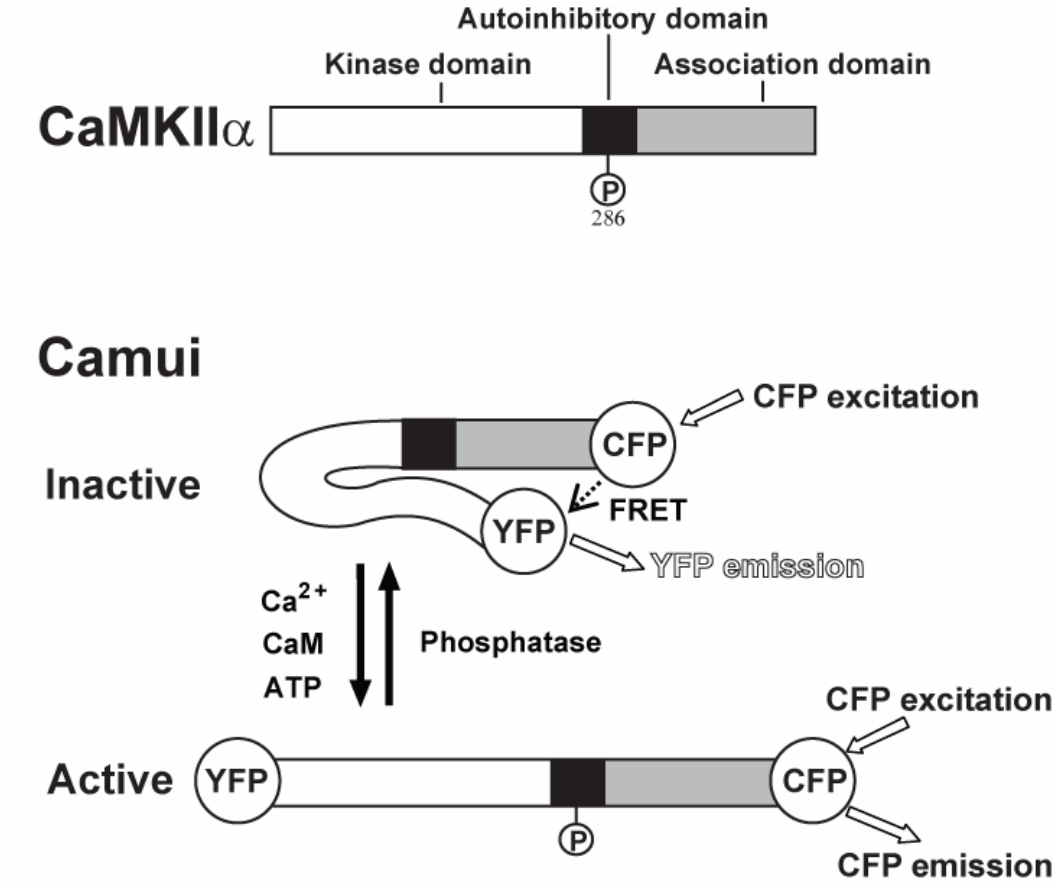

Figure 1. Schematic diagram of Camui. In its inactive state, the distance small distance between CFP and YFP allows FRET to occur. However, activation induced conformational change increase the distance between the two fluorophores such that FRET cannot occur. The ratio of CFP/YFP reflects the relative activation state of Camui (higher CFP/YFP=higher CaMKIIα activity).

(donor) excites the second fluorophore (acceptor) leading to the occurrence of FRET. When the donor and acceptor fluorophores are farther apart from one another, this FRET does not occur. Therefore, Takao *et al*. took advantage of the conformational changes associated with CaMKIIα activation and designed Camui by fusing CFP (donor) and YFP (acceptor) to the two termini of CaMKIIα. CFP emission overlaps with the excitation spectrum of YFP and thus by monitoring the emission spectrum of the two, FRET can be measured. This method is called ratiometric FRET. Another method for detecting FRET is via measurement of the fluorescence lifetime of the donor, termed fluorescence lifetime imaging (FLIM) [212].

Camui, a YFP-CaMKIIα-CFP tandem fusion protein, which is extensively characterized in our previous study [210], is shown in the schematic diagram in Figure 1. Camui shows FRET in its inactive state. In the presence of ATP and CaM, stimulation with Ca^{2+} causes a rapid (<1 min) decrease in FRET. This change arises from a conformational change due to both binding with Ca^{2+}/CaM and autophosphorylation, as is evident by the persistence of FRET after the addition of the Ca^{2+} chelator ethylene glycol tetraacetic acid (EGTA) . This persistent, Ca^{2+}-independent change in FRET was abolished by omitting ATP or by eliminating the kinase activity with a point mutation (lysine 42 to arginine) at the catalytic core. Therefore, a process involving autophosphorylation, most likely the autophosphorylation at T286 on the autoinhibitory domain, is contributing to this persistent change. In fact, a phosphoblocking mutation (T286A) stops the persistent change in FRET, whereas a phosphomimicking mutation (T286D) is sufficient to induce a change in FRET without Ca^{2+} stimulation. Therefore,

Camui detects the activation of CaMKIIα by the binding of Ca^{2+}/CaM and subsequent autophosphorylation.

Using Camui, we can now investigate the spatial and temporal regulation of CaMKIIα in rapid OD plasticity events in layer II/III of ferret visual cortex, which is also where inputs from two eyes mix for the first time along the visual pathway. In addition, it the superficial location of layer II/III makes it perfectly suited for in vivo two-photon imaging studies. Camui will also allow us to identify synapses undergoing plastic changes *in vivo* and to estimate the number of such changing synapses on a given neuron in a particular eye domain. Furthermore, subcellular observation of CaMKIIα activity changes using Camui will allow us to determine the distribution of visual input at the single spine, dendrite and a neuron level. Indeed, a recent *in vitro* study using the FLIM version of Camui in rat (hippocampal) slice culture has demonstrated that the activation profile of CaMKIIα at a single spine by glutamate uncaging can be monitored [213]. This provides promising evidence that CaMKIIα activity can be detected *in vivo* using the ratiometric Camui FRET probe.

1.3. Acknowledgment

Work described in this thesis is supported by funding from the Brain Science Institute, RIKEN, Japan and the National Institutes of Health Grant R01 DA-17310.

1.4. References

1. Wiesel, T.N. and D.H. Hubel, *Single-cell response in striate cortex of kittens deprived of vision in one eye.* J Neurophysiol, 1963. **26**(6): p. 1003-1017.

2. Movshon, J.A. and M.R. Dursteler, *Effects of brief periods of unilateral eye closure on the kitten's visual system.* J Neurophysiol, 1977. **40**(6): p. 1255-65.

3. Wiesel, T.N. and D.H. Hubel, *Comparison of the effects of unilateral and bilateral eye closure on cortical unit responses in kittens.* J Neurophysiol, 1965. **28**(6): p. 1029-40.

4. Sur, M. and J.L.R. Rubenstein, *Patterning and Plasticity of the Cerebral Cortex.* Science, 2005. **310**(5749): p. 805-810.

5. Crowley, J.C. and L.C. Katz, *Development of ocular dominance columns in the absence of retinal input.* Nat Neurosci, 1999. **2**(12): p. 1125-1130.

6. Katz, L.C. and C.J. Shatz, *Synaptic Activity and the Construction of Cortical Circuits.* Science, 1996. **274**(5290): p. 1133-1138.

7. Olson, C.R. and R.D. Freeman, *Progressive changes in kitten striate cortex during monocular vision.* J Neurophysiol, 1975. **38**(1): p. 26-32.

8. Simon Le Vay, T.N.W.D.H.H., *The development of ocular dominance columns in normal and visually deprived monkeys.* The Journal of Comparative Neurology, 1980. **191**(1): p. 1-51.

9. Hubel, D.H., T.N. Wiesel, and S. LeVay, *Plasticity of ocular dominance columns in monkey striate cortex.* Philos Trans R Soc Lond B Biol Sci, 1977. **278**(961): p. 377-409.

10. Hubel, D.H., T.N. Wiesel, and S. LeVay, *Functional architecture of area 17 in normal and monocularly deprived macaque monkeys.* Cold Spring Harb Symp Quant Biol, 1976. **40**: p. 581-9.

11. Issa, N.P., et al., *The Critical Period for Ocular Dominance Plasticity in the Ferret's Visual Cortex.* J. Neurosci., 1999. **19**(16): p. 6965-6978.

12. Mower, A.F., et al., *cAMP/Ca2+ response element-binding protein function is essential for ocular dominance plasticity.* J Neurosci, 2002. **22**(6): p. 2237-45.

13. Heynen, A.J., et al., *Molecular mechanism for loss of visual cortical responsiveness following brief monocular deprivation.* Nat Neurosci, 2003. **6**(8): p. 854-62.

14. Fagiolini, M., et al., *Functional postnatal development of the rat primary visual cortex and the role of visual experience: Dark rearing and monocular deprivation.* Vision Research, 1994. **34**(6): p. 709.

15. Gordon, J.A. and M.P. Stryker, *Experience-Dependent Plasticity of Binocular Responses in the Primary Visual Cortex of the Mouse.* J. Neurosci., 1996. **16**(10): p. 3274-3286.

16. Frenkel, M.Y. and M.F. Bear, *How Monocular Deprivation Shifts Ocular Dominance in Visual Cortex of Young Mice.* Neuron, 2004. **44**(6): p. 917.

17. Wiesel, T.N. and D.H. Hubel, *Comparison of the effects of unilateral and bilateral eye closure on cortical unit responses in kittens.* J Neurophysiol, 1965. **28**(6): p. 1029-1040.

18. Hubel, D.H. and T.N. Wiesel, *The period of susceptibility to the physiological effects of unilateral eye closure in kittens.* J Physiol, 1970. **206**(2): p. 419-436.

19. Horton, J.C. and D.R. Hocking, *Timing of the critical period for plasticity of ocular dominance columns in macaque striate cortex.* J Neurosci, 1997. **17**(10): p. 3684-709.

20. Garraghty, P.E. and S. Mriganka, *: Morphology of single intracellularly stained axons terminating in area 3b of macaque monkeys.* : The Journal of Comparative Neurology, 1990. **294**: p. 583-93.

21. LeVay, S. and C.D. Gilbert, *Laminar patterns of geniculocortical projection in the cat.* Brain Research, 1976. **113**(1): p. 1.

22. Hubel, D.H. and N.W. Torsten, *: Laminar and columnar distribution of geniculo-cortical fibers in the macaque monkey.* : The Journal of Comparative Neurology, 1972. **146** (4): p. 421-50.

23. Bolz, J., C.D. Gilbert, and T.N. Wiesel, *Pharmacological analysis of cortical circuitry.* Trends in Neurosciences, 1989. **12**(8): p. 292.

24. Buonomano, D.V. and M.M. Merzenich, *CORTICAL PLASTICITY: From Synapses to Maps.* Annual Review of Neuroscience, 1998. **21**(1): p. 149-186.

25. Freeman, R.D. and C. Olson, *Brief periods of monocular deprivation in kittens: effects of delay prior to physiological study.* J Neurophysiol, 1982. **47**(2): p. 139-150.

26. Miller, K.D., J.B. Keller, and M.P. Stryker, *Ocular Dominance Column Development: Analysis and Simulation.* Science, 1989. **245**(4918): p. 605.

27. Shatz, C.J. and M.P. Stryker, *Ocular dominance in layer IV of the cat's visual cortex and the effects of monocular deprivation.* J Physiol, 1978. **281**(1): p. 267-283.

28. Ruthazer, E.S. and M.P. Stryker, *The Role of Activity in the Development of Long-Range Horizontal Connections in Area 17 of the Ferret.* J. Neurosci., 1996. **16**(22): p. 7253-7269.

29. Crair, M.C., D.C. Gillespie, and M.P. Stryker, *The Role of Visual Experience in the Development of Columns in Cat Visual Cortex.* Science, 1998. **279**(5350): p. 566-570.

30. Crair, M.C., et al., *Ocular Dominance Peaks at Pinwheel Center Singularities of the Orientation Map in Cat Visual Cortex.* J Neurophysiol, 1997. **77**(6): p. 3381-3385.

31. Trachtenberg, J.T., C. Trepel, and M.P. Stryker, *Rapid Extragranular Plasticity in the Absence of Thalamocortical Plasticity in the Developing Primary Visual Cortex.* Science, 2000. **287**(5460): p. 2029-2032.

32. Liu, C.-H., et al., *Cannabinoid Receptor Blockade Reveals Parallel Plasticity Mechanisms in Different Layers of Mouse Visual Cortex.* Neuron, 2008. **58**(3): p. 340.

33. Antonini, A., M. Fagiolini, and M.P. Stryker, *Anatomical Correlates of Functional Plasticity in Mouse Visual Cortex.* J. Neurosci., 1999. **19**(11): p. 4388-4406.

34. Hata, Y. and M.P. Stryker, *Control of thalamocortical afferent rearrangement by postsynaptic activity in developing visual cortex.* Science, 1994. **265**(5179): p. 1732-1735.

35. Desai, N.S., et al., *Critical periods for experience-dependent synaptic scaling in visual cortex.* Nat Neurosci, 2002. **5**(8): p. 783-9.

36. Sherman, S.M. and J. Stone, *Physiological normality of the retina in visually deprived cats.* Brain Research, 1973. **60**(1): p. 224.

37. Sur, M., A.L. Humphrey, and S.M. Sherman, *Monocular deprivation affects X- and Y-cell retinogeniculate terminations in cats.* Nature, 1982. **300**(5888): p. 183.

38. Kalil, R., *Quantitative study of the effects of monocular enucleation and deprivation on cell growth in the dorsal lateral geniculate nucleus of the cat.* J Comp Neurol, 1980. **189**(3): p. 483-524.

39. Sherman, M.S. and K.J. Sanderson, *Binocular interaction on cells of the dorsal lateral geniculate nucleus of visually deprived cats.* Brain Research, 1972. **37**(1): p. 126.

40. LeVay, S. and D. Ferster, *Relay cell classes in the lateral geniculate nucleus of the cat and the effects of visual deprivation.* J Comp Neurol, 1977. **172**(4): p. 563-84.

41. Lehmkuhle, S., et al., *Effects of early monocular lid suture on spatial and temporal sensitivity of neurons in dorsal lateral geniculate nucleus of the cat.* J Neurophysiol, 1980. **43**(2): p. 542-56.

42. Friedlander, M.J., L.R. Stanford, and S.M. Sherman, *Effects of monocular deprivation on the structure-function relationship of individual neurons in the cat's lateral geniculate nucleus.* J Neurosci, 1982. **2**(3): p. 321-30.

43. Wiesel, T.N. and D.H. Hubel, *Effects of visual deprivation on morphology and physiology of cells in the cat's lateral geniculate body.* J Neurophysiol, 1963. **26**(6): p. 978-993.

44. LeVay, S., T.N. Wiesel, and D.H. Hubel, *The development of ocular dominance columns in normal and visually deprived monkeys.* J Comp Neurol, 1980. **191**(1): p. 1-51.

45. Antonini, A. and M.P. Stryker, *Plasticity of geniculocortical afferents following brief or prolonged monocular occlusion in the cat.* The Journal of Comparative Neurology, 1996. **369**(1): p. 64-82.

46. Antonini, A. and M.P. Stryker, *Rapid remodeling of axonal arbors in the visual cortex.* Science, 1993. **260**(5115): p. 1819-1821.

47. Friedlander, M.J., K.A. Martin, and D. Wassenhove-McCarthy, *Effects of monocular visual deprivation on geniculocortical innervation of area 18 in cat.* J. Neurosci., 1991. **11**(10): p. 3268-3288.

48. Konur, S. and R. Yuste, *Developmental regulation of spine and filopodial motility in primary visual cortex: reduced effects of activity and sensory deprivation.* J Neurobiol, 2004. **59**(2): p. 236-46.

49. Majewska, A. and M. Sur, *Motility of dendritic spines in visual cortex in vivo: changes during the critical period and effects of visual deprivation.* Proc Natl Acad Sci U S A, 2003. **100**(26): p. 16024-9.

50. Mataga, N., Y. Mizuguchi, and T.K. Hensch, *Experience-Dependent Pruning of Dendritic Spines in Visual Cortex by Tissue Plasminogen Activator.* Neuron, 2004. **44**(6): p. 1031.

51. Oray, S., A. Majewska, and M. Sur, *Dendritic spine dynamics are regulated by monocular deprivation and extracellular matrix degradation.* Neuron, 2004. **44**(6): p. 1021-30.

52. Hayashi, Y. and A.K. Majewska, *Dendritic Spine Geometry: Functional Implication and Regulation.* Neuron, 2005. **46**(4): p. 529.

53. Majewska, A., A. Tashiro, and R. Yuste, *Regulation of spine calcium dynamics by rapid spine motility.* J Neurosci, 2000. **20**(22): p. 8262-8.

54. Nimchinsky, E.A., B.L. Sabatini, and K. Svoboda, *Structure and function of dendritic spines.* Annu Rev Physiol, 2002. **64**: p. 313-53.

55. Bonhoeffer, T. and R. Yuste, *Spine Motility: Phenomenology, Mechanisms, and Function.* Neuron, 2002. **35**(6): p. 1019.

56. Lendvai, B., et al., *Experience-dependent plasticity of dendritic spines in the developing rat barrel cortex in vivo.* Nature, 2000. **404**(6780): p. 876-81.

57. Dailey, M.E. and S.J. Smith, *The dynamics of dendritic structure in developing hippocampal slices.* J Neurosci, 1996. **16**(9): p. 2983-94.

58. Fischer, M., et al., *Rapid actin-based plasticity in dendritic spines.* Neuron, 1998. **20**(5): p. 847-54.

59. Dunaevsky, A., et al., *Developmental regulation of spine motility in the mammalian central nervous system.* Proc Natl Acad Sci U S A, 1999. **96**(23): p. 13438-43.

60. Korkotian, E. and M. Segal, *Regulation of dendritic spine motility in cultured hippocampal neurons.* J Neurosci, 2001. **21**(16): p. 6115-24.

61. Oray, S., A. Majewska, and M. Sur, *Effects of synaptic activity on dendritic spine motility of developing cortical layer v pyramidal neurons.* Cereb Cortex, 2006. **16**(5): p. 730-41.

62. Okamoto, K., et al., *Rapid and persistent modulation of actin dynamics regulates postsynaptic reorganization underlying bidirectional plasticity.* Nat Neurosci, 2004. **7**(10): p. 1104-12.

63. Matsuzaki, M., et al., *Structural basis of long-term potentiation in single dendritic spines.* Nature, 2004. **429**(6993): p. 761-6.

64. Lang, C., et al., *Transient expansion of synaptically connected dendritic spines upon induction of hippocampal long-term potentiation.* Proc Natl Acad Sci U S A, 2004. **101**(47): p. 16665-70.

65. Zhou, Q., K.J. Homma, and M.M. Poo, *Shrinkage of dendritic spines associated with long-term depression of hippocampal synapses.* Neuron, 2004. **44**(5): p. 749-57.

66. Trachtenberg, J.T., et al., *Long-term in vivo imaging of experience-dependent synaptic plasticity in adult cortex.* Nature, 2002. **420**(6917): p. 788-94.

67. Holtmaat, A.J., et al., *Transient and persistent dendritic spines in the neocortex in vivo.* Neuron, 2005. **45**(2): p. 279-91.

68. Bienenstock, E.L., L.N. Cooper, and P.W. Munro, *Theory for the development of neuron selectivity: orientation specificity and binocular interaction in visual cortex.* J Neurosci, 1982. **2**(1): p. 32-48.

69. Bear, M.F., *A synaptic basis for memory storage in the cerebral cortex.* Proc Natl Acad Sci U S A, 1996. **93**(24): p. 13453-9.

70. Cooper, L.N., F. Liberman, and E. Oja, *A theory for the acquisition and loss of neuron specificity in visual cortex.* Biol Cybern, 1979. **33**(1): p. 9-28.

71. Hebb, D.O., *Organization of behavior.* 1949, New York: John Wiley & Sons.

72. Heynen, A.J., W.C. Abraham, and M.F. Bear, *Bidirectional modification of CA1 synapses in the adult hippocampus in vivo.* Nature, 1996. **381**(6578): p. 163-6.

73. Kirkwood, A., et al., *Common forms of synaptic plasticity in the hippocampus and neocortex in vitro.* Science, 1993. **260**(5113): p. 1518-21.

74. Dudek, S.M. and M.F. Bear, *Homosynaptic long-term depression in area CA1 of hippocampus and effects of N-methyl-D-aspartate receptor blockade.* Proc Natl Acad Sci U S A, 1992. **89**(10): p. 4363-7.

75. Mulkey, R.M., et al., *Involvement of a calcineurin/inhibitor-1 phosphatase cascade in hippocampal long-term depression.* Nature, 1994. **369**(6480): p. 486-8.

76. Thiels, E., G. Barrionuevo, and T.W. Berger, *Excitatory stimulation during postsynaptic inhibition induces long-term depression in hippocampus in vivo.* J Neurophysiol, 1994. **72**(6): p. 3009-16.

77. Kirkwood, A., et al., *Common forms of synaptic plasticity in the hippocampus and neocortex in vitro.* Science, 1993. **260**(5113): p. 1518-1521.

78. Castro-Alamancos, M.A., J.P. Donoghue, and B.W. Connors, *Different forms of synaptic plasticity in somatosensory and motor areas of the neocortex.* J Neurosci, 1995. **15**(7 Pt 2): p. 5324-33.

79. Artola, A., S. Brocher, and W. Singer, *Different voltage-dependent thresholds for inducing long-term depression and long-term potentiation in slices of rat visual cortex.* Nature, 1990. **347**(6288): p. 69-72.

80. Heynen, A.J. and M.F. Bear, *Long-term potentiation of thalamocortical transmission in the adult visual cortex in vivo.* J Neurosci, 2001. **21**(24): p. 9801-13.

81. Kirkwood, A., M.C. Rioult, and M.F. Bear, *Experience-dependent modification of synaptic plasticity in visual cortex.* Nature, 1996. **381**(6582): p. 526-8.

82. Crozier, R.A., et al., *Deprivation-induced synaptic depression by distinct mechanisms in different layers of mouse visual cortex.* Proceedings of the National Academy of Sciences, 2007. **104**(4): p. 1383-1388.

83. Maffei, A., et al., *Potentiation of cortical inhibition by visual deprivation.* Nature, 2006. **443**(7107): p. 81.

84. Sawtell, N.B., et al., *NMDA Receptor-Dependent Ocular Dominance Plasticity in Adult Visual Cortex.* Neuron, 2003. **38**(6): p. 977.

85. Cho, K.K.A., et al., *The ratio of NR2A/B NMDA receptor subunits determines the qualities of ocular dominance plasticity in visual cortex.* Proceedings of the National Academy of Sciences, 2009. **106**(13): p. 5377-5382.

86. Mioche, L. and W. Singer, *Chronic recordings from single sites of kitten striate cortex during experience-dependent modifications of receptive-field properties.* J Neurophysiol, 1989. **62**(1): p. 185-97.

87. Mrsic-Flogel, T.D., et al., *Homeostatic Regulation of Eye-Specific Responses in Visual Cortex during Ocular Dominance Plasticity.* Neuron, 2007. **54**(6): p. 961.

88. Smith, G.B., A.J. Heynen, and M.F. Bear, *Bidirectional synaptic mechanisms of ocular dominance plasticity in visual cortex.* Philosophical Transactions of the Royal Society B: Biological Sciences, 2009. **364**(1515): p. 357-367.

89. Turrigiano, G.G., *The self-tuning neuron: synaptic scaling of excitatory synapses.* Cell, 2008. **135**(3): p. 422-35.

90. Turrigiano, G.G., et al., *Activity-dependent scaling of quantal amplitude in neocortical neurons.* Nature, 1998. **391**(6670): p. 892-6.

91. Goel, A., et al., *Cross-modal regulation of synaptic AMPA receptors in primary sensory cortices by visual experience.* Nat Neurosci, 2006. **9**(8): p. 1001.

92. Turrigiano, G.G. and S.B. Nelson, *Homeostatic plasticity in the developing nervous system.* Nat Rev Neurosci, 2004. **5**(2): p. 97-107.

93. Berardi, N., et al., *Molecular basis of plasticity in the visual cortex.* Trends Neurosci, 2003. **26**(7): p. 369-78.

94. Nedivi, E., *Molecular analysis of developmental plasticity in neocortex.* J Neurobiol, 1999. **41**(1): p. 135-47.

95. Tropea, D., A. Van Wart, and M. Sur, *Molecular mechanisms of experience-dependent plasticity in visual cortex.* Philos Trans R Soc Lond B Biol Sci, 2009. **364**(1515): p. 341-55.

96. Quinlan, E.M., et al., *Rapid, experience-dependent expression of synaptic NMDA receptors in visual cortex in vivo.* Nat Neurosci, 1999. **2**(4): p. 352.

97. Quinlan, E.M., D.H. Olstein, and M.F. Bear, *Bidirectional, experience-dependent regulation of N-methyl-d-aspartate receptor subunit composition in the rat visual cortex during postnatal development.* Proceedings of the National Academy of Sciences of the United States of America, 1999. **96**(22): p. 12876-12880.

98. Chen, W.S. and M.F. Bear, *Activity-dependent regulation of NR2B translation contributes to metaplasticity in mouse visual cortex.* Neuropharmacology, 2007. **52**(1): p. 200-14.

99. Hensch, T.K. and M.P. Stryker, *Columnar Architecture Sculpted by GABA Circuits in Developing Cat Visual Cortex.* Science, 2004. **303**(5664): p. 1678-1681.

100. Reiter, H.O. and M.P. Stryker, *Neural plasticity without postsynaptic action potentials: less-active inputs become dominant when kitten visual cortical cells are pharmacologically inhibited.* Proc Natl Acad Sci U S A, 1988. **85**(10): p. 3623-7.

101. Fagiolini, M., et al., *Specific GABAA Circuits for Visual Cortical Plasticity.* Science, 2004. **303**(5664): p. 1681-1683.

102. Guo, Y., et al., *Expression of two forms of glutamic acid decarboxylase (GAD67 and GAD65) during postnatal development of the cat visual cortex.* Brain Res Dev Brain Res, 1997. **103**(2): p. 127-41.

103. Reetz, A., et al., *GABA and pancreatic beta-cells: colocalization of glutamic acid decarboxylase (GAD) and GABA with synaptic-like microvesicles suggests their role in GABA storage and secretion.* Embo J, 1991. **10**(5): p. 1275-84.

104. Martin, D.L., et al., *Regulatory properties of brain glutamate decarboxylase (GAD): the apoenzyme of GAD is present principally as the smaller of two molecular forms of GAD in brain.* J. Neurosci., 1991. **11**(9): p. 2725-2731.

105. Hensch, T.K., et al., *Local GABA Circuit Control of Experience-Dependent Plasticity in Developing Visual Cortex.* Science, 1998. **282**(5393): p. 1504-1508.

106. Beaver, C.J., et al., *Cyclic AMP-dependent protein kinase mediates ocular dominance shifts in cat visual cortex.* Nat Neurosci, 2001. **4**(2): p. 159-63.

107. Gordon, J.A., et al., *Deficient Plasticity in the Primary Visual Cortex of [alpha]-Calcium/Calmodulin-Dependent Protein Kinase II Mutant Mice.* Neuron, 1996. **17**(3): p. 491-499.

108. Taha, S., et al., *Autophosphorylation of [alpha]CaMKII Is Required for Ocular Dominance Plasticity.* Neuron, 2002. **36**(3): p. 483-491.

109. Taha, S.A. and M.P. Stryker, *Ocular dominance plasticity is stably maintained in the absence of alpha calcium calmodulin kinase II (alphaCaMKII) autophosphorylation.* Proc Natl Acad Sci U S A, 2005. **102**(45): p. 16438-42.

110. Di Cristo, G., et al., *Requirement of ERK activation for visual cortical plasticity.* Science, 2001. **292**(5525): p. 2337-40.

111. Yang, Y., et al., *Reversible blockade of experience-dependent plasticity by calcineurin in mouse visual cortex.* Nat Neurosci, 2005. **8**(6): p. 791.

112. Mulkey, R.M., et al., *Involvement of a calcineurin/ inhibitor-1 phosphatase cascade in hippocampal long-term depression.* Nature, 1994. **369**(6480): p. 486.

113. Lieberman, D.N. and I. Mody, *Regulation of NMDA channel function by endogenous Ca(2+)-dependent phosphatase.* Nature, 1994. **369**(6477): p. 235-9.

114. Tong, G., D. Shepherd, and C.E. Jahr, *Synaptic desensitization of NMDA receptors by calcineurin.* Science, 1995. **267**(5203): p. 1510-2.

115. Torii, N., et al., *An inhibitor for calcineurin, FK506, blocks induction of long-term depression in rat visual cortex.* Neuroscience Letters, 1995. **185**(1): p. 1.

116. Funauchi, M., H. Haruta, and T. Tsumoto, *Effects of an inhibitor for calcium/calmodulin-dependent protein phosphatase, calcineurin, on induction of long-term potentiation in rat visual cortex.* Neuroscience Research, 1994. **19**(3): p. 269.

117. Deisseroth, K., H. Bito, and R.W. Tsien, *Signaling from synapse to nucleus: postsynaptic CREB phosphorylation during multiple forms of hippocampal synaptic plasticity.* Neuron, 1996. **16**(1): p. 89-101.

118. Silva, A.J., et al., *CREB and memory.* Annu Rev Neurosci, 1998. **21**: p. 127-48.

119. Impey, S. and R.H. Goodman, *CREB Signaling-Timing Is Everything.* Sci. STKE, 2001. **2001**(82): p. pe1-.

120. Sheng, M., M.A. Thompson, and M.E. Greenberg, *CREB: a Ca(2+)-regulated transcription factor phosphorylated by calmodulin-dependent kinases.* Science, 1991. **252**(5011): p. 1427-30.

121. Mayr, B. and M. Montminy, *Transcriptional regulation by the phosphorylation-dependent factor CREB.* Nat Rev Mol Cell Biol, 2001. **2**(8): p. 599-609.

122. Deisseroth, K., E.K. Heist, and R.W. Tsien, *Translocation of calmodulin to the nucleus supports CREB phosphorylation in hippocampal neurons.* Nature, 1998. **392**(6672): p. 198-202.

123. Matthews, R.P., et al., *Calcium/calmodulin-dependent protein kinase types II and IV differentially regulate CREB-dependent gene expression.* Mol Cell Biol, 1994. **14**(9): p. 6107-16.

124. Bito, H., K. Deisseroth, and R.W. Tsien, *CREB phosphorylation and dephosphorylation: a Ca(2+)- and stimulus duration-dependent switch for hippocampal gene expression.* Cell, 1996. **87**(7): p. 1203-14.

125. Pham, T.A., et al., *CRE-mediated gene transcription in neocortical neuronal plasticity during the developmental critical period.* Neuron, 1999. **22**(1): p. 63-72.

126. Pizzorusso, T., et al., *Reactivation of ocular dominance plasticity in the adult visual cortex.* Science, 2002. **298**(5596): p. 1248-51.

127. Bear, M.F. and W. Singer, *Modulation of visual cortical plasticity by acetylcholine and noradrenaline.* Nature, 1986. **320**(6058): p. 172-6.

128. Gu, Q. and W. Singer, *Involvement of serotonin in developmental plasticity of kitten visual cortex.* Eur J Neurosci, 1995. **7**(6): p. 1146-53.

129. Putignano, E., et al., *Developmental downregulation of histone posttranslational modifications regulates visual cortical plasticity.* Neuron, 2007. **53**(5): p. 747-59.

130. Huang, Z.J., et al., *BDNF Regulates the Maturation of Inhibition and the Critical Period of Plasticity in Mouse Visual Cortex.* Cell, 1999. **98**(6): p. 739.

131. Tropea, D., et al., *Gene expression changes and molecular pathways mediating activity-dependent plasticity in visual cortex.* Nat Neurosci, 2006. **9**(5): p. 660-668.

132. Kaneko, M., et al., *Tumor necrosis factor-alpha mediates one component of competitive, experience-dependent plasticity in developing visual cortex.* Neuron, 2008. **58**(5): p. 673-80.

133. Wayman, G.A., et al., *Calmodulin-Kinases: Modulators of Neuronal Development and Plasticity.* Neuron, 2008. **59**(6): p. 914.

134. Bennett, M.K., N.E. Erondu, and M.B. Kennedy, *Purification and characterization of a calmodulin-dependent protein kinase that is highly concentrated in brain.* J. Biol. Chem., 1983. **258**(20): p. 12735-12744.

135. Erondu, N.E. and M.B. Kennedy, *Regional distribution of type II Ca2+/calmodulin-dependent protein kinase in rat brain.* J. Neurosci., 1985. **5**(12): p. 3270-3277.

136. Hendry, S.H. and M.B. Kennedy, *Immunoreactivity for a calmodulin-dependent protein kinase is selectively increased in macaque striate cortex after monocular deprivation.* Proc Natl Acad Sci U S A, 1986. **83**(5): p. 1536-40.

137. Tighilet, B., T. Hashikawa, and E.G. Jones, *Cell- and Lamina-Specific Expression and Activity-Dependent Regulation of Type II Calcium/Calmodulin-Dependent Protein Kinase Isoforms in Monkey Visual Cortex.* J. Neurosci., 1998. **18**(6): p. 2129-2146.

138. Ouimet, C.C., T.L. McGuinness, and P. Greengard, *Immunocytochemical localization of calcium/calmodulin-dependent protein kinase II in rat brain.* Proc Natl Acad Sci U S A, 1984. **81**(17): p. 5604-8.

139. Erondu, N.E. and M.B. Kennedy, *Regional distribution of type II Ca2+/calmodulin-dependent protein kinase in rat brain.* J Neurosci, 1985. **5**(12): p. 3270-7.

140. Kennedy, M.B., M.K. Bennett, and N.E. Erondu, *Biochemical and immunochemical evidence that the "major postsynaptic density protein" is a subunit of a calmodulin-dependent protein kinase.* Proc Natl Acad Sci U S A, 1983. **80**(23): p. 7357-61.

141. Chen, X., et al., *Mass of the postsynaptic density and enumeration of three key molecules.* Proceedings of the National Academy of Sciences of the United States of America, 2005. **102**(32): p. 11551-11556.

142. Petersen, J.D., et al., *Distribution of Postsynaptic Density (PSD)-95 and Ca2+/Calmodulin-Dependent Protein Kinase II at the PSD.* J. Neurosci., 2003. **23**(35): p. 11270-11278.

143. Asrican, B., J. Lisman, and N. Otmakhov, *Synaptic strength of individual spines correlates with bound Ca2+-calmodulin-dependent kinase II.* J Neurosci, 2007. **27**(51): p. 14007-11.

144. Lisman, J., H. Schulman, and H. Cline, *The molecular basis of CaMKII function in synaptic and behavioural memory.* Nat Rev Neurosci, 2002. **3**(3): p. 175-190.

145. Soderling, T.R. and J.T. Stull, *Structure and regulation of calcium/calmodulin-dependent protein kinases.* Chem Rev, 2001. **101**(8): p. 2341-52.

146. Rosenberg, O.S., et al., *Structure of the Autoinhibited Kinase Domain of CaMKII and SAXS Analysis of the Holoenzyme.* Cell, 2005. **123**(5): p. 849.

147. Gaertner, T.R., et al., *Comparative analyses of the three-dimensional structures and enzymatic properties of alpha, beta, gamma and delta isoforms of Ca2+-calmodulin-dependent protein kinase II.* J Biol Chem, 2004. **279**(13): p. 12484-94.

148. Morris, E.P. and K. Torok, *Oligomeric structure of alpha-calmodulin-dependent protein kinase II.* J Mol Biol, 2001. **308**(1): p. 1-8.

149. Kolodziej, S.J., et al., *Three-dimensional reconstructions of calcium/calmodulin-dependent (CaM) kinase IIalpha and truncated CaM kinase IIalpha reveal a unique organization for its structural core and functional domains.* J Biol Chem, 2000. **275**(19): p. 14354-9.

150. Woodgett, J.R., M.T. Davison, and P. Cohen, *The calmodulin-dependent glycogen synthase kinase from rabbit skeletal muscle. Purification, subunit structure and substrate specificity.* Eur J Biochem, 1983. **136**(3): p. 481-7.

151. Thaler, C., et al., *Structural rearrangement of CaMKIIÎ± catalytic domains encodes activation.* Proceedings of the National Academy of Sciences, 2009: p. -.

152. Hudmon, A., et al., *A mechanism for Ca2+/calmodulin-dependent protein kinase II clustering at synaptic and nonsynaptic sites based on self-association.* J Neurosci, 2005. **25**(30): p. 6971-83.

153. Soderling, T.R. and V.A. Derkach, *Postsynaptic protein phosphorylation and LTP.* Trends in Neurosciences, 2000. **23**(2): p. 75-80.

154. Hanson, P.I., et al., *Expression of a multifunctional Ca2+/calmodulin-dependent protein kinase and mutational analysis of its autoregulation.* Neuron, 1989. **3**(1): p. 59-70.

155. Smith, M.K., et al., *Functional determinants in the autoinhibitory domain of calcium/calmodulin-dependent protein kinase II. Role of His282 and multiple basic residues.* J Biol Chem, 1992. **267**(3): p. 1761-8.

156. Mukherji, S. and T.R. Soderling, *Regulation of Ca2+/calmodulin-dependent protein kinase II by inter- and intrasubunit-catalyzed autophosphorylations.* J. Biol. Chem., 1994. **269**(19): p. 13744-13747.

157. Meyer, T., et al., *Calmodulin trapping by calcium-calmodulin-dependent protein kinase.* Science, 1992. **256**(5060): p. 1199-202.

158. Hanson, P.I., et al., *Dual role of calmodulin in autophosphorylation of multifunctional CaM kinase may underlie decoding of calcium signals.* Neuron, 1994. **12**(5): p. 943-56.

159. De Koninck, P. and H. Schulman, *Sensitivity of CaM Kinase II to the Frequency of Ca2+ Oscillations.* Science, 1998. **279**(5348): p. 227-230.

160. Rich, R.C. and H. Schulman, *Substrate-directed Function of Calmodulin in Autophosphorylation of Ca2+/Calmodulin-dependent Protein Kinase II.* J. Biol. Chem., 1998. **273**(43): p. 28424-28429.

161. Shen, K. and T. Meyer, *Dynamic control of CaMKII translocation and localization in hippocampal neurons by NMDA receptor stimulation.* Science, 1999. **284**(5411): p. 162-6.

162. Bayer, K.U., et al., *Interaction with the NMDA receptor locks CaMKII in an active conformation.* Nature, 2001. **411**(6839): p. 801-5.

163. Bayer, K.U., et al., *Transition from Reversible to Persistent Binding of CaMKII to Postsynaptic Sites and NR2B.* J. Neurosci., 2006. **26**(4): p. 1164-1174.

164. Gardoni, F., et al., *Calcium/calmodulin-dependent protein kinase II is associated with NR2A/B subunits of NMDA receptor in postsynaptic densities.* J Neurochem, 1998. **71**(4): p. 1733-41.

165. Thiels, E., et al., *Transient and persistent increases in protein phosphatase activity during long-term depression in the adult hippocampus in vivo.* Neuroscience, 1998. **86**(4): p. 1023-9.

166. Chen, J., B.L. Martin, and D.L. Brautigan, *Regulation of protein serine-threonine phosphatase type-2A by tyrosine phosphorylation.* Science, 1992. **257**(5074): p. 1261-4.

167. Fukunaga, K., et al., *Decreased protein phosphatase 2A activity in hippocampal long-term potentiation.* J Neurochem, 2000. **74**(2): p. 807-17.

168. Strack, S., et al., *Differential inactivation of postsynaptic density-associated and soluble Ca2+/calmodulin-dependent protein kinase II by protein phosphatases 1 and 2A.* J Neurochem, 1997. **68**(5): p. 2119-28.

169. Yoshimura, Y., Y. Sogawa, and T. Yamauchi, *Protein phosphatase 1 is involved in the dissociation of Ca2+/calmodulin-dependent protein kinase II from postsynaptic densities.* FEBS Lett, 1999. **446**(2-3): p. 239-42.

170. Pi, H.J. and J.E. Lisman, *Coupled phosphatase and kinase switches produce the tristability required for long-term potentiation and long-term depression.* J Neurosci, 2008. **28**(49): p. 13132-8.

171. Mayford, M., et al., *The 3'-untranslated region of CaMKII alpha is a cis-acting signal for the localization and translation of mRNA in dendrites.* Proc Natl Acad Sci U S A, 1996. **93**(23): p. 13250-5.

172. Miller, S., et al., *Disruption of dendritic translation of CaMKIIalpha impairs stabilization of synaptic plasticity and memory consolidation.* Neuron, 2002. **36**(3): p. 507-19.

173. Rook, M.S., M. Lu, and K.S. Kosik, *CaMKIIalpha 3' untranslated region-directed mRNA translocation in living neurons: visualization by GFP linkage.* J Neurosci, 2000. **20**(17): p. 6385-93.

174. Giovannini, M.G., et al., *Mitogen-activated protein kinase regulates early phosphorylation and delayed expression of Ca2+/calmodulin-dependent protein kinase II in long-term potentiation.* J Neurosci, 2001. **21**(18): p. 7053-62.

175. Ouyang, Y., et al., *Tetanic stimulation leads to increased accumulation of Ca(2+)/calmodulin-dependent protein kinase II via dendritic protein synthesis in hippocampal neurons.* J Neurosci, 1999. **19**(18): p. 7823-33.

176. Wang, X., et al., *The phosphorylation of eukaryotic initiation factor eIF4E in response to phorbol esters, cell stresses, and cytokines is mediated by distinct MAP kinase pathways.* J Biol Chem, 1998. **273**(16): p. 9373-7.

177. Bliss, T.V.P. and T. Lomo, *Long-lasting potentiation of synaptic transmission in the dentate area of the anaesthetized rabbit following stimulation of the perforant path.* J Physiol, 1973. **232**(2): p. 331-356.

178. Wang, X.F. and N.W. Daw, *Long term potentiation varies with layer in rat visual cortex.* Brain Research, 2003. **989**(1): p. 26.

179. Regehr, W.G. and D.W. Tank, *Postsynaptic NMDA receptor-mediated calcium accumulation in hippocampal CA1 pyramidal cell dendrites.* Nature, 1990. **345**(6278): p. 807-10.

180. Nowak, L., et al., *Magnesium gates glutamate-activated channels in mouse central neurones.* Nature, 1984. **307**(5950): p. 462-5.

181. Malinow, R., *LTP: desperately seeking resolution.* Science, 1994. **266**(5188): p. 1195-6.

182. Nicoll, R.A., J.A. Kauer, and R.C. Malenka, *The current excitement in long-term potentiation.* Neuron, 1988. **1**(2): p. 97-103.

183. Harris, E.W., A.H. Ganong, and C.W. Cotman, *Long-term potentiation in the hippocampus involves activation of N-methyl-D-aspartate receptors.* Brain Res, 1984. **323**(1): p. 132-7.

184. Malenka, R.C., et al., *An essential role for postsynaptic calmodulin and protein kinase activity in long-term potentiation.* Nature, 1989. **340**(6234): p. 554-557.

185. Malinow, R., D.V. Madison, and R.W. Tsien, *Persistent protein kinase activity underlying long-term potentiation.* Nature, 1988. **335**(6193): p. 820-4.

186. Malinow, R., H. Schulman, and R.W. Tsien, *Inhibition of postsynaptic PKC or CaMKII blocks induction but not expression of LTP.* Science, 1989. **245**(4920): p. 862-866.

187. Ito, I., H. Hidaka, and H. Sugiyama, *Effects of KN-62, a specific inhibitor of calcium/calmodulin-dependent protein kinase II, on long-term potentiation in the rat hippocampus.* Neurosci Lett, 1991. **121**(1-2): p. 119-21.

188. Silva AJ, S.C., Tonegawa S, Wang Y., *Deficient hippocampal long-term potentiation in alpha-calcium-calmodulin kinase II mutant mice.* Science, 1992. **257**(5067): p. 201-6.

189. Hinds, H.L., S. Tonegawa, and R. Malinow, *CA1 long-term potentiation is diminished but present in hippocampal slices from alpha-CaMKII mutant mice.* Learn Mem, 1998. **5**(4-5): p. 344-54.

190. Giese, K.P., et al., *Autophosphorylation at Thr286 of the [alpha]-calcium-calmodulin kinase II in LTP and learning.* Science, 1998. **279**: p. 870-873.

191. Otmakhova, N.A., et al., *Inhibition of the cAMP pathway decreases early long-term potentiation at CA1 hippocampal synapses.* J Neurosci, 2000. **20**(12): p. 4446-51.

192. Kleschevnikov, A.M. and A. Routtenberg, *PKC activation rescues LTP from NMDA receptor blockade.* Hippocampus, 2001. **11**(2): p. 168-75.

193. Lledo, P.M., et al., *Calcium/calmodulin-dependent kinase II and long-term potentiation enhance synaptic transmission by the same mechanism.* Proc Natl Acad Sci U S A, 1995. **92**(24): p. 11175-9.

194. Pettit, D.L., S. Perlman, and R. Malinow, *Potentiated transmission and prevention of further LTP by increased CaMKII activity in postsynaptic hippocampal slice neurons.* Science, 1994. **266**(5192): p. 1881-1885.

195. Benke, T.A., et al., *Modulation of AMPA receptor unitary conductance by synaptic activity.* Nature, 1998. **393**(6687): p. 793-7.

196. Barria, A., V. Derkach, and T. Soderling, *Identification of the Ca2+/calmodulin-dependent protein kinase II regulatory phosphorylation site in the alpha-amino-3-hydroxyl-5-methyl-4-isoxazole-propionate-type glutamate receptor.* J Biol Chem, 1997. **272**(52): p. 32727-30.

197. Derkach, V., A. Barria, and T.R. Soderling, *Ca2+/calmodulin-kinase II enhances channel conductance of alpha-amino-3-hydroxy-5-methyl-4-isoxazolepropionate type glutamate receptors.* Proc Natl Acad Sci U S A, 1999. **96**(6): p. 3269-74.

198. Lee, H.K., et al., *Regulation of distinct AMPA receptor phosphorylation sites during bidirectional synaptic plasticity.* Nature, 2000. **405**(6789): p. 955-9.

199. Shi, S.H., et al., *Rapid spine delivery and redistribution of AMPA receptors after synaptic NMDA receptor activation.* Science, 1999. **284**(5421): p. 1811-6.

200. Hayashi, Y., et al., *Driving AMPA receptors into synapses by LTP and CaMKII: requirement for GluR1 and PDZ domain interaction.* Science, 2000. **287**(5461): p. 2262-7.

201. Poncer, J.C., J.A. Esteban, and R. Malinow, *Multiple Mechanisms for the Potentiation of AMPA Receptor-Mediated Transmission by alpha - Ca2+/Calmodulin-Dependent Protein Kinase II.* J. Neurosci., 2002. **22**(11): p. 4406-4411.

202. Hayashi, Y., et al., *Driving AMPA Receptors into Synapses by LTP and CaMKII: Requirement for GluR1 and PDZ Domain Interaction.* Science, 2000. **287**(5461): p. 2262-2267.

203. Lisman, J.E. and A.M. Zhabotinsky, *A model of synaptic memory: a CaMKII/PP1 switch that potentiates transmission by organizing an AMPA receptor anchoring assembly.* Neuron, 2001. **31**(2): p. 191-201.

204. Lee, H.-K., et al., *Regulation of distinct AMPA receptor phosphorylation sites during bidirectional synaptic plasticity.* Nature, 2000. **405**(6789): p. 955-959.

205. Feng, T.P., *The involvement of PKC and multifunctional CaM kinase II of the postsynaptic neuron in induction and maintenance of long-term potentiation.* Prog Brain Res, 1995. **105**: p. 55-63.

206. Stevens, C.F., S. Tonegawa, and Y. Wang, *The role of calcium-calmodulin kinase II in three forms of synaptic plasticity.* Current Biology, 1994. **4**(8): p. 687-693.

207. Mayford, M., et al., *CaMKII regulates the frequency-response function of hippocampal synapses for the production of both LTD and LTP.* Cell, 1995. **81**(6): p. 891-904.

208. Thiagarajan, T.C., E.S. Piedras-Renteria, and R.W. Tsien, *alpha- and betaCaMKII. Inverse regulation by neuronal activity and opposing effects on synaptic strength.* Neuron, 2002. **36**(6): p. 1103-14.

209. Brocke, L., et al., *Functional Implications of the Subunit Composition of Neuronal CaM Kinase II.* J. Biol. Chem., 1999. **274**(32): p. 22713-22722.

210. Takao, K., et al., *Visualization of Synaptic Ca2+ /Calmodulin-Dependent Protein Kinase II Activity in Living Neurons.* J. Neurosci., 2005. **25**(12): p. 3107-3112.

211. Stryer, L., *Fluorescence Energy Transfer as a Spectroscopic Ruler.* Annual Review of Biochemistry, 1978. **47**(1): p. 819-846.

212. Yasuda, R., *Imaging spatiotemporal dynamics of neuronal signaling using fluorescence resonance energy transfer and fluorescence lifetime imaging microscopy.* Current Opinion in Neurobiology, 2006. **16**(5): p. 551-561.

213. Lee, S.-J.R., et al., *Activation of CaMKII in single dendritic spines during long-term potentiation.* Nature, 2009. **458**(7236): p. 299.

CHAPTER 2 – *In vivo* detection of CaMKIIα activity in ferret visual cortex

2.1. Abstract

OD plasticity is a well studied model for experience-dependent cortical plasticity which is believed to be the neural correlate of memory and learning processes in the brain. The synaptic mechanisms underlying this form of plasticity are not well understood. It is generally agreed that Hebbian mechanisms such as homosynaptic LTP) and LTD play an important role. However, recent studies show that homeostatic regulations are also involved in OD plasticity. Here we further investigate the involvement of these two mechanisms at a single spine level by using two-photon imaging of Camui, a CaMKIIα activity reporter and intrinsic signal optical imaging in ferrets *in vivo*. We found that after only 4 hrs of MD, the overall CaMKIIα activity in spines and the adjacent dendritic regions of neurons in the deprived eye domain increases significantly. This increase is also seen in the binocular eye domain. In the open eye domain, however, this overall increase in CaMKIIα activity is absent. These observations are specific to MD as control experiments did not show such changes. Our results lend support to the model that both Hebbian, as well as homeostatic compensatory mechanism can subserve OD plasticity.

2.2. Introduction

OD plasticity has been the paradigmatic model for studying the role of sensory experience in shaping cortical neural circuits. Visual manipulation by MD induces a dramatic shift of cortical responsiveness in favor of the open eye [1-7]. The underlying synaptic mechanisms for OD plasticity have been intensively studied. An emerging model was put forth by Frenkel and Bear after their observations that there are two temporally distinctive phases in MD induced OD plasticity [5]. First, the deprived eye response depresses. Second, a delayed open eye response potentiates after longer MD. After integrating the theoretical framework of BCM theory [8-10] and other supporting evidence for the existence of a modification threshold [11], they propose that the delay is necessary for lowering the modification threshold to provide a permissive condition for the open eye potentiation. There is now a wealth of data to suggest that MD induces LTD in the deprived cortex in the deprived cortex [6, 12] and there is emerging evidence for the idea that open eye potentiation is mediated by NMDA receptor dependent LTP [13, 14].

In addition to Hebbian mechanisms such LTP and LTD, homeostatic regulation has been discovered to play a critical role in OD plasticity [15]. Homeostatic plasticity is a mechanism to prevent neural circuits from becoming hyper- or hypoactive when challenged by large alterations in input strength. Desai et al. demonstrated that 2 days of MD by TTX injection increases the mEPSC amplitude of pyramidal neurons in the deprived hemisphere *in vivo*. This scaling up of excitatory synaptic strength could explain the potentiation of the non-deprived eye responses after MD. A recent study in mouse visual cortex using two-photon calcium imaging offered important insights into the

interplay of Hebbian and homeostatic mechanisms in OD plasticity [16]. Their results showed that MD-induced response shifts in layer II/III depends on the relative amount of visual input a neuron receives from each eye. In neurons receiving both open-eye and deprived-eye input, deprived-eye responses were reduced and those of the open eye increased. However, the deprived-eye responses of neurons receiving predominantly the deprived-eye inputs were surprisingly enhanced after a few days of MD. They concluded that the direction of shift of the deprived-eye responses in each cell depends on the amount of open-eye input and that homeostatic mechanisms can directly regulate neuronal responsiveness during MD. This eye-specific input dependent response modification after MD calls for a close investigation of plasticity at the level of a single synapse plasticity.

We reason that for alterations in neuronal responsiveness to be detected after days of MD at somatic level, rapid plasticity processes at the individual synapses that initiate these changes must take place earlier, especially in layer II/III where fast plasticity processes reside [2]. CaMKIIα, a major component of the postsynaptic density, is well suited for serving as a marker for synaptic strength [17, 18]. Activation of CaMKII is required for LTP induction as its inhibitor blocks LTP [19-22]. Constitutively active CaMKII increases synaptic transmission by inserting AMPARs into the synapses and prevents further LTP, indicative of a shared mechanism between activation of CaMKII and LTP induction [23-26]. CaMKII is also required for OD plasticity [27]. Moreover, the unique activation by autophosphorylation at Thrs286 and inactivation mechanisms of CaMKII have made it a candidate molecular switch for memory [18, 28, 29]. Thus, the goal of the current study was to examine, at a single spine level, the alterations in

postsynaptic strength of cortical neurons in layer II/III after 4 hrs of MD in ferret visual cortex, a model system for studies of experience-dependent plasticity [30-32].

2.3. Materials and Methods

2.3.1. Construction of the CaMKII activity reporter (Camui) and *in vitro* characterization

Construction of monomeric Camui (mCamui) and controls

The prototypic Camui construct is described in a previous study [33]. Camui is a FRET construct that allows the detection of CaMKIIα activity by measuring the CFP/YFP ratio. An increase in CFP/YFP ratio indicates an increase in CaMKIIα activity and vice versa. To avoid non-specific protein aggregation, single mutation was introduced at A206K (A=alanine, K=lysine) in CFP and YFP moieties to monomerize them [34, 35] using Quikchange site-directed mutagenesis (Stratagene). Furthermore, to improve the brightness of mCamui, CFP and YFP were replaced with brighter variants, Cerulean [36] and Ypet [37], respectively, and monomerized in the same manner. An mCamui-T305D/T306D (T=threonine, D=aspartic acid) mutant was also generated according to the same protocol followed by replacement of CFP and YFP by mYpet-mCerulean via recombination. The T305D/T306D mutation renders CaMKII inactive to Ca^{2+}/calmodulin.

Generation of herpes simplex virus

All of the above constructs were subcloned into the herpes simplex virus (HSV) type I amplicon pHSVPrpUC and packaged as described [38]. Briefly, the resultant recombinant amplicon plasmid is transfected into 2-2 cells using Lipofectamine 2000

(Invitrogen). After 24-30 hrs, when 95% of the cells show cytopathic effects, cells are superinfected with a replication-incompetent helper virus (the IE2 deletion mutant 5dl1.2, derived from the KOS strain). The virus from this initial transfection/infection is then passaged three times in 2-2 cells to increase both the vector to helper ratio and the total amount of virus. The virus is then purified on a sucrose gradient (10%, 30% and 60% sucrose) to separate the virus from the cytotoxic elements in crude cell lysates. The virus that is harvested at the interface of 30% and 60% sucrose is then concentrated by ultracentrifugation and resuspended in 10% sucrose. The titer of the virus ranges from 0.8 – 5 $x10^7$ infectious units/ml, depending on the batch.

Characterization of mCamui FRET in infected HEK239T cell lysate

After infection by HSV-mCamuiα virus for ~24 hrs, HEK239T cells were collected by centrifugation in PBS at 4°C for 1 min at 16000 x g. The resultant cell pellet was homogenized in a buffer containing 40 mM HEPES-Na (pH 8.0), 5 mM magnesium acetate, 0.1 mM EGTA 0.01% Tween-20, and protease inhibitor cocktail (1mM phenymethylsulfonyl fluoride; 260 μM N-α-p-tosyl-L-arginine methyl ester hydrochloride; 10 mM benzamidine) [33]. The fluorescence profile was measured using a spectrofluorometer (Shimazu RF-5301-PC) with 120 μl of the cleared supernatant (sup) after centrifugation at 16000 x g for 1 min. The excitation wavelength was 433 nm. The spectrum was first obtained with 120 μl of sup. The CaMKII reaction was started at room temperature by adding a 20 μl mixture of $CaCl_2$, ATP, and bovine calmodulin (Calbiochem) (final concentration: 1 mM, 50 μM and 1 μM respectively). Ca^{2+} was chelated after 3 min by adding 1 μl of 200 mM EGTA (final concentration was 1.4 mM). Fluorescence intensity was adjusted according to volume changes. FRET is calculated as

the ratio of peak CFP/YFP emission intensity. CFP peaks at 477 nm and YFP peaks at 528 nm. An increase in CFP/YFP indicated an increase in CaMKII activity and vice versa.

2.3.2. *In vivo* imaging of CaMKII activity

HSV-mCamui injection and window implantation

All procedures were conducted under sterile conditions according to the protocol approved by the Department of Comparative Medicine at Massachusetts Institute of Technology and IACUC.

Ferrets at the critical period for OD plasticity (P42-50) were premedicated with atropine (to decrease bronchial secretions, 0.04 mg/kg, intramuscular injection (im)), methylprednisolone sodium succinate (MPSS, to prevent cortical swelling, 60 mg/kg, im) and buprenorphine hydrochloride (Buprenex, analgesic, 0.1 mg/kg, subcutaneous injection (sc)) 20 minutes prior to induction of anesthesia. Anesthesia was induced in a chamber containing 5% isoflurane in O_2. The endotracheal tube for anesthesia maintenance was coated in lidocaine gel (local anesthetic and lubricant) before insertion, and anesthesia was maintained with isoflurane (1.5-2.0%) in O_2. The depth of anesthesia was continuously monitored and periodically adjusted based on variability in heart rate (HRS), saturation of peripheral oxygen (spO2), endo-tidal CO_2 concentration, respiration rate (RR), and paw-pinch reflex. If the animal showed any response to aversive stimuli, or if the HRS or respiration rate deviated by more than 10% above baseline, anesthetic concentration was increased. Body temperature was maintained at 37 ºC using a thermostatic blanket with a rectal probe.

The inner ears of the anesthetized animal were lubricated with topical lidocaine gel application and the head affixed with ear bars in a stereotaxic frame. A small

craniotomy was performed and the dura removed. A micropipette containing virus was lowered to 500 µm and 250 µm below the cortical surface and 0.5-0.75 µl of viral solution was injected at each depth using an infusion pump at a rate of 5µl/minute. The micropipette was removed, the cortex covered with 0.005 inch thick artificial dura (Specialty Manufacturing Inc.) and then with a layer of sterile agarose (1.5% in PBS containing ampicillin (antibiotics, 100 µg/ml)) (Figure 1A). The craniotomy was then sealed with a glass window, and a head plate was affixed to the skull with dental cement for reproducible head positioning during *in vivo* chronic imaging sessions. The wound was sutured and the edges of the skin sealed with dental cement. For analgesic, Buprenex (0.1 mg/kg, sc) and MPSS (30mg/kg, im) were administered 45 minutes before anesthetic gases were discontinued. Buprenex (0.1 mg/kg, sc) and MPSS (15 mg/kg at 12 hrs, 7.5 mg/kg at 24 hrs, 3.75 mg/kg at 36 hrs, im) were injected additionally 12, 24, and 36 hrs after the surgery and thereafter if necessary. Enrofloxacin (Baytril, 5 mg/kg, im) was given prophylactically once per day for 3-5 days, after which it was discontinued if no signs of infection existed.

Chronic in vivo two-photon microscopy

Ferrets were premedicated, anesthetized and intubated as described. The depth of anesthesia was continuously monitored by observing variability in HRS, RR, $ETCO_2$ and paw-pinch reflex and increased if the animal showed any response to aversive stimuli, or if HRS deviated more than 10% from the baseline. Once anesthetized, the animal's head was fixed to a stereotaxic frame via the head plate and positioned under the objective lens of a 2-photon microscope. FRET was visualized at an excitation wavelength of 800 nm. Emission was separated into two channels by a 505 nm long-pass dichroic mirror and detected by two separate PMTs each equipped with band-pass filters: 480/30 nm (CFP

emission), and 535/26 nm (YFP emission). The output from the two PMTs was fed into Olympus Fluoview software and recorded (Figure 1B). Our emission filter combination allows approximately 30% leak of CFP signal into the YFP channel. Since this bleed-through is purely optical and always constant irrespective of FRET condition, it was not compensated for. The craniotomy was first identified using a 20X lens (XL UMPlanFI/0.95, Olympus), after which images of the superficial projections of neurons and surrounding neuropil containing the blood vessel pattern (seen as areas devoid of label within the injection site) are collected. Two-photon images of spines 10-150 µm below the pial surface were then collected using the same 20X or 40X (NA 0.9, Olympus) lens, under digital zoom (up to 10X. All images were acquired as z stacks with individual z-planes collected at 1 -10 µm apart. Following the first 2-photon imaging session (basal time point), while anesthesia was maintained, the ferret's eyelid was sutured closed (Ethicon sutures, 7.0 prolene), and the sutured eyelid coated with topical Vetropolycin ophthalmic ointment (a mixture of bacitracin, neomycin, and polymyxin B) to prevent infection. In most cases, the eye contralateral to the imaged hemisphere was sutured, with the exception of one experiment in which the ipsilateral eye was sutured. For comparison, ODI values from this experiment were adjusted and scaled similarly to those values obtained when closing the contralateral eye. Results were similar regardless of which eye was sutured and were therefore pooled together in the final analysis. The animal was then allowed to recover and returned to the cage for access to food and water. The ferret was then observed for the next ~4 hrs to ensure that the animal received adequate monocular vision through the open eye and did not fall asleep, although two to three 15 min naps were allowed. Following ~4 hrs of monocular vision the above 2-

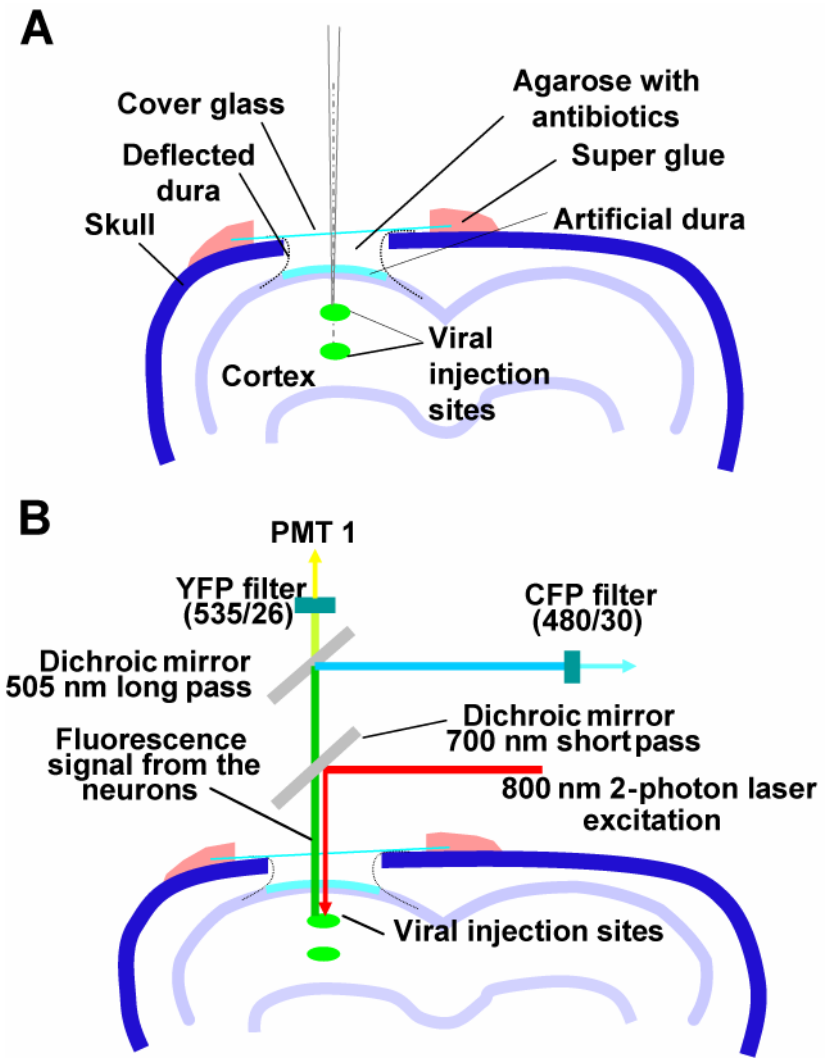

Figure 1. Schematic diagrams showing (A) the cranial window preparation and viral injection and (B) the excitation and emission light paths during two-photon microscopic imaging. Virus was injected at two depths (250 µm and 500 µm green ovals) and typically resulted in expression in layers I, II/III and IV although spines and dendrites were not imaged at this depth.

photon imaging procedure was repeated (4 hrs MD time point). Blood vessel patterns from the basal time point were used to align the low power images, followed by alignment of high power images using previously recorded x,y coordinates, allowing for chronic imaging of the same spines between time points. Following 2-photon imaging the eyelid was unsutured, and trimmed eyelid margins were covered with topical Vetropolycin ophthalmic ointment to prevent infection. The animal was then allowed to recover and returned to its cage.

Analysis of two-photon microscopic images

Image analysis was performed using Metamorph (Molecular Devices). Images were separated into two channels and regions of interest were manually placed on the image of the CFP channel. Each spine region and the adjacent dendritic region pair shared a common nearby background region, used for background subtraction. Fluorescence intensity of these regions was measured and recorded from both the CFP and YFP channel images. The best focal plane, with the highest fluorescence intensity (background subtracted) for the individual spine and dendritic regions, were then determined according to the CFP channel image and used for calculating the CFP/YFP ratio for each region. This CFP/YFP (FRET) provides a quantitative measurement for assessing CaMKII activity, and changes therein, with an increase in CFP/YFP indicating an increase in CaMKII activity. For calculation of spine width, we followed the methods described in a previous study [39]. Briefly, a line was drawn across the widest width of a spine, perpendicular to the spine neck at its predetermined best focal plane, determined using the color combined image of the two channels. Full width, at half maximum (FWHM, μm), of the Gaussian fitted fluorescence intensity profile of the line was obtained and used as the spine width.

2.3.3. Intrinsic signal optical imaging and determination of OD

Intrinsic signal optical imaging

12-24 hrs after the second two-photon imaging session, optical imaging of intrinsic signals was performed. The animal was anesthetized and fixed to a stereotaxic frame as described above. Pupils were dilated with atropine sulfate (0.5%) and the nictitating membranes retracted with phenylephrine hydrochloride (2%) eye drops. The cortical surface was illuminated with a tungsten halogen light source, and a slow-scan video camera equipped with a tandem macro-lens arrangement was used to acquire images of intrinsic signals (Optical Imaging, Imager 3001). In order to obtain a reference image of the surface blood vessels, the cortical surface was illuminated with a green filter (546 /15 nm bandpass). The focal plane was then adjusted to ~400 um below the cortical surface and a red filter (630/30 nm bandpass) used for the acquisition of intrinsic signal maps. To obtain OD maps, drifting gratings (4 orientations, spatial frequency of 0.125 cycles/deg, temporal frequency of 1 Hz) were presented to each eye individually. The data acquisition started 3 s before and ended 4 s after the drifting gratings, thus 7 frames (1 frame/s) were obtained for each single condition map. An eye shutter was used to randomly interleave the stimulation of each eye.

Analysis of intrinsic signal optical imaging data

First frame analysis was performed on each single condition map. The last 4 frames (raw signal) were averaged and divided by the average of the first 3 frames (baseline), effectively reducing the slow background noise. Then, 4 single orientation maps from the stimulation of each eye were averaged to obtain a contralateral (C) and ipsilateral (I) eye response map. The contralateral eye map was subtracted from the

ipsilateral eye map to generate the OD map. OD index (ODI) was calculated by (C-I)/(C+I)*1000, both eye responses were from the red light reflectance.

Statistics

Initial data analysis was performed using Microsoft Excel and GraphPad software. Plots were made in GraphPad. Statistical differences in values after 4 hrs MD were calculated in comparison to their respective basal values with either Kolmogorov-Smirnov test (online software [40]) or a two-tailed, paired Student's t-test (Excel). Pearson's correlation coefficient was also calculated in Excel.

2.4. Results

2.4.1. Monomerization and improvement of Camui

When the original Camui was expressed in the ferret visual cortex using a herpes virus expression system, we found that it forms non-specific aggregates in the soma of the neurons, which was not obvious in our previous work using plasmid expression vector *in vitro*. This likely affects the detection of CaMKII activity (Figure 2). We considered that this may be caused by the tendency of GFP family proteins, including YFP and CFP, to dimerize at high concentrations [35]. This may be exaggerated in the Camui since it has two GFP moieties flanking CaMKII and CaMKII itself is oligomerized [33, 41]. Therefore, we introduced a point mutation (A206K, A=alanine, K=lysine) into the CFP and YFP moieties to disrupt the hydrophobic interaction at the interface between the two proteins [35]. This mutation causes no significant alterations in the spectral properties [35]. To test the feasibility, we first monomerized enhanced CFP (mECFP) (Clontech) and Venus (mVenus). The expression of this new monomeric

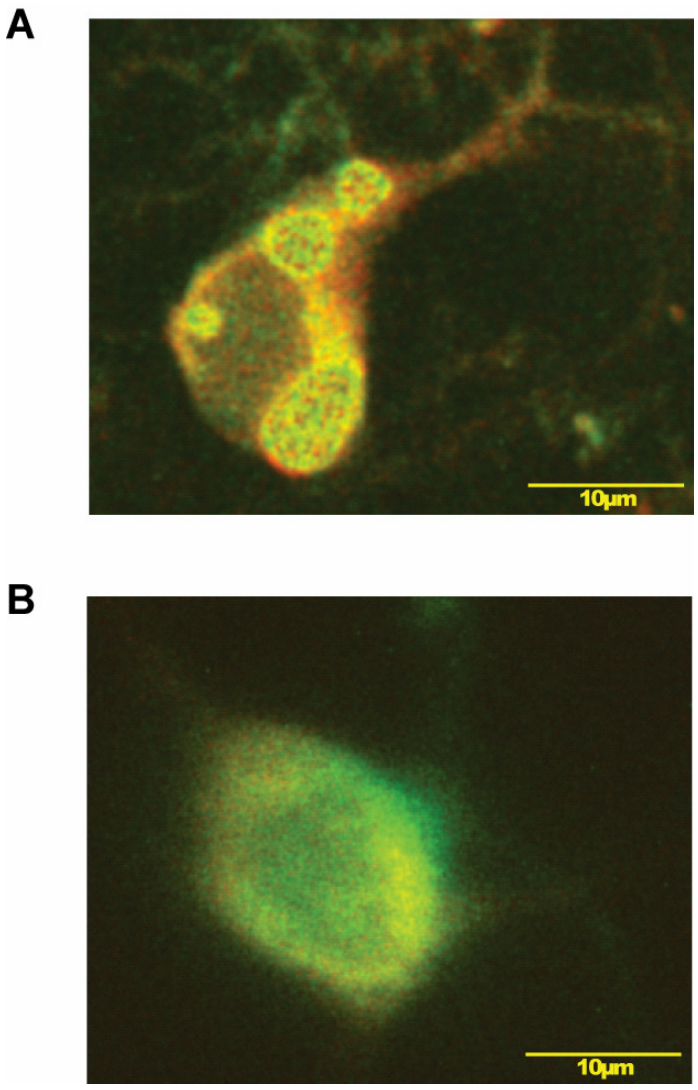

Figure 2. ***In vivo*** **image of a neuron soma expressing Camuiα (A) and monomerized Camuiα (B). A. Clear non-specific aggregates are seen in the soma. B. Point mutation, (A206K, A=alanine, K=lysine) of the CFP and YFP moieties of Camui resulted in diffuse expression. A and B are CFP and YFP color combined images.**

Camui (mCamui) showed no aggregates and was diffuse in neurons as shown in Figure 2.

Next, we wanted to improve the overall brightness and dynamic range of mCamui to enhance the signal to noise ratio of spine images. We tried a number of different fluorophore combinations including mVenus and mStrawberry or mOrange [42] and decided to replace the original Camui's CFP and YFP by their respective brighter variants monomeric Cerulean (mCerulean) [36] and Ypet (mYpet) [37]. HEK293T cells expressing the improved mCamui-mYpet/mCerulean have an overall brighter appearance than those infected by the original HSV mCamui (data not shown). The spectral analysis of the homogenate of cells expressing the two versions of mCamui revealed a similar emission spectrum (Figure 3). However, the improved mCamui-mYpet/mCerulean construct had higher basal FRET as evident from the higher YFP peak at 528 nm (Figure 3A). Upon Ca^{2+} stimulation, both mCamui constructs showed a decrease in the YFP peak and a corresponding increase in the CFP peak. This change in FRET, presented by change in peak CFP/YFP ratio (see Materials and Methods for peak wavelengths) is indicative of activation of CaMKIIα [33]. Ca^{2+} stimulation induced a higher FRET change in the mCamui-mYpet/mCerulean (from 1 to 2.61) than in the original mCamui (from 1 to 2.07) (Figure 3B). After chelating Ca^{2+} with EGTA, the CFP peak decreasedand the YFP peak increased, but they did not return to the basal level (Figure 3). This persistent activation is attributed to the autophosphorylation at T286, which is calcium independent, as previously shown by Takao et al. [33]. The improved mCamui had higher autonomous activity upon Ca^{2+} chelation by EGTA (Figure 3B). Thus, the mCamui-mYpet/mCerulean is better suited for *in vivo* imaging studies as it is brighter and has a better dynamic range than the original mCamui. In the following part of this

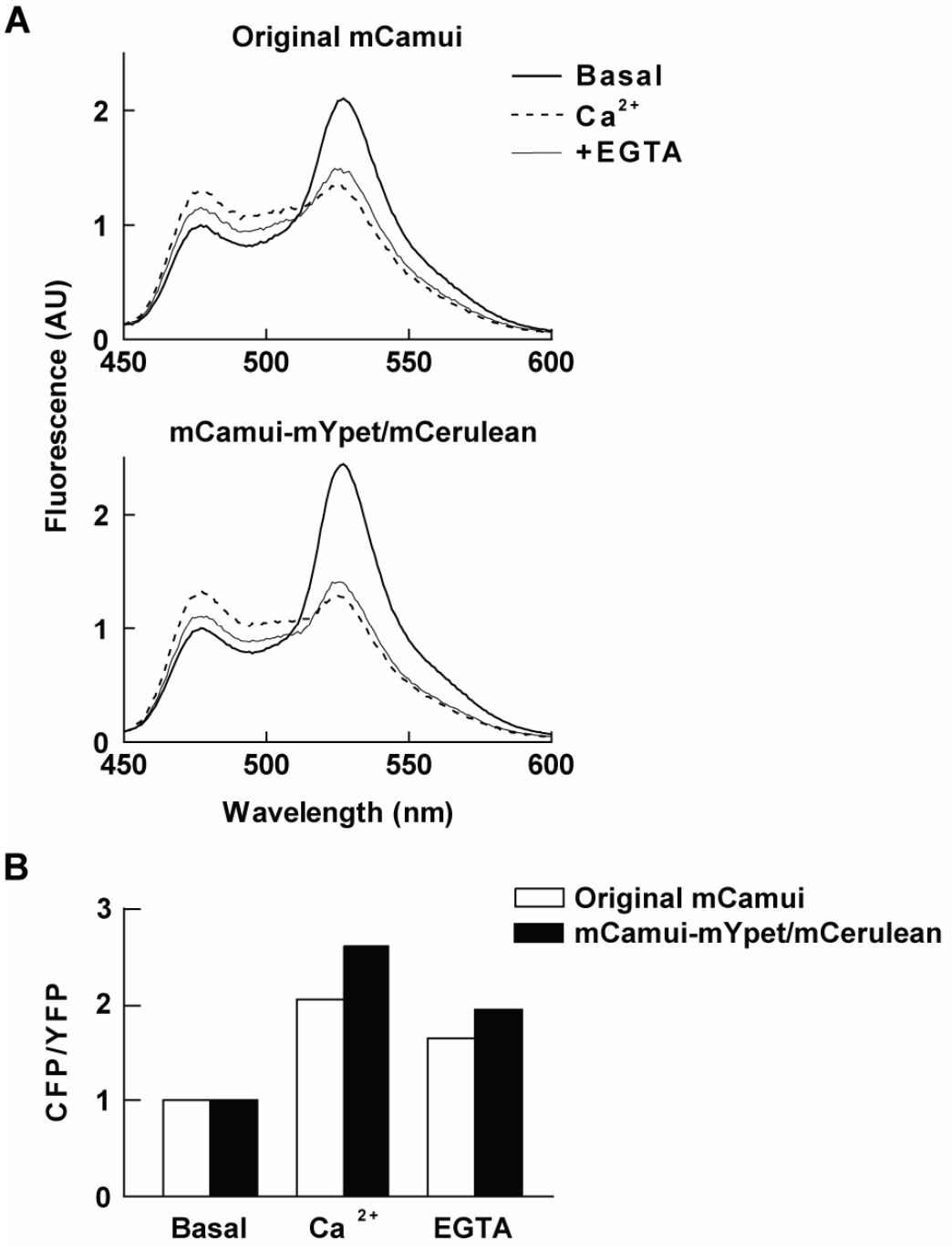

Figure 3. mCamui-mYpet/mCerulean had a similar emission spectrum to mCamui but better dynamic range upon stimulation. (A) Sample emission spectra of the original mCamui and mCamui with mYpet/mCerulean combination measured using HEK293T cell lysate expressing each construct before, 3 min after the addition of Ca2+, and 3 min after the addition of EGTA, at CFP specific excitation (433 nm). (B) Quantification of FRET changes in both versions of mCamui by calculating the peak CFP/YFP ratio from the emission spectra in (A).

study, we used mCamui-mYpet/mCerulean (Camui) unless otherwise noted.

2.4.2. Construction and characterization of mCamui controls

In light of variables, such as changes in cerebral blood flow and level of blood oxygenation, that might confound our *in vivo* imaging results, we prepared two controls for mCamui. First, mCamuiα-T305DT306D mutant that is deficient in binding to Ca^{2+}/calmodulin [43-46]. Lack of response to Ca^{2+} stimulation and EGTA chelation demonstrated that mCamuiα-T305D/T306D mutant is well suited as a negative control for mCamui activation (Figure 4B,D). Next, to control for the cortical scattering of fluorescence of different wavelengths, we constructed a direct fusion protein of mYpet and mCerulean. HSV infected HEK293T cell lysate was used to measure the emission spectrum of the fusion protein (Figure 4C). It has a slightly higher FRET than the mCamui at the basal level indicating the more efficient energy transfer. This improved energy transfer is attributed to the lack of CaMKIIα between the two fluorophores, which reduces the distance permissive for the transfer. Thus, this fusion protein shows constant FRET and serves as another negative control.

2.4.3. Imaging of CaMKII activity in specific eye-domain

In order to monitor activity of CaMKIIα associated with visual cortical plasticity during the critical period, we expressed Camui in the ferret (P42-50) visual cortex. The ferret was chosen because its entire visual cortex is binocular and it has OD columns. Moreover, ferrets have a relatively immature visual system at birth [32] and late peaking critical period (~ postnatal day 42, P42) compared with other species. This allows for handling of the animal, as the body size of a ferret at P42 reaches that of an adult rat.

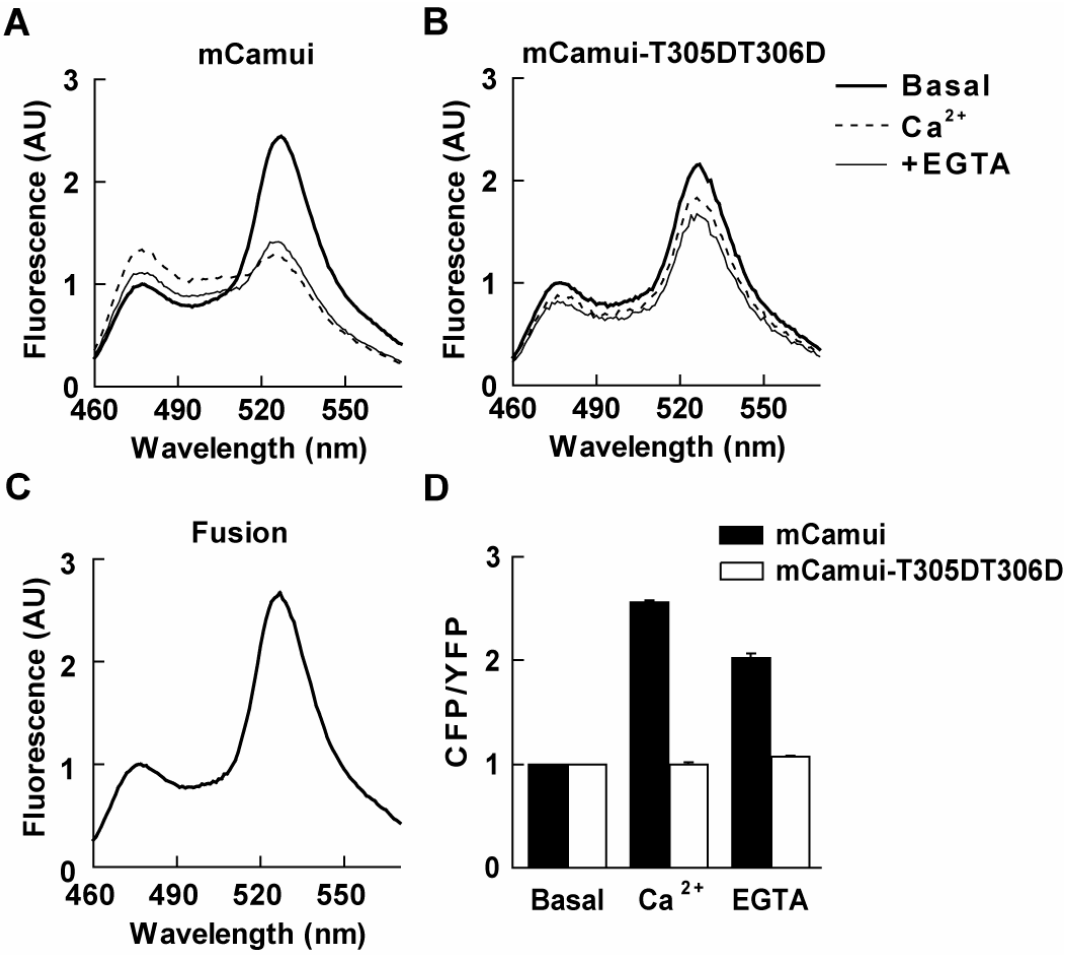

Figure 4. Control constructs for mCamui. (A-C) Sample emission spectra of mCamui (A), mCamui-T305DT306D (B), and mYpet-mCerulean fusion (C) under different conditions. Measurements were performed as in Figure 3. mCamui spectra (A, D) used here for comparison with the two controls are the same as those shown in Figure 3. (D) Quantification of FRET changes in mCamui and mCamui-T305DT306D. Calculation done as in Figure 3 (n=3 each). Error bars represent SEM.

Infected cortical neurons were repeatedly imaged through a cranial window. A zoomed out image of a part of the injection site obtained using *in vivo* two-photon laser scanning microscopy (Figure 5A) was aligned with the ocular dominance (OD) domains obtained using intrinsic signal optical imaging (Figure 5A) by comparing blood vessel patterns visible with both imaging techniques.

Numerous neuronal cell bodies diffusely expressing mCamui were clearly visible and the blood vessel pattern could be recognized as dark regions devoid of label (Figure 5A). The vast majority of the infected neurons were pyramidal cells with typical morphology (Figure 5A). Higher resolution two-photon microscopic images, at the level of dendritic spines were obtained in both the CFP and YFP channels and were located on the OD map to assign their respective OD index (Figure 5C). This method allowed us to examine the differential states of CaMKIIα activity in the designated OD domains before and after manipulation of visual input.

2.4.4. CFP/YFP ratio is stable over the course of imaging

First we tested the stability of the CFP/YFP ratio *in vivo*, over time, in the visual cortex of normal (receiving no MD) ferrets. We repeatedly imaged the soma of mCamui-mECFP/mVenus infected neurons (Figure 6). When comparing the CFP/YFP ratio at all time points to the initial time point (0 min), there was no statistically significant difference (paired t-test, $p>0.05$), indicating that the experimental design and imaging process itself did not affect the CFP/YFP ratio over time in normal ferrets.

2.4.5. Four hrs of MD induced changes in CaMKIIα activity

Next, we monitored the change in CaMKIIα activity associated with visual

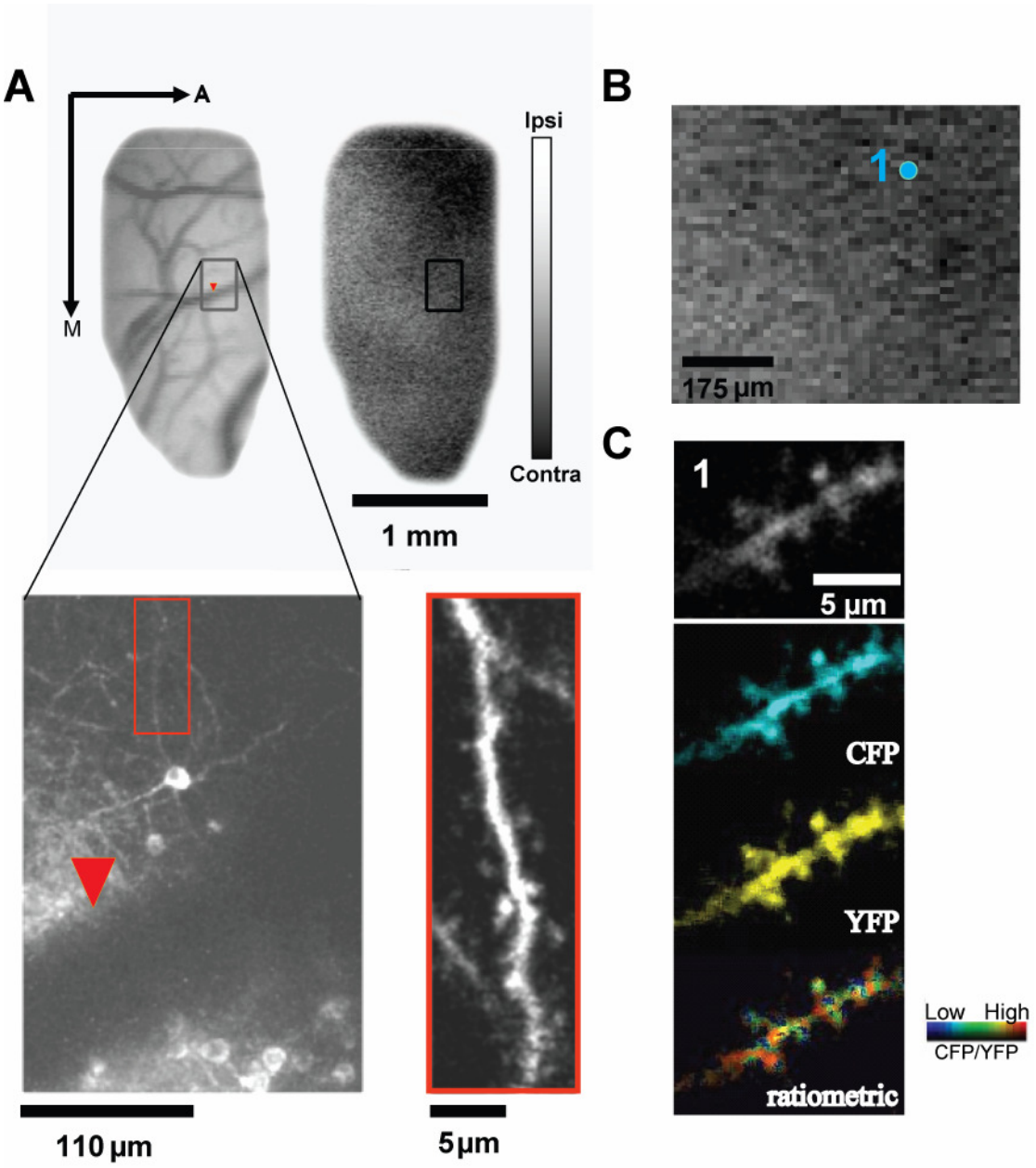

Figure 5. Alignment of the two-photon images with (OD) domains. (A) Blood vessel map and OD domains obtained using intrinsic signal optical imaging (upper panel, A: interior; M: Medial). Blood vessels (red arrow head) that are visible in both optical imaging and two-photon imaging are used to align the injection sites to the OD domains. Lower panel shows a portion of an injection site and a dendritic segment (10X digital zoom=200X), highlighted by the red box. Gray scale bar indicates the range of OD (white=ipsilateral eye dominated, black=contralateral eye dominated). (B) A portion of the OD map, blue dot indicating the location of dendritic segment shown in (C). (C) Channel separated images (CFP and YFP) of dendrite 1 (10X digital zoom=200X) are shown together with an intensity modulated display mode image (ratiometric) indicating the CFP/YFP ratio. Warmer hue represents higher CaMKII activity. All gray scale images were made from original color combine images of both channels.

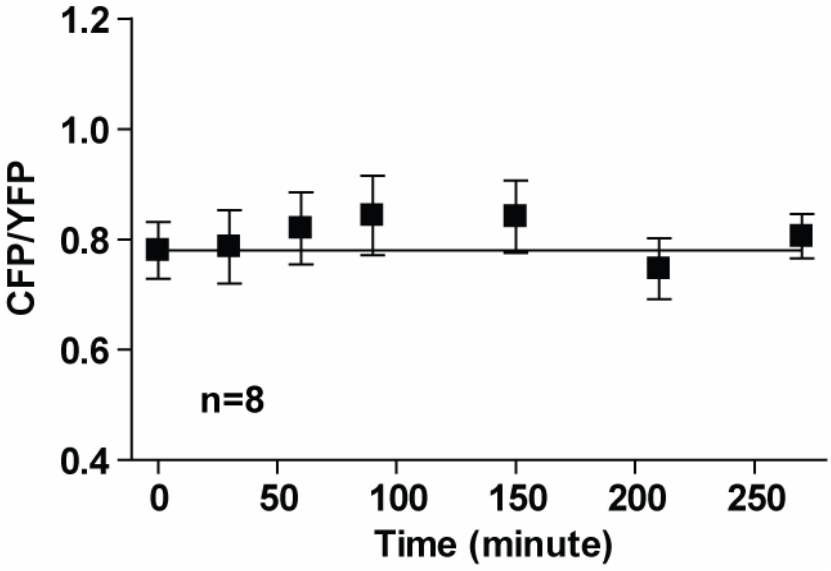

Figure 6. The average CFP/YFP ratio calculated from a population of neuronal cell bodies is stable when chronically imaged over hrs in visual cortex of normal ferrets (no MD performed). Paired Student's t-test, all time points compared to initial time point, $p > 0.05$. Error bars represent SEM

cortical plasticity, focusing on the early stage of synaptic plasticity at 4 hrs of MD for several reasons: 1) functional changes in cortical responsiveness are observed starting at approximately 4 hrs post MD [4, 47, 48]; 2) 6 hrs of MD is sufficient to initiate biochemical changes such as phosphorylation of AMPARs [6] and 3) CaMKII is activated following the induction of plasticity [49-52]. After acquiring the basal images of the dendritic shafts and spines, the animal's contralateral eyelid was sutured closed. It was then allowed to experience monocular vision for 4 hrs. During this period, we closely monitored the animal to ensure that it was awake and receiving visual input. Next, the same dendrites and spines were imaged again to assess the change in CaMKIIα activity. Intrinsic signal optical imaging was then performed to determine the ocular dominance profile of the same cortical region.

We found that CaMKIIα activity, indicated as the CFP/YFP ratio, showed a significant increase in both spines and the adjacent dendritic regions after 4 hrs of MD in the deprived eye domain, (Figure 7, basal versus 4 hrs MD, KS test, $p < 0.01$ for both cases). The change was not observed in neurons expressing mCamui-T305D/T306D mutant that cannot be activated by Ca^{2+}/calmodulin (Figure 8, KS test, $p > 0.05$) or those expressing mYpet-mCerulean direct fusion protein (Figure 9, KS test, $p > 0.05$). Therefore, the observed change in the CFP/YFP ratio seen with Camui was associated with CaMKIIα activation resulting from 4 hrs of MD.

In contrast, CaMKIIα activity did not show a change in either the spines or dendritic regions after 4 hrs of MD within the open eye domain (Figure 10, KS test, $p > 0.05$). In the binocular region, we observed an intermediate result; a smaller increase in CaMKIIα activity in dendritic regions after 4hrs of MD (Figure 11, KS test, $p < 0.01$).

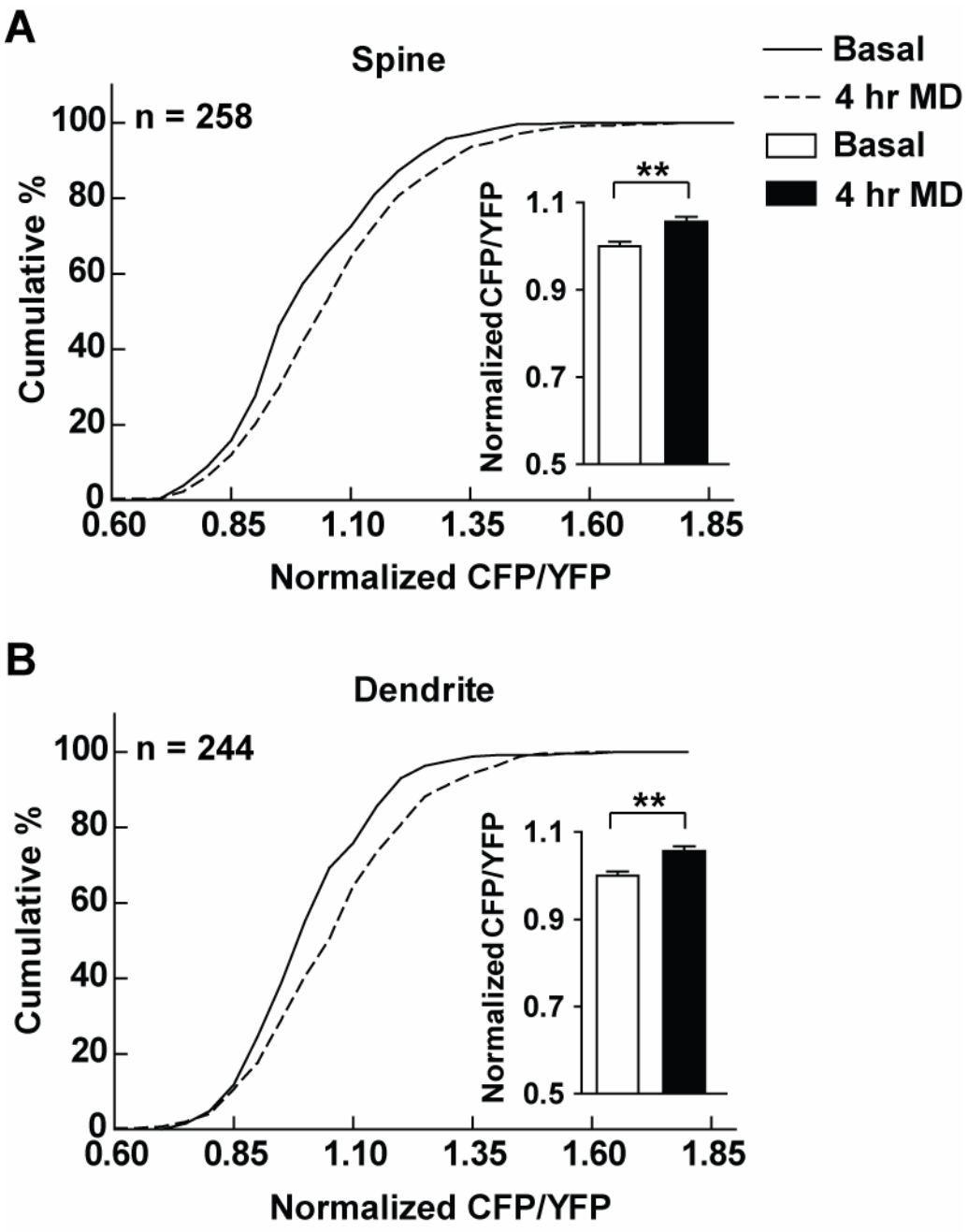

Figure 7. Increased CaMKIIα activity levels in deprived eye dominated regions after 4 hrs MD. (A) Camui CFP/YFP in individual spines normalized to the average CFP/YFP of all spines within the respective injection site before (basal) and after 4 hrs MD are represented as cumulative histograms or as group means presented in the inset. (B) Dendritic region data plotted as in (A). Error bars represent SEM. Data were from 4 ferrets. **p < 0.01 (paired, 2-tailed t-test).

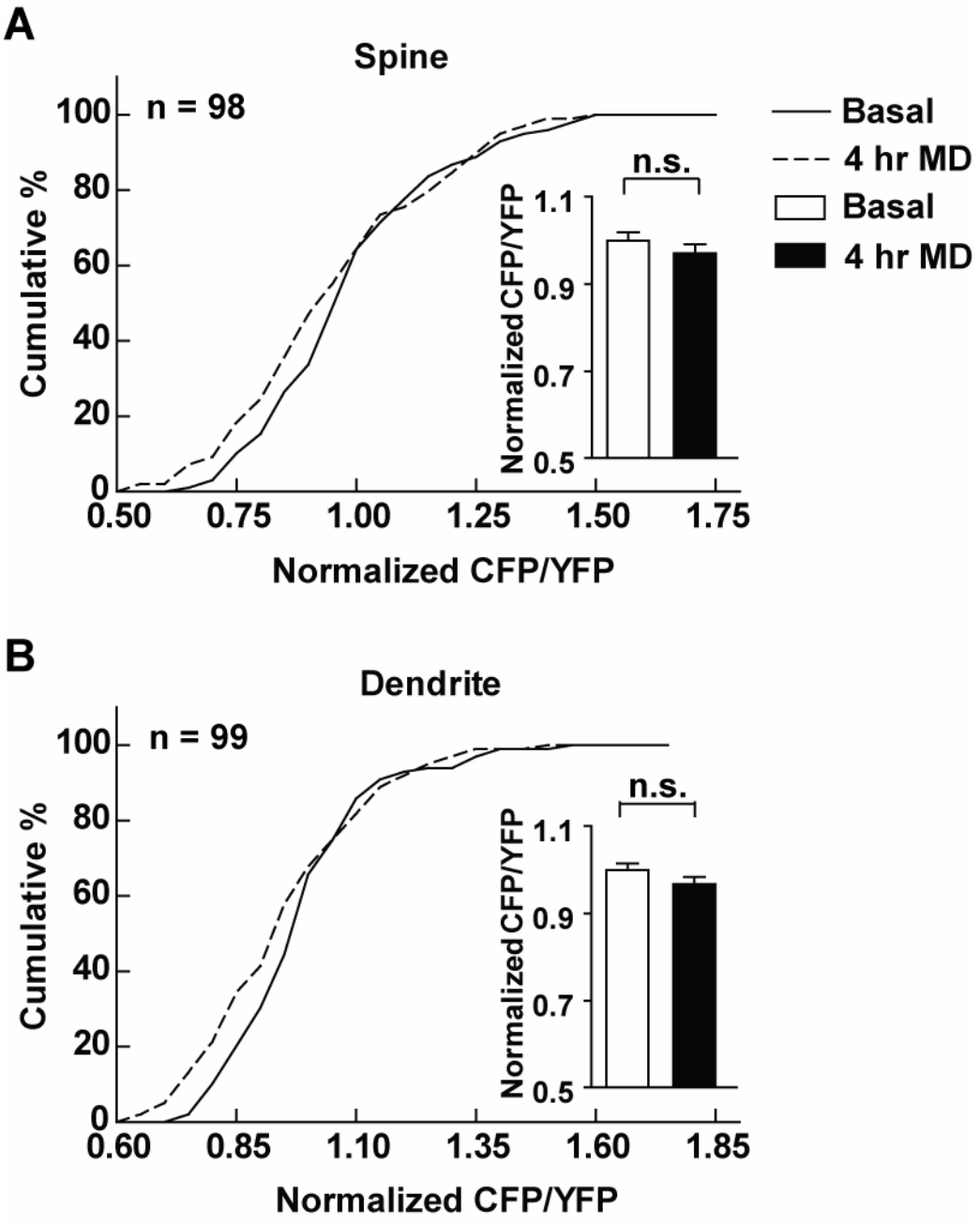

Figure 8. CaMKIIα-T305DT306D activity level did not change in deprived eye dominated regions after 4 hrs MD. (A) Camui-T305DT306D CFP/YFP in individual spines, normalized to the average CFP/YFP of all spines within the respective injection site before (basal) and after 4 hrs MD are represented as cumulative histograms or as group means presented in the inset. (B) Dendritic region data plotted as in (A). Error bars represent SEM. Data were from 2 ferrets. $p > 0.05$ (paired, 2-tailed t-test).

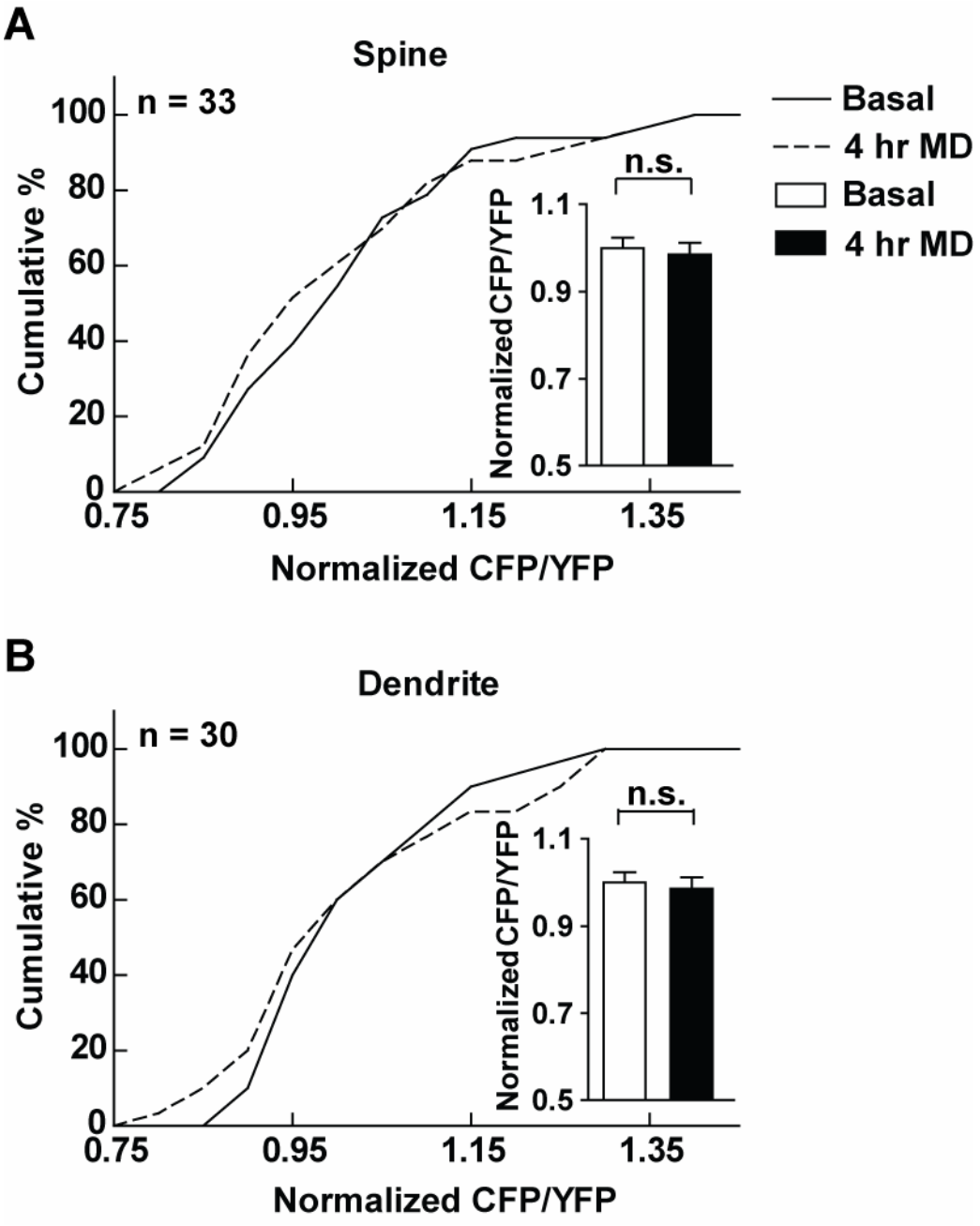

Figure 9. mYpet-mCerulean fusion protein FRET did not change in deprived eye dominated regions after 4 hrs MD. (A) mYpet-mCerulean fusion CFP/YFP in individual spines, normalized to the average CFP/YFP of all spines within the respective injection site before (basal) and after MD (4hrs MD) are represented as cumulative histograms or as group means presented in the inset. (B) Dendritic region data plotted as in (A). Error bars represent SEM. Data were from 2 ferrets. $p > 0.05$ (paired, 2-tailed t-test).

CaMKIIα in spines also showed a tendency to increase although the increase was not statistically significant (Figure 11A, KS test, p = 0.155).

To summarize these results, we plotted the OD index (ODI) versus the observed change in FRET (Figure 12). Overall, there was a statistically significant correlation between ODI and change in CFP/YFP ratio (Pearson's correlation coefficient (r) for spines: -0.70; dendritic regions' r = -0.30). In spines of the closed eye domain, there was an increase CFP/YFP ratio (Figure 12A), indicative of an increase in CaMKII activity while in the open eye domain, there was no change. The dendritic regions followed the same general tendency although the correlation is weaker than that seen for spines (Figure 12B).The binocular domain fell in between. Negative control constructs, Camui-T305D/T306D and mYpet-mCerulean fusion protein fell outside of this correlation, showing almost no change in CFP/YFP ratio, confirming the specificity of the observed change to Camui with MD.

2.4.6. Change in CaMKIIα at individual spine level

We next wondered if the observed activation of CaMKIIα took place in all synapses or not. Our FRET-based live imaging provides versatile information to this point because we can compare CaMKIIα activity before and after 4 hrs of MD of the same spine and dendritic region (Figure 13A). First, we examined the relationship between the spine size and the basal level of CaMKIIα activity (Figure 13B) and found smaller (or larger) spines would be more likely to have increased (or decreased) CaMKIIα activity after 4 hrs of MD. The correlation analysis showed a lack of such that there is no correlation between the two (r = 0.11). This indicates that while the bound amount of CaMKII in a spine is positively correlated with the spine size [53, 54],

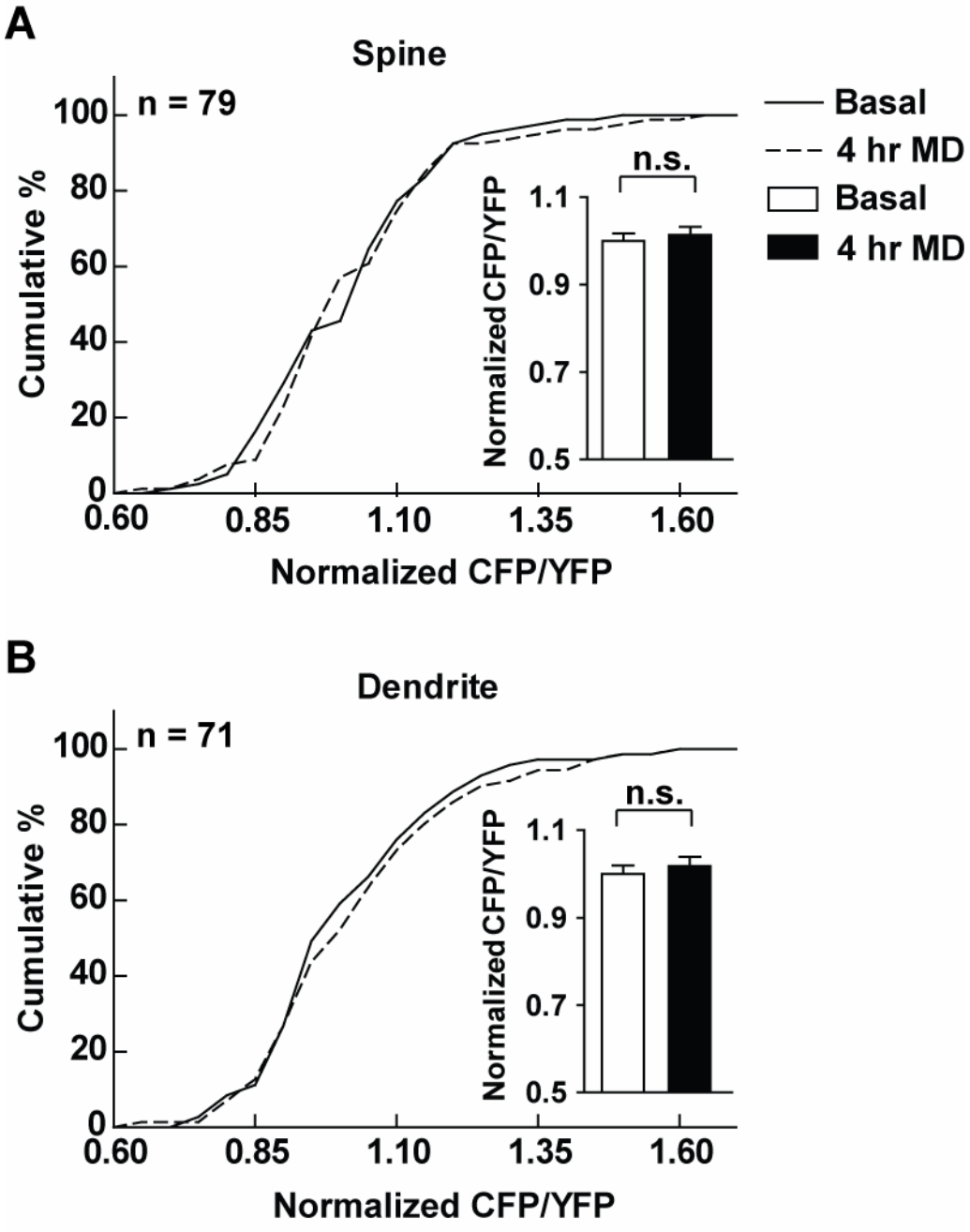

Figure 10. CaMKIIα activity level did not change in the open eye dominated regions after 4 hrs MD. (A) Camui CFP/YFP in individual spines, normalized to the average CFP/YFP of all spines within the respective injection site before (basal) and after 4 hrs MD are represented as cumulative histograms or as group means presented in the inset. (B) Dendritic region data plotted as in (A). Error bars represent SEM. Data were from 2 ferrets. $p > 0.05$ (paired, 2-tailed t-test).

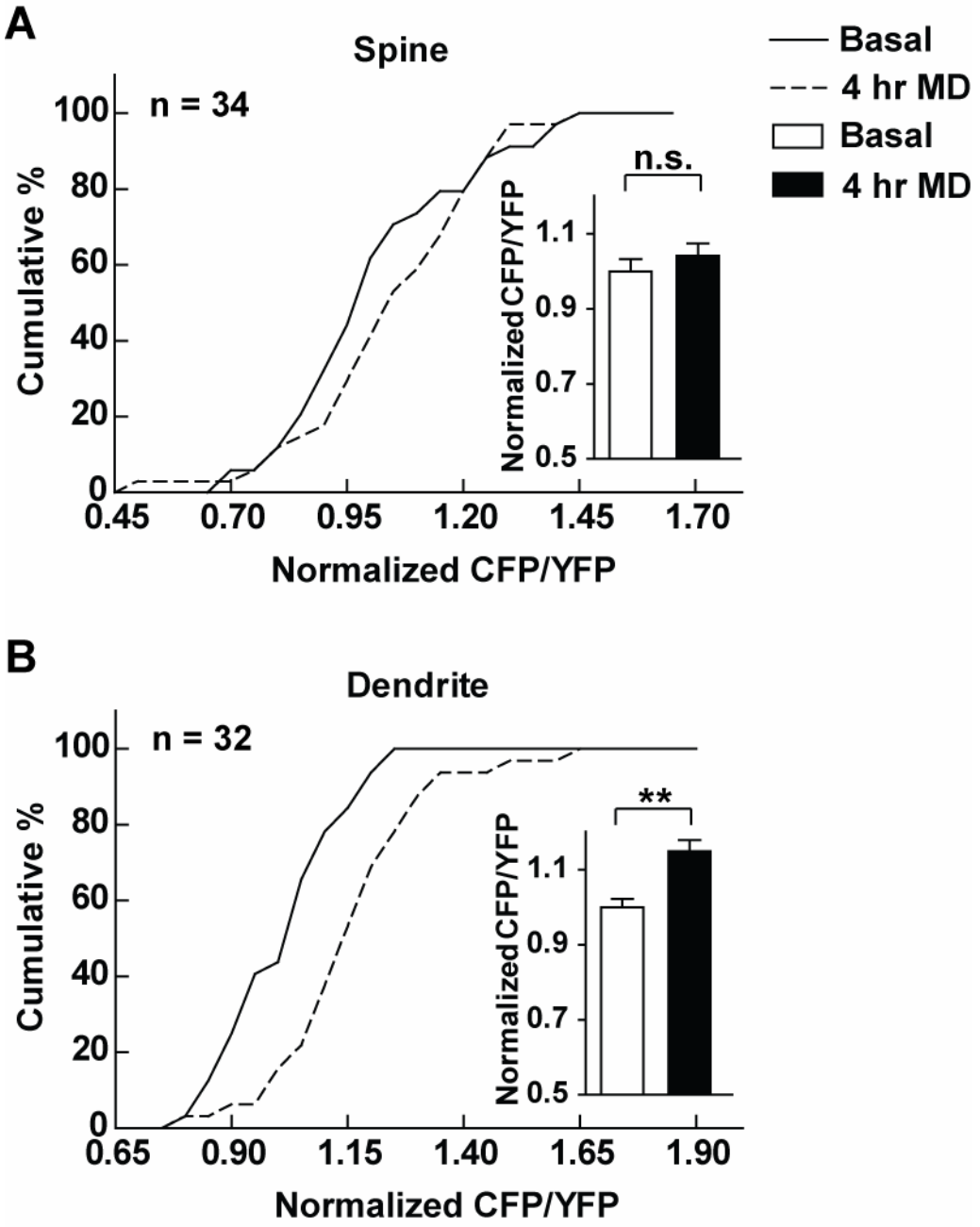

Figure 11. Increased CaMKIIα activity level in the binocular regions after 4 hrs MD. (A) Camui CFP/YFP in individual spines, normalized to the average CFP/YFP of all spines within the respective injection site before (basal) and after 4 hrs MD are represented as cumulative histograms or as group means presented in the inset. (B) Dendritic region data plotted as in (A). Error bars represent SEM. Data were from 2 ferrets. $p > 0.05$, $^{**}p < 0.01$ (paired, 2-tailed t-test).

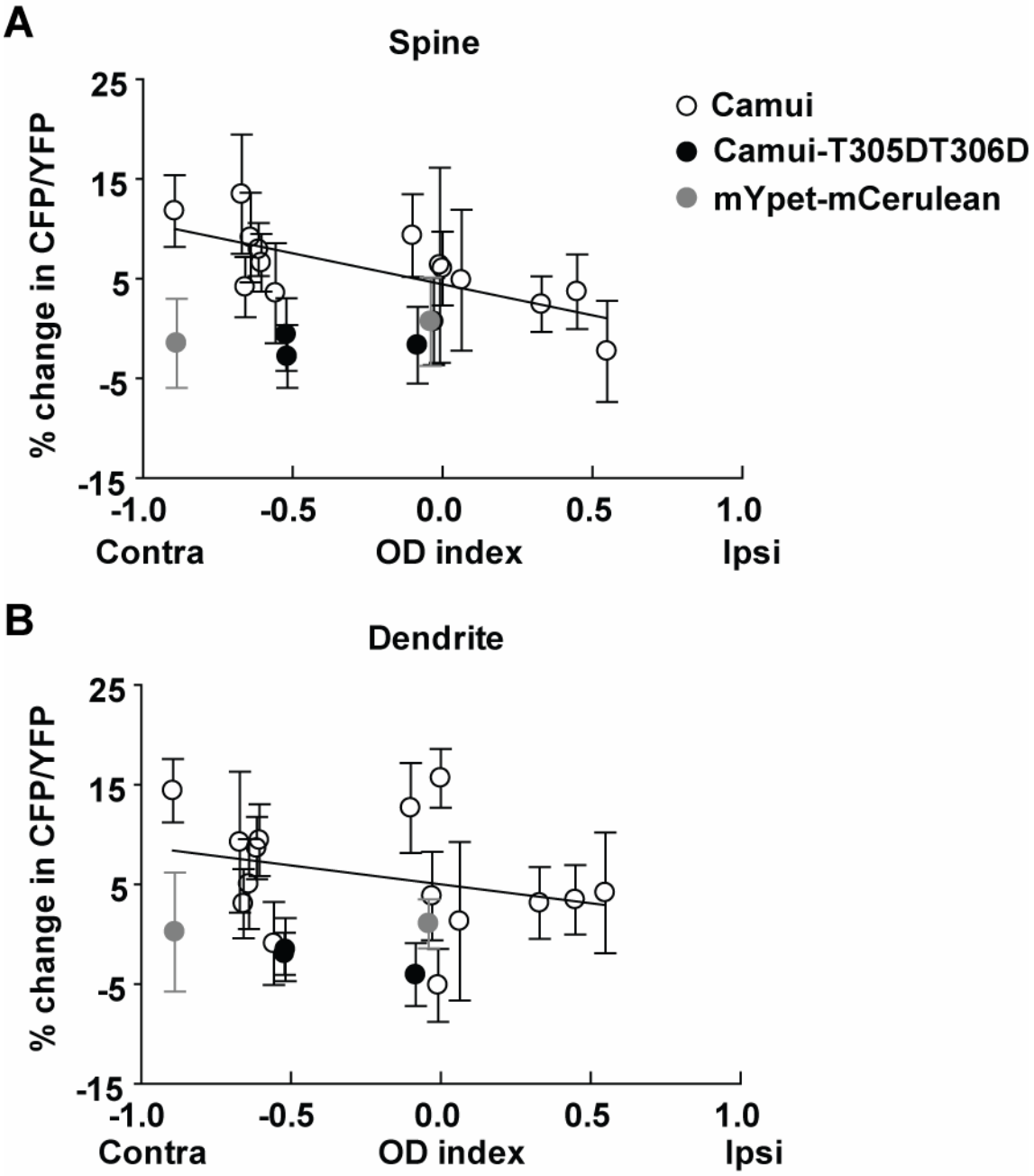

Figure 12. Change in CaMKIIα activity in spines strongly correlates with OD index but not in dendrites. (A) Each circle shows the mean of percent change in CFP/YFP or FRET level of fusion protein in spines after 4 hrs MD within one imaging site. (B) Dendritic region data presented as in (A). Data were from 9 ferrets. Error bars represent SEM.

CaMKII activity level does not predict the size of a spine. Second, we wanted to know if relationship (Figure 13C, r = 0.09). Third, we determined that cortical depth at which the analyzed spines and dendritic regions reside was not correlated with the percent change in CaMKIIα activity (Figure 13D, r = 0.13).

We then rank ordered each spine in the deprived eye domain by their basal CFP/YFP ratio, smallest to largest, and plotted these values together with the respective ratio after 4 hrs of MD (Figure 14A). In order to test statistical significance, the data were further binned every 20% according to the rank order and the statistical significance was calculated in each bin. Basal CaMKIIα activity varied considerably. However, there was a clear tendency for spines that had high basal CaMKIIα activity to show relatively small increases in CaMKIIα activation, while a large number of spines and dendritic regions with minimal to moderate CaMKIIα activity showed a larger increase (Figure 14B). The same analysis performed for data from the open eye domain showed that unlike the deprived eye domain, the spines and dendritic regions with minimal to moderate basal CaMKIIα activation did not show a significant increase after 4 hrs of MD (Figure 15). As for the data in the binocular domain, although we have a small sample size, dendritic regions showed an increase in CaMKIIα activity similar to the deprived eye domain while CaMKIIα activity changes in spines followed the observations from the open eye domain (Figure 16). In sum, the observed increase in CaMKIIα activity as a result of 4 hrs of MD seems to arise from the population of spines with minimal to moderate basal CaMKIIα activity.

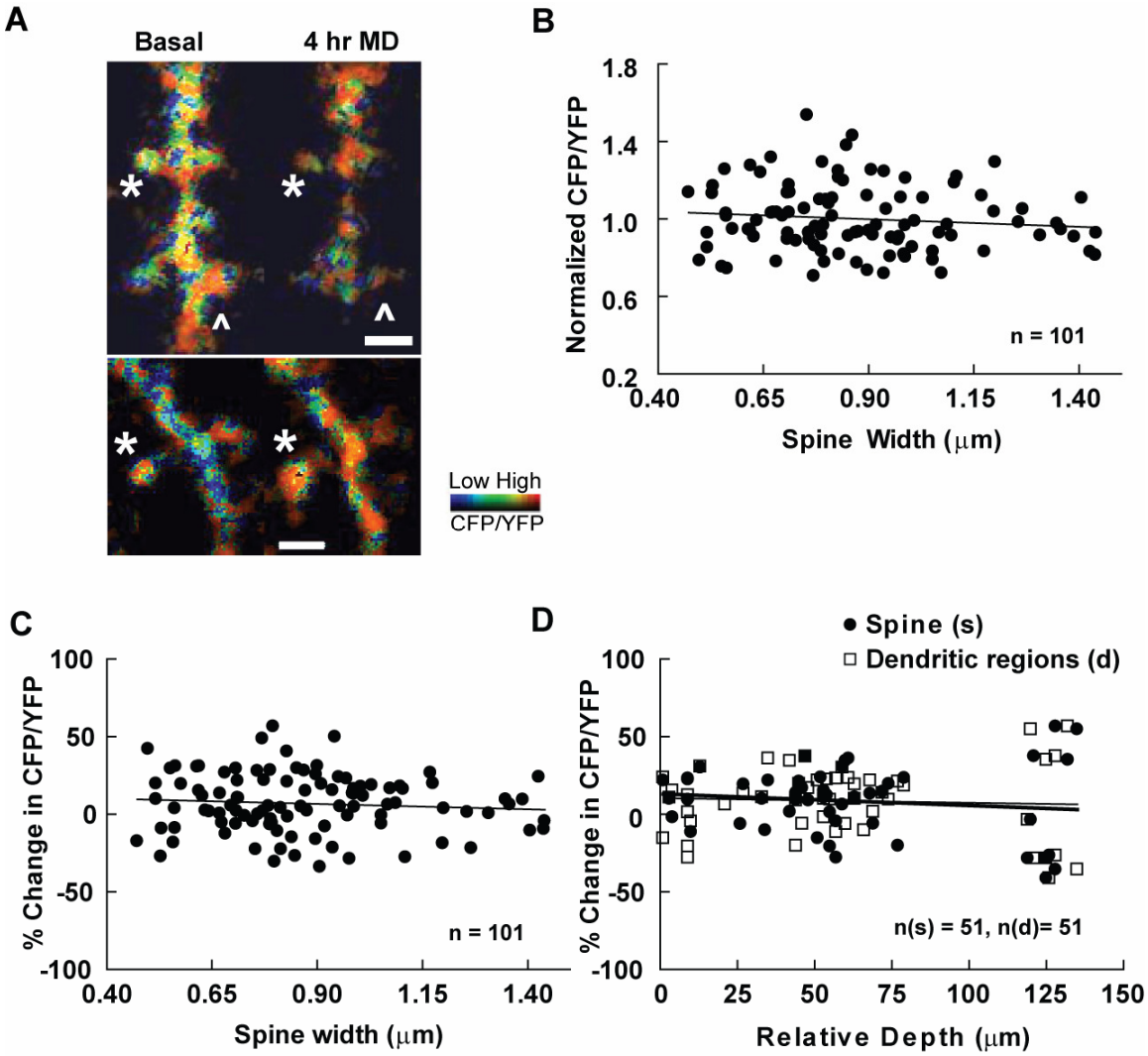

Figure 13. Single spine analysis. (A) Ratiometric images of individual dendritic segments and spines in intensity modulated display mode. * indicates spines with increased CaMKII activity after 4 hrs MD. ^ indicates spines with decreased CaMKII activity after 4 hrs MD. Scale bar: 2 µm. (B) Plot of site average normalized basal CFP/YFP ratio in individual spines against the spine width. (C) Plot of percent change in CFP/YFP ratio in individual spines after 4 hrs MD against the spine width. (D) Plot of percent change in CFP/YFP ratio in individual spines after 4 hrs MD against the relative cortical depth at which each spine or dendrite was located. Data were from 1 ferret.

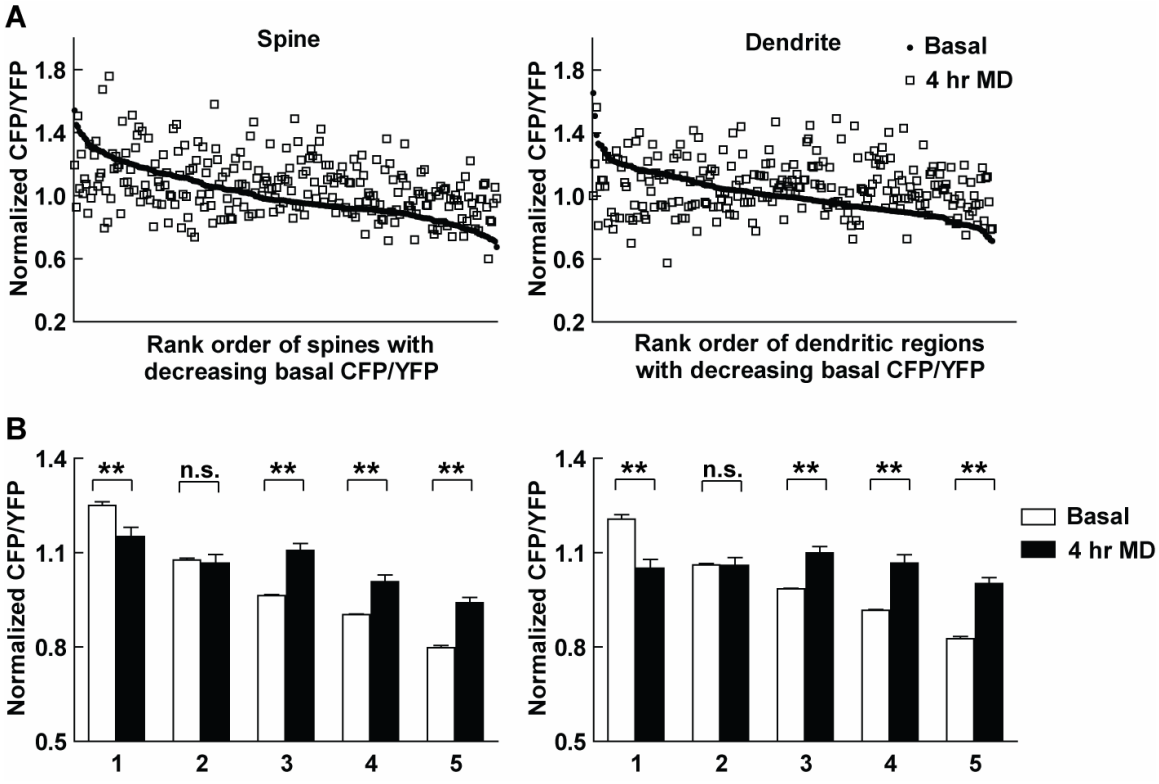

Figure 14. Population analysis of individual spines and dendritic regions in the deprived eye domain. (A) Normalized basal CFP/YFP ratios in individual spines (left) and dendritic regions (right) are ranked and plotted in the decreasing order. Each region's respective 4 hrs MD ratio is also plotted. (B) Mean of the binned 20% of the data is plotted according to rank order. Numbers (1-5) on the x-axis denote the first to fifth binned 20% percent of data. Left: spine. Right: dendritic region. Error bars represent SEM. p > 0.05; **p < 0.01 (paired 2-tailed t-test).

2.4.7. Basal CaMKII activity in spines that were eliminated after 4 hrs of MD was lower than the average activity of the surrounding population of labeled neurons

While many spines are stable over long periods of time, a subset of spines undergoes activity dependent turn over. Yu et al. found that there is an elimination of dendritic spines under the same MD paradigm in ferret visual cortex [48]. For this reason we looked for spines that were eliminated after 4 hrs of MD and compared them to the average activity of the surrounding population of spines within the same injection site (site average). We found 8 dendritic spines out of 266 spines in the deprived eye domain that were eliminated following 4 hrs of MD. Interestingly, their basal CaMKIIα activity was significantly lower than their site average (Figure 17A, $p < 0.05$ (paired t-test)). However, the analysis of the dendritic regions that were adjacent to those eliminated spines, and that remained after 4 hrs of MD, showed that their basal CaMKIIα activity was not different from the site average (Figure 17B, $p > 0.8$ (paired t-test)). This indicated that, although the majority of spines with low basal CaMKIIα activity were still maintained and even gained higher CaMKIIα activity after 4 hrs of MD, a small population was eliminated; those with higher basal CaMKII were resistant to elimination.

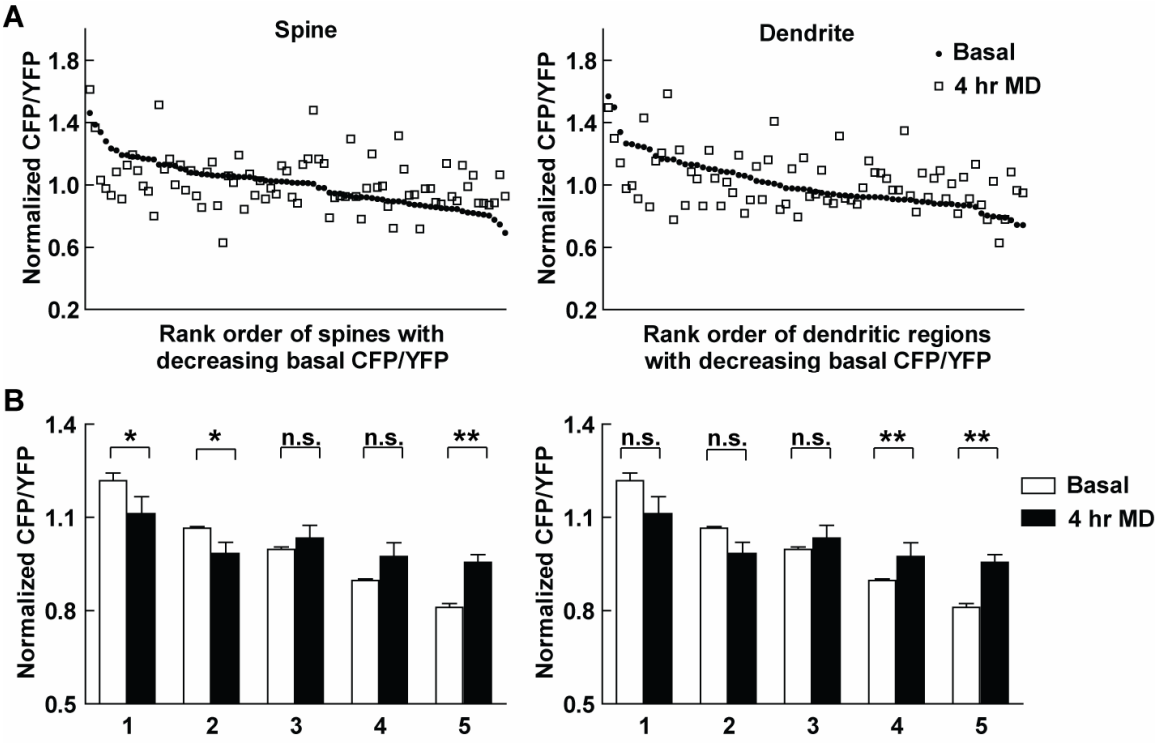

Figure 15. Population analysis of individual spines and dendritic regions in the open eye domain. (A) Normalized basal CFP/YFP ratios in individual spines (left) and dendritic regions (right) are ranked and plotted in decreasing order. Each region's respective 4 hrs MD ratio is also plotted. (B) Mean of the binned 20% of the data is plotted according to rank order. Numbers (1-5) on the x-axis denote the first to fifth binned 20% of data. Left: spine. Right: dendritic region. Error bars represent SEM. $p > 0.05$; *$p < 0.05$; **$p < 0.01$ (paired, 2-tailed t-test).

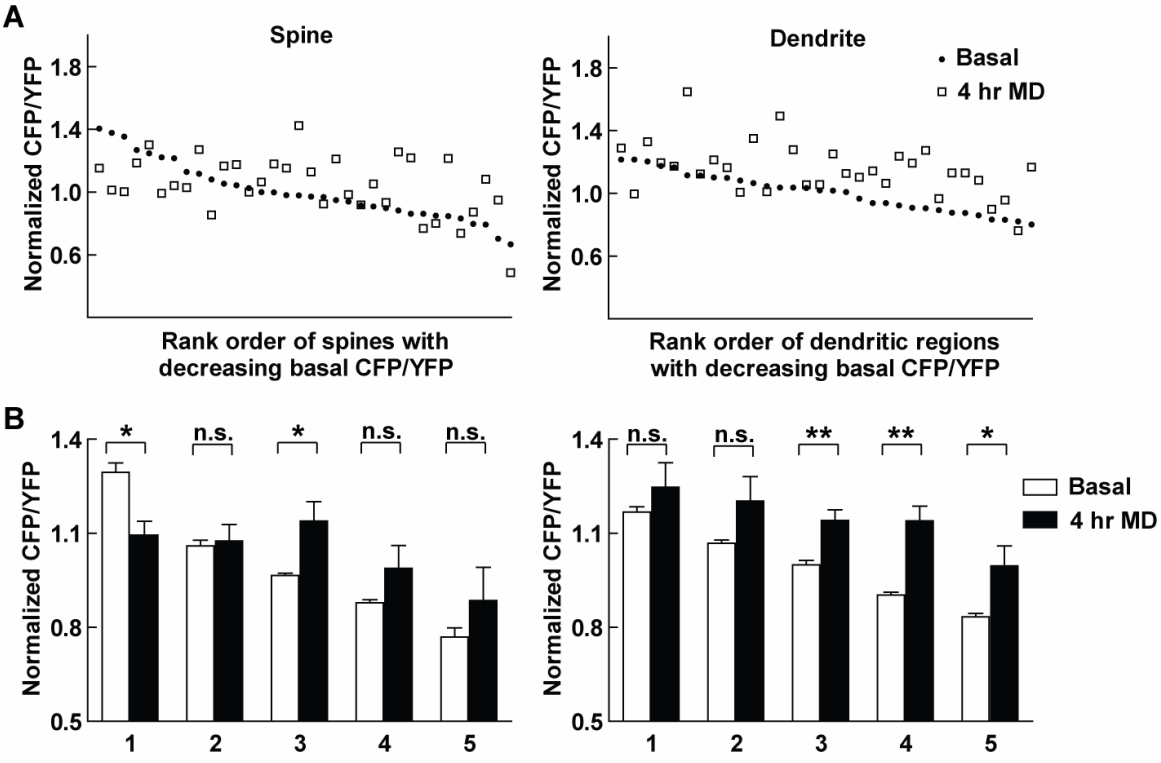

Figure 16. Population analysis of individual spines and dendritic regions in the binocular domain. (A) Normalized basal CFP/YFP ratios in individual spines (left) and dendritic regions (right) are ranked and plotted in decreasing order. Each region's respective 4 hrs MD ratio is also plotted. (B) Mean of the binned 20% of the data is plotted according to rank order. Numbers (1-5) on the x-axis denote the first to fifth binned 20% of data. Left: spine. Right: dendritic region. Error bars represent SEM. $p > 0.05$; *$p < 0.05$; **$p < 0.01$ (paired 2-tailed t-test).

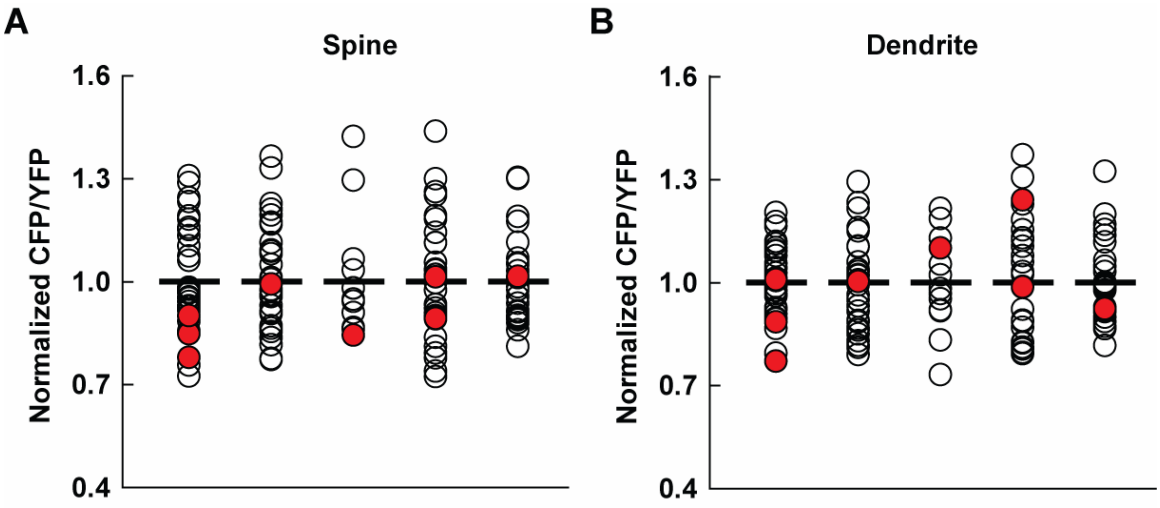

Figure 17. Basal CaMKII activity in eliminated spines was significantly lower than the average population within the same injection site. (A) Each circle represents CaMKII activity in a spine and the horizontal bar is the site average of the vertically aligned spines. Red dots indicate the spines that were eliminated after 4 hrs MD. (B) Data for dendritic regions adjacent to eliminated spines, shown as in (A). Data were from 3 ferrets.

2.5. Discussion

To investigate the synaptic mechanisms of OD plasticity, we combined chronic *in vivo* two-photon imaging and intrinsic signal optical imaging techniques to monitor the changes of a CaMKIIα activity reporter, Camui, before and after 4 hrs of MD at the level of individual spines. We found that spines, and their adjacent dendritic regions, showed a significant increase in CaMKIIα activity after only 4 hrs of MD in the deprived eye domain. This effect was also observed in the binocular domain, although to a lesser extent. However, in the open eye domain this increase was not observed. Detailed single spine analysis showed that this increase can be attributed to a higher CaMKIIα activity level of a specific population of spines and dendritic regions that had a minimal to moderate level of basal CaMKIIα activity. Furthermore, we observed no correlation between CaMKIIα activity in spines and spine size. We also found, that in the deprived eye domain, spines that were eliminated after 4 hrs of MD had basal CaMKIIα activity levels that were significantly lower than the site average activity. This lower CaMKIIα activity was however not seen in the immediate adjacent dendritic regions. Taken together, our results show that there is a strong correlation between deprived eye dominance and the increase in CaMKIIα activity.

2.5.1. Chronic *in vivo* imaging of CaMKII at single spine level

The current study is a proof of principle that opens the door to the possibility of monitoring molecular events underlying plasticity processes *in vivo*. The unique combination of using a viral delivery system, an optical reporter of a biochemical process (CaMKII activation), chronic *in vivo* two-photon imaging, and intrinsic signal optical imaging empowered us to 1) express a functional protein in a temporally and spatially

restricted manner, 2) repeatedly monitor important biochemical processes underlying plasticity events at a subcellular level, and 3) investigate the roles of these biochemical processes in different functional domains of the cortex. Previous studies in mutant mice assessing the role of CaMKIIα activity in OD plasticity concluded that it is required for this form of plasticity [27]. However, it is difficult to address the temporal and spatial regulation of CaMKIIα activity that is apparently important for OD plasticity in these mice. Now, using our method, this detailed mechanistic dissection can be accomplished *in vivo* and in the same subcellular structures before and after alterations in visual experience.

2.5.2. Hebbian and Homeostatic mechanisms in OD plasticity

Our main observation of elevated CaMKIIα activity in single spines within the deprived eye domain after only 4 hrs of MD is best reconciled by homeostatic mechanisms [15, 55-57]. Although we did see spines with decreased CaMKII activity in the deprived eye domain, pointing to a Hebbian mechanism, the majority of spines showed an increase in the face of declining presynaptic drive. These observations are in agreement with a recent study that used calcium-sensitive dye *in vivo* imaging to study OD plasticity in mice by Mrsic-Flogel et. al. [16]. In the binocular cortex of mice, the deprived eye responses of neurons receiving predominantly deprived eye input were surprisingly enhanced after MD. Similar observations were made when they looked at the monocular cortex that receives exclusive deprived eye input. They concluded that homeostatic mechanisms are recruited to increase neuronal responsiveness when cortical neurons are challenged by degraded vision and thereby maintain the firing rates within an

optimal range. Our results support this view in that CaMKII activity increases the most in the regions of the cortex that are dominated by the deprived eye (Figure 12).

Homeostatic regulation is thought to be a global scaling up or down to preserve the relative weight of individual synapses in the entire network [15, 56, 58], whereas the Hebbian mechanisms change the synaptic strength of an individual synapses whose activity are modulated [59]. Considering the roles of these two mechanisms in our observed results, it is apparent that both mediate the changes that occur in synaptic strength with short term MD as we saw the synaptic changes in spines along the same dendritic shaft vary both in magnitude and in direction as well as the CaMKII activity in the majority of spines increased. Therefore, it would be interesting to monitor how CaMKII activity changes in a population of spines from a single neuron affect the firing rate of that neuron simultaneously. This way, we could potentially determine the eye preference of a single neuron and correlate that preference to the percent of synapses receiving input from that eye.

2.5.3 The role of activated CaMKII in the deprived eye domain

It is generally accepted that CaMKII plays a role in experience-dependent synaptic rearrangements *in vivo* as mutant CaMKII mice showed disrupted cortical plasticity [27, 60-62]. Our analysis revealed that spines with low basal CaMKIIα activity had the propensity to be eliminated following 4 hrs of MD (Figure 17). We therefore speculate that an increase in CaMKII activity in a given spine after 4 hrs of MD might protect that spine from being eliminated. Therefore, spines with low basal CaMKII activity could have two outcomes following 4 hrs of MD: 1) persistent low CaMKII activity, which may make them candidates for elimination or 2) increased CaMKII

activation, which may serve to protect or maintain these synapses. These "protected" spines might have a weakening presynaptic partner as the deprived eye drive is decreasing. This could account for the initial deprived eye depression. On the other hand, maintenance of the postsynaptic spine by activated CaMKII could facilitate the delayed potentiation process of building new functional synapses with the open eye contacts [5, 16].

2.5.4. Other considerations

A recent study using the same probe but different fluorophore combination and detection modality reported that CaMKIIα activation in a spine stimulated by either glutamate uncaging alone or paired with postsynaptic depolarization lasts only 2 minutes [50]. These results are at odds with our results in which CaMKII activation after 4 hrs of MD was detected. We speculate that several differences between the two studies might account for the discrepancy. Since we did not attempt *in vivo* imaging earlier than 4 hrs of MD, we have no way of confirming the starting point of CaMKII activation. Also, there could be different phases of CaMKII activation: a transient rise in activation followed by a delayed second phase of prolonged activation, with the second phase being what our experimental design captured. Furthermore, LTP induction at a single spine level differs significantly from physiological presynaptic changes in a population of neurons after MD. It is likely that changes in the balance of deprived and open eye input to a large number of synapses trigger mechanisms other than Hebbian mechanisms and these mechanisms have an effect in the entire neuron including the synapse. Therefore, when the different forms of plasticity processes operate simultaneously, the activation profile of CaMKII is no longer the same as seen under the Hebbian rule.

2.5.5. Conclusion

In this study, we combined *in vivo* two-photon imaging and intrinsic signal optical imaging techniques to monitor CaMKIIα activity changes in a single spine as a means of determining alterations in synaptic strength during OD plasticity. We found that an increase in CaMKIIα activity is positively correlated with deprived eye. This finding is consistent with previous results in that homeostatic regulation and Hebbian mechanisms are both involved in OD plasticity.

2.6. Statement of involvement

This project was done in collaboration with Dr. Mriganka Sur's laboratory. In particular, Dr. Amanda Mower worked closely with me throughout the entire project. Dr. Hongbo Yu performed intrinsic optical imaging. Dr. Ania Majewska showed us how to use the two-photon microscope that she built and took part in imaging the first few ferrets. Dr. Kenichi Okamoto provided advice on the fluorescent proteins and imaging. My role in conducting the experiments included molecular cloning, HSV generation, *in vitro* characterization of various constructs and assisting Dr. Mower in the window implant surgery. We imaged ferrets under the two-photon microscope together. I helped with the intrinsic signal optical imaging, although majority of experiments were done by Drs. Mower and Yu. Alignment of the viral injection sites to the ocular dominance domains was performed by Dr. Mower and ocular dominance index was determined by Dr. Yu. Dr. Mower performed most of the cell body analysis. I performed all of the spine and dendritic region analysis with the help of automated programs written by Kayi Lee.

2.7. References

1. Gordon, J.A. and M.P. Stryker, *Experience-Dependent Plasticity of Binocular Responses in the Primary Visual Cortex of the Mouse.* J. Neurosci., 1996. **16**(10): p. 3274-3286.

2. Trachtenberg, J.T., C. Trepel, and M.P. Stryker, *Rapid Extragranular Plasticity in the Absence of Thalamocortical Plasticity in the Developing Primary Visual Cortex.* Science, 2000. **287**(5460): p. 2029-2032.

3. Shatz, C.J. and M.P. Stryker, *Ocular dominance in layer IV of the cat's visual cortex and the effects of monocular deprivation.* J Physiol, 1978. **281**(1): p. 267-283.

4. Freeman, R.D. and C. Olson, *Brief periods of monocular deprivation in kittens: effects of delay prior to physiological study.* J Neurophysiol, 1982. **47**(2): p. 139-150.

5. Frenkel, M.Y. and M.F. Bear, *How Monocular Deprivation Shifts Ocular Dominance in Visual Cortex of Young Mice.* Neuron, 2004. **44**(6): p. 917.

6. Heynen, A.J., et al., *Molecular mechanism for loss of visual cortical responsiveness following brief monocular deprivation.* Nat Neurosci, 2003. **6**(8): p. 854-62.

7. Liu, C.-H., et al., *Cannabinoid Receptor Blockade Reveals Parallel Plasticity Mechanisms in Different Layers of Mouse Visual Cortex.* Neuron, 2008. **58**(3): p. 340.

8. Bienenstock, E.L., L.N. Cooper, and P.W. Munro, *Theory for the development of neuron selectivity: orientation specificity and binocular interaction in visual cortex.* J Neurosci, 1982. **2**(1): p. 32-48.

9. Cooper, L.N., F. Liberman, and E. Oja, *A theory for the acquisition and loss of neuron specificity in visual cortex.* Biol Cybern, 1979. **33**(1): p. 9-28.

10. Bear, M.F., *A synaptic basis for memory storage in the cerebral cortex.* Proc Natl Acad Sci U S A, 1996. **93**(24): p. 13453-9.

11. Kirkwood, A., M.C. Rioult, and M.F. Bear, *Experience-dependent modification of synaptic plasticity in visual cortex.* Nature, 1996. **381**(6582): p. 526-8.

12. Smith, G.B., A.J. Heynen, and M.F. Bear, *Bidirectional synaptic mechanisms of ocular dominance plasticity in visual cortex.* Philosophical Transactions of the Royal Society B: Biological Sciences, 2009. **364**(1515): p. 357-367.

13. Sawtell, N.B., et al., *NMDA Receptor-Dependent Ocular Dominance Plasticity in Adult Visual Cortex.* Neuron, 2003. **38**(6): p. 977.

14. Cho, K.K.A., et al., *The ratio of NR2A/B NMDA receptor subunits determines the qualities of ocular dominance plasticity in visual cortex.* Proceedings of the National Academy of Sciences, 2009. **106**(13): p. 5377-5382.

15. Desai, N.S., et al., *Critical periods for experience-dependent synaptic scaling in visual cortex.* Nat Neurosci, 2002. **5**(8): p. 783-9.

16. Mrsic-Flogel, T.D., et al., *Homeostatic Regulation of Eye-Specific Responses in Visual Cortex during Ocular Dominance Plasticity.* Neuron, 2007. **54**(6): p. 961.

17. Kennedy, M.B., M.K. Bennett, and N.E. Erondu, *Biochemical and immunochemical evidence that the "major postsynaptic density protein" is a subunit of a calmodulin-dependent protein kinase.* Proc Natl Acad Sci U S A, 1983. **80**(23): p. 7357-61.

18. Lisman, J., H. Schulman, and H. Cline, *The molecular basis of CaMKII function in synaptic and behavioural memory.* Nat Rev Neurosci, 2002. **3**(3): p. 175-190.

19. Malinow, R., H. Schulman, and R.W. Tsien, *Inhibition of postsynaptic PKC or CaMKII blocks induction but not expression of LTP.* Science, 1989. **245**(4920): p. 862-866.

20. Malinow, R., D.V. Madison, and R.W. Tsien, *Persistent protein kinase activity underlying long-term potentiation.* Nature, 1988. **335**(6193): p. 820-4.

21. Malenka, R.C., et al., *An essential role for postsynaptic calmodulin and protein kinase activity in long-term potentiation.* Nature, 1989. **340**(6234): p. 554-7.

22. Ito, I., H. Hidaka, and H. Sugiyama, *Effects of KN-62, a specific inhibitor of calcium/calmodulin-dependent protein kinase II, on long-term potentiation in the rat hippocampus.* Neurosci Lett, 1991. **121**(1-2): p. 119-21.

23. Shirke, A.M. and R. Malinow, *Mechanisms of potentiation by calcium-calmodulin kinase II of postsynaptic sensitivity in rat hippocampal CA1 neurons.* J Neurophysiol, 1997. **78**(5): p. 2682-92.

24. Lledo, P.M., et al., *Calcium/calmodulin-dependent kinase II and long-term potentiation enhance synaptic transmission by the same mechanism.* Proc Natl Acad Sci U S A, 1995. **92**(24): p. 11175-9.

25. Pettit, D.L., S. Perlman, and R. Malinow, *Potentiated transmission and prevention of further LTP by increased CaMKII activity in postsynaptic hippocampal slice neurons.* Science, 1994. **266**(5192): p. 1881-1885.

26. Hayashi, Y., et al., *Driving AMPA receptors into synapses by LTP and CaMKII: requirement for GluR1 and PDZ domain interaction.* Science, 2000. **287**(5461): p. 2262-7.

27. Gordon, J.A., et al., *Deficient Plasticity in the Primary Visual Cortex of [alpha]-Calcium/Calmodulin-Dependent Protein Kinase II Mutant Mice.* Neuron, 1996. **17**(3): p. 491-499.

28. Lisman, J.E. and M.A. Goldring, *Feasibility of long-term storage of graded information by the Ca2+/calmodulin-dependent protein kinase molecules of the postsynaptic density.* Proc Natl Acad Sci U S A, 1988. **85**(14): p. 5320-4.

29. Lisman, J., *The CaM kinase II hypothesis for the storage of synaptic memory.* Trends in Neurosciences, 1994. **17**(10): p. 406-412.

30. Chapman, B. and M.P. Stryker, *Development of orientation selectivity in ferret visual cortex and effects of deprivation.* J Neurosci, 1993. **13**(12): p. 5251-62.

31. Mower, A.F., et al., *cAMP/Ca2+ response element-binding protein function is essential for ocular dominance plasticity.* J Neurosci, 2002. **22**(6): p. 2237-45.

32. Issa, N.P., et al., *The Critical Period for Ocular Dominance Plasticity in the Ferret's Visual Cortex.* J. Neurosci., 1999. **19**(16): p. 6965-6978.

33. Takao, K., et al., *Visualization of Synaptic Ca2+ /Calmodulin-Dependent Protein Kinase II Activity in Living Neurons.* J. Neurosci., 2005. **25**(12): p. 3107-3112.

34. Yang, F., L.G. Moss, and G.N. Phillips, *The molecular structure of green fluorescent protein.* Nat Biotech, 1996. **14**(10): p. 1246-1251.

35. Zacharias, D.A., et al., *Partitioning of Lipid-Modified Monomeric GFPs into Membrane Microdomains of Live Cells.* Science, 2002. **296**(5569): p. 913-916.

36. Rizzo, M.A., et al., *An improved cyan fluorescent protein variant useful for FRET.* Nat Biotechnol, 2004. **22**(4): p. 445-9.

37. Nguyen, A.W. and P.S. Daugherty, *Evolutionary optimization of fluorescent proteins for intracellular FRET.* Nat Biotechnol, 2005. **23**(3): p. 355-60.

38. Lim, F. and R.L. Neve, *Generation of High-Titer Defective HSV-1 Vectors.* Current Protocols in Neuroscience, 1999: p. 4.13.1-4.13.17.

39. Beique, J.-C., et al., *Synapse-specific regulation of AMPA receptor function by PSD-95.* Proceedings of the National Academy of Sciences, 2006. **103**(51): p. 19535-19540.

40. http://www.physics.csbsju.edu/stats/KS-test.n.plot_form.html

41. Rosenberg, O.S., et al., *Oligomerization states of the association domain and the holoenyzme of Ca2+/CaM kinase II.* FEBS Journal, 2006. **273**(4): p. 682-694.

42. Shaner, N.C., et al., *Improved monomeric red, orange and yellow fluorescent proteins derived from Discosoma sp. red fluorescent protein.* Nat Biotechnol, 2004. **22**(12): p. 1567-72.

43. Colbran, R.J. and T.R. Soderling, *Calcium/calmodulin-independent autophosphorylation sites of calcium/calmodulin-dependent protein kinase II. Studies on the effect of phosphorylation of threonine 305/306 and serine 314 on calmodulin binding using synthetic peptides.* J Biol Chem, 1990. **265**(19): p. 11213-9.

44. Rich, R.C. and H. Schulman, *Substrate-directed Function of Calmodulin in Autophosphorylation of Ca2+/Calmodulin-dependent Protein Kinase II.* J. Biol. Chem., 1998. **273**(43): p. 28424-28429.

45. Patton, B.L., S.G. Miller, and M.B. Kennedy, *Activation of type II calcium/calmodulin-dependent protein kinase by Ca2+/calmodulin is inhibited by autophosphorylation of threonine within the calmodulin-binding domain.* J. Biol. Chem., 1990. **265**(19): p. 11204-11212.

46. Jackson, C.A. and T.L. Hickey, *Use of ferrets in studies of the visual system.* Lab Anim Sci, 1985. **35**(3): p. 211-5.

47. Mioche, L. and W. Singer, *Chronic recordings from single sites of kitten striate cortex during experience-dependent modifications of receptive-field properties.* J Neurophysiol, 1989. **62**(1): p. 185-97.

48. Yu, H., A. Majewska, and M. Sur. *Rearrangement of dendritic spines during short term monocular deprivation in the primary visual cortex of the ferret in vivo*. in *Neuronscience Meeting Planner, Program No 7148*. 2005. Washingotn, DC: Society for Neuroscience.

49. Fukunaga, K., D. Muller, and E. Miyamoto, *Increased Phosphorylation of Ca^{2+}/Calmodulin-dependent Protein Kinase II and Its Endogenous Substrates in the Induction of Long Term Potentiation.* J. Biol. Chem., 1995. **270**(11): p. 6119-6124.

50. Lee, S.-J.R., et al., *Activation of CaMKII in single dendritic spines during long-term potentiation.* Nature, 2009. **458**(7236): p. 299.

51. Fukunaga, K., et al., *Long-term potentiation is associated with an increased activity of Ca2+/calmodulin-dependent protein kinase II.* J Biol Chem, 1993. **268**(11): p. 7863-7.

52. Ouyang, Y., et al., *Visualization of the Distribution of Autophosphorylated Calcium/Calmodulin-Dependent Protein Kinase II after Tetanic Stimulation in the CA1 Area of the Hippocampus.* J. Neurosci., 1997. **17**(14): p. 5416-5427.

53. Asrican, B., J. Lisman, and N. Otmakhov, *Synaptic strength of individual spines correlates with bound Ca2+-calmodulin-dependent kinase II.* J Neurosci, 2007. **27**(51): p. 14007-11.

54. Otmakhov, N., et al., *Persistent accumulation of calcium/calmodulin-dependent protein kinase II in dendritic spines after induction of NMDA receptor-dependent chemical long-term potentiation.* J Neurosci, 2004. **24**(42): p. 9324-31.

55. Turrigiano, G.G., et al., *Activity-dependent scaling of quantal amplitude in neocortical neurons.* Nature, 1998. **391**(6670): p. 892-6.

56. Turrigiano, G.G. and S.B. Nelson, *Homeostatic plasticity in the developing nervous system.* Nat Rev Neurosci, 2004. **5**(2): p. 97-107.

57. Turrigiano, G.G., *The self-tuning neuron: synaptic scaling of excitatory synapses.* Cell, 2008. **135**(3): p. 422-35.

58. Turrigiano, G., *Homeostatic signaling: the positive side of negative feedback.* Current Opinion in Neurobiology, 2007. **17**(3): p. 318-324.

59. Hebb, D.O., *Organization of behavior.* 1949, New York: John Wiley & Sons.

60. Taha, S., et al., *Autophosphorylation of [alpha]CaMKII Is Required for Ocular Dominance Plasticity.* Neuron, 2002. **36**(3): p. 483-491.

61. Glazewski, S., et al., *Requirement for alpha-CaMKII in experience-dependent plasticity of the barrel cortex.* Science, 1996. **272**: p. 421-423.

62. Glazewski, S., et al., *The role of alpha-CaMKII autophosphorylation in neocortical experience-dependent plasticity.* Nature Neurosci., 2000. **3**: p. 911-918.

CHAPTER 3: Genetically encoded probe for fluorescence lifetime imaging of CaMKII activity

3.1. Abstract

Ca^{2+}/calmodulin-dependent protein kinase II (CaMKII) is highly enriched in excitatory synapses in the central nervous system and is critically involved in synaptic plasticity, learning, and memory. Previously, we generated a ratiometric FRET probe, Camui, to monitor the CaMKII activity *in vivo*. Here, we attempted to generate a new version of Camui for fluorescence lifetime imaging (FLIM) of CaMKII activity that is better suited for *in vivo* imaging studies. We first optimized the combinations of fluorescent proteins by taking advantage of expansion of fluorescent proteins towards longer wavelength in fluorospectrometric assay. Then using digital frequency domain FLIM (DFD-FLIM), we demonstrated that the resultant protein can indeed detect CaMKII activation in living cells. These FLIM versions of Camui could be useful for elucidating the function of CaMKII both *in vitro* and *in vivo*.

3.2. Introduction

Ca^{2+}/calmodulin-dependent protein kinase II (CaMKII) is a serine/threonine protein kinase crucial for synaptic plasticity in the central nervous system [1]. It can serve as a valuable synaptic strength reporter in many plasticity processes. To detect CaMKII activation *in vivo*, we previously designed an approach to observe CaMKII activity by detecting conformational change of CaMKII associated with its activation. This was accomplished by constructing a tandem fusion of YFP, CaMKII, and CFP, the engineered sensor named Camui, and measuring its fluorescence resonance energy transfer (FRET) [2].

Camui showed FRET in its inactive state. In the presence of ATP and calmodulin, the stimulation with Ca^{2+} causes a rapid (<1 min) decrease of FRET. This change arises from a conformational change due to both binding with Ca^{2+}/calmodulin and autophosphorylation. Even after the addition of EGTA, the change in FRET persists. This persistent, Ca^{2+}-independent change in FRET is abolished by omitting ATP or by eliminating the kinase activity (K42R) with a point mutation at the catalytic core. Therefore, a process involving autophosphorylation is contributing to the persistent change, most likely the autophosphorylation at threonine 286 (T286) on the autoinhibitory domain. In fact, a phosphoblocking mutation (T286A) blocks the persistent change in FRET, whereas a phosphomimicking mutation (T286D) is sufficient to induce change in FRET without Ca^{2+} stimulation. Therefore, Camui detects the activation of CaMKII by the Ca^{2+}/calmodulin binding and the subsequent autophosphorylation.

Recent studies pointed out certain advantages of FLIM imaging over other

imaging modalities to detect protein interaction or conformational change using FRET [3-6]. FLIM imaging detects FRET-induced changes in nanosecond-order fluorescence decay-time of the donor fluorescence after excitation. The decay time-constant of donor fluorescence is independent of the concentration of the probe [4], and can circumvent some of the difficulties associated with the ratiometric imaging of FRET such as change in tissue scattering or absorption. However, the CFP-YFP pair, used for many FRET probes including our original Camui, is not suitable for FLIM because of a complex fluorescence decay-time of CFP [7]. Also, CFP is not the brightest of the GFP-family proteins, which makes the overall signal dim, and the spectral bleed-through reduces the dynamic range. In fact, a probe for FLIM-based FRET imaging requires different properties compared with the ratiometric FRET imaging. 1) The fluorescent decay-time of the donor is ideally single exponential. 2) The acceptor can be dim, or better, shows no fluorescence at all.

A recent expansion of GFP-related fluorescent protein family will allow us to explore the ideal combination of fluorescent proteins for a FLIM probe. In this study, motivated by the new additions of the family towards longer wavelength [8], we first tested various red-shifted fluorescent proteins as well as a novel quencher mDarkVenus as the acceptor proteins. This allowed us to use GFP or YFP as a donor, which both have single exponential fluorescence decay-time constant and are significantly brighter than CFP. After determining the optimal pairs with a fluorospectroscopic assay in cell homogenate, we tested the applicability of one of such pair to the FLIM imaging in live cells. Consequently, we identified several promising versions of Camui that could be useful for elucidating the function of CaMKII both i*n vitro* and *in vivo*.

3.3. Materials and Methods

Construction of Camui Series

YFP (Venus variant) [9] was a gift from Drs. T. Nagai (Hokkaido University) and A. Miyawaki (RIKEN); mRFP, mOrange, and mStrawberry from Dr. Roger Tsien (UCSD); pEGFP-C1, pDsRed2-C1 and pDsRed-monomer-C1 were purchased from Clontech; TagRFP from Evrogen (Moscow, Russia). All variants of Camui were constructed from rat CaMKIIα, with donor and acceptor fluorophore proteins fused at amino- and carboxyl-termini similarly to described [2] with standard molecular biological methods. They were in a mammalian expression vector based on Clontech's pEGFP-C1 series downstream to the CMV promoter. We describe the constructs here by "*N-terminal fluorophore/C-terminal fluorophore"*. See Table. 1.

Fluorospectrometric Measurement of FRET

Camui variants were transfected in HEK293T cells by a liposome-mediated method (Lipofectamine 2000, Invitrogen, Carlsbad, CA). After 1-2 days, the cells were homogenized in CaMKII assay buffer composed of 40 mM HEPES-Na (pH 8.0), 0.1 mM EGTA, 5 mM magnesium acetate, 0.01% Tween-20, 1 mM DTT, and protease inhibitor cocktail (1 mM phenylmethylsulfonyl fluoride; 260 μM *N*-α-*p*-tosyl-L-arginine methyl ester hydrochloride; 10 mM benzamidine). After centrifugation, the supernatant was used for measurement. Fluorescence spectra were obtained with a spectrofluorophotometer (RF-5301PC, Shimadzu, Kyoto, Japan). To stimulate Camui, Ca^{2+} (1 mM) was added in the presence of 1 μM calmodulin and 50 μM ATP at room temperature. The reaction was stopped by 1.5 mM EGTA. Fluorescence intensity was adjusted according to the volume changes. Spectroscopic parameters are in Table 1.

Table 1 Constructs tested in this study

Name (N-terminus/C-terminus)	Förster distance (nm)	Excitation wavelength (nm) used	Donor emission peak (nm)	Acceptor emission peak (nm)
Venus/CFP 26R/N164H	5.21	433	477	528
mRFP/GFP	5.06	475	510	600
GFP/mRFP	5.06	475	510	600
mOrange/GFP	5.55	475	510	587
mStrawberry/GFP	5.66	475	510	608
TagRFP/GFP	5.05	475	510	577
mRFP/Venus	5.47	480	528	609
mOrange/Venus	5.67	480	528	557
mStrawberry/Venus	6.04	500	528	598
TagRFP/Venus	5.87	500	528	580
DsRed monomer/Venus	5.14	490	528	585
mDarkYFP/mGFP	5.81	457	510	N.D.[b]
mDarkVenus/mGFP	N.D.[a]	457	510	N.D.[b]

Förster distance was calculated as described [7] for each pair of donor and acceptor. The spectra for GFP, mOrange, mStrawberry, and Venus were obtained from the laboratory webpage of Dr. Roger Tsien; TagRFP from webpage of Evrogen (www.evrogen.com); others determined in-house. Quantum yield and extinction coefficient data for GFP, mOrange, mStrawberry, Venus, TagRFP, DsRed monomer from [8]; mRFP from [10]; CFP K26R/N164H by personal communication from Drs. Tomoo Ohashi and Harold P. Erickson (the extincition coefficient, 24,000 $M^{-1}cm^{-1}$ and the quantum yield, 0.63). Those for mDarkYFP have not been determined and the values for non-monomerized version (REACh2) were used [11].

[a]: Not determined due to lack of data the extinction coefficient of mDarkVenus.

[b]: None or negligible fluorescence emission.

Expression and Imaging of GFP

The coding region for GFP (EGFP, Clontech) was PCR-amplified and subcloned into the pET-21d vector (Novagen, San Diego, CA). GFP protein was expressed in BL21(DE3) cells and then purified to homogeneity by using the Ni-NTA agarose (Qiagen, Hilden, Germany). Imaging was done using 20 μM GFP in 20 mM Tris-HCl buffer (pH 7.4).

Expression and Imaging of Camui in HEK293T cells

HEK293T cells were transfected as above. The cells were imaged as described [2]. Digital frequency domain FLIM (DFD-FLIM) images (Figure 3 and 4) were taken with a custom-made, photon counting two-photon microscopy system [12], by digitally heterodyning emission photons with a 79.916 MHz frequency generated from the 80 MHz laser in a field-programmable gate array (FPGA) chip (Xilinx Spartan 3E, XC3S100E, San Jose, CA). The fluorescence emission was detected with photo-multiplier tube (PMT) (R7400U-04, Hamamatsu Photonics, Hamamatsu, Japan), amplified (ACA-4-35-N 35 dB; 1.8 GHz, Becker & Hickl, Berlin, Germany) and digitized (Model 6915, Philips Scientifics, Mahwah, NJ) prior to the heterodyning. The laser repetition signal was provided by the photodiode output on the Spectra-Physics 3930 unit, amplified and digitized (Model 6930, Philips Scientifics) before arriving at the FGPA chip. Excitation wavelength was set at 910 nm. GFP emission was detected with a band-pass filter 525/50 nm. The FLIM images were processed with Globals for Images software (Laboratory for Fluorescence Dynamics, University of California, Irvine).

3.4. Results

3.4.1. Improvement of Camui using GFP-mRFP pair

We first used fluorospectrometry for testing constructs as it offers a quantitative comparison of FRET among multiple samples. The criteria we used are: (1) the extent of change in FRET efficiency in response to Ca^{2+}-stimulation as measured by dequenching of donor channel, (2) the brightness of acceptor channel (darker is better).

We employed a monomeric version of DsRed, monomeric red fluorescent protein (mRFP) [10] to construct mRFP/GFP- and GFP/mRFP-Camui, which is indeed reported as a fluorophore pair for FLIM imaging (Figureure 1 A and B) [3, 4]. Observing transfected cells using fluorescent microscope at their optimum excitation wavelengths showed a reasonable green and red fluorescence (not shown). In the spectral analyses of the homogenate of the cells expressing these proteins upon GFP specific excitation at 475 nm, we could observe a distinct peak corresponding to GFP emission but the mRFP peak was very small, barely seen over the skew of GFP peak (Figure 1A). Stimulation Ca^{2+} led to a rapid (<1 min) and stable increase in GFP peak by 53.2 ± 0.7% and eliminated the mRFP peak (Figure 1A and B). After the addition of EGTA, the GFP peak decreased but to 25.8 ± 1.1% still above the initial level. Therefore, although mRFP peak was barely visible, FRET indeed occurred in mRFP/GFP-Camui and GFP was quenched by it. This is not surprising considering the modest extinction coefficient (44,000 $M^{-1}cm^{-1}$) and low fluorescence quantum yield (0.25) of mRFP [10]. This is, in fact, beneficial for application to FLIM imaging as it requires only the donor fluorescence and contamination with the acceptor fluorescence can distort the measured lifetime of the donor. Notably, the extent of donor dequenching in mRFP/GFP-Camui was larger than

Venus/CFP-Camui under the same conditions, which was approximately 31.8 ± 2.0% by the addition of Ca^{2+} and 17.8 ± 1.9% after the chelation with EGTA (Figure 1A and B). In a control construct where Ca^{2+}/calmodulin binding site is mutated so that it does not bind with Ca^{2+}/calmodulin complex (T305D/T306D of CaMKIIα)[2], the spectral profile was unchanged even after the addition of Ca^{2+}/calmodulin (Figure 1A and B). Therefore, this FRET change was associated with the activation of the CaMKII moiety of the construct through Ca^{2+}/calmodulin binding. The reverse construct, GFP/mRFP-Camui exhibited an overall smaller response with the same manipulation, indicating that the steric arrangement of two fluorophores is important (Figure 1A and B).

We imaged HEK293T cells expressing mRFP/GFP-Camui and stimulated them with Ca^{2+}-ionophore, 4-Br-A23187. Consistent with the observation from cell homogenates, there was an increase in GFP fluorescence by the stimulation (Figure 1C and D). The response was slower than in cell homogenate, likely due to the time lag of the perfusing system and the drug effect. In fact, when we pre-permeabilize the cells expressing YFP/CFP-Camui with 4-Br-A23187 in Ca^{2+}-free extracellular solution and locally puff-applied Ca^{2+}-containing extracellular solution, the FRET started changing within 10 sec and reached maximum within 1 min (K. Takao and Y. Hayashi, unpublished).

3.4.2. Comparison among spectral variants of mRFP and GFP

Recent expansion of the mRFP family encouraged us to explore additional members of the family [8]. We selected mOrange and mStrawberry to replace mRFP because of the better absorbance compared with the original mRFP (extinction coefficient, 71,000 and 90,000 $M^{-1}cm^{-1}$ for mOrange and mStrawberry, respectively [8]). Also, in

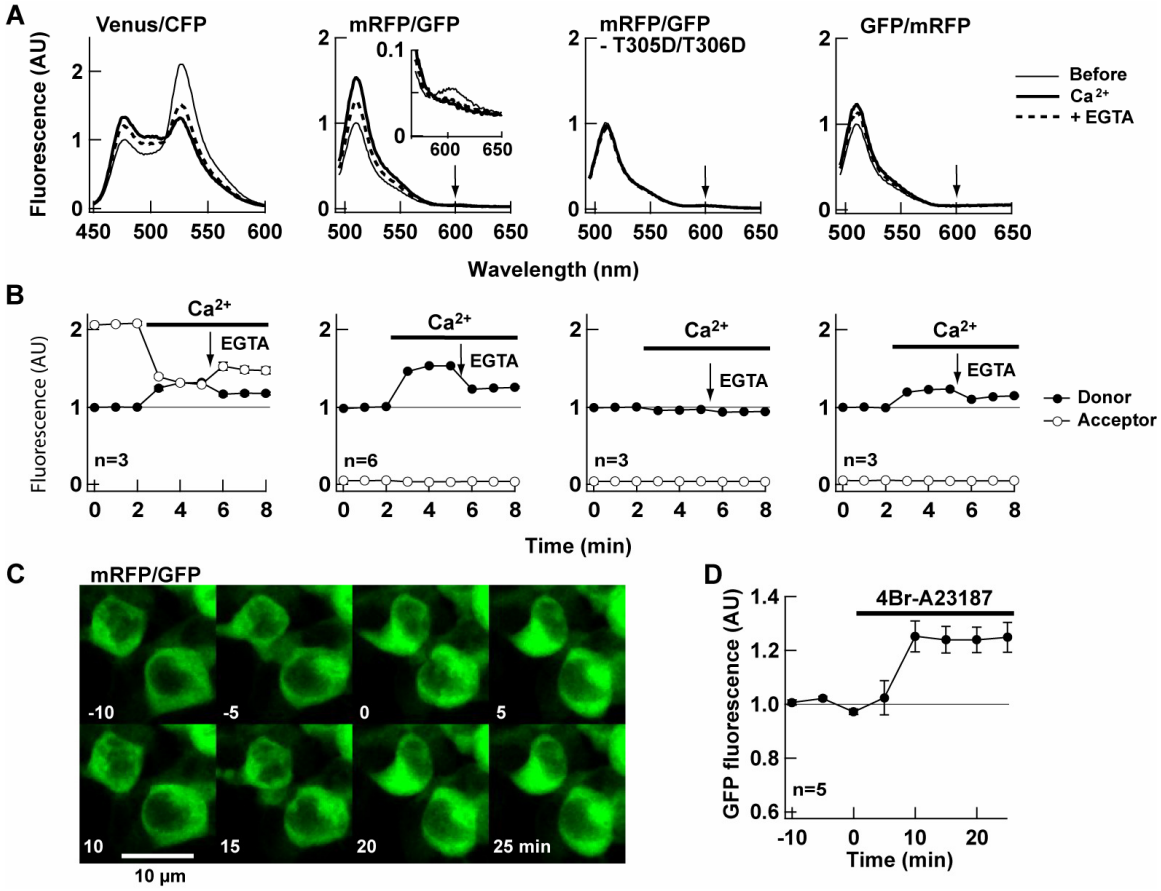

Figure 1. mRFP/GFP-Camui showed a significant dequenching upon stimulation. (A) The emission spectra of the Venus/CFP-Camui, mRFP/GFP-Camui, mRFP/GFP-Camui with T305D/T306D mutations and GFP/mRFP-Camui made with the HEK293T cell lysate expressing each construct before, 3 min after the addition of 1 mM Ca2+, and 3 min after the addition of 1.5 mM EGTA, at the donor specific excitation. The expected positions of acceptor peaks are shown by downward arrows. A 10-fold magnification of the mRFP emission peak is shown in the inset for mRFP/GFP-Camui. (B) A plot of donor and acceptor peak intensity over time, normalized by the donor peak intensity before application of Ca2+. The response was monitored every 1 min. (C) GFP fluorescence image of HEK293T cells expressing mRFP/GFP-Camui. (D) A summary of GFP fluorescence intensity in HEK293T cells. Intensity was normalized to the average intensity prior to stimulation for each cell. The error bars are s.e.m.

order to improve the spectral overlap of donor emission with acceptor excitation, GFP was replaced with Venus version of YFP. We focused on the constructs with the acceptor and donor at the N- and C-termini respectively as mRFP/GFP showed better dequenching than GFP/mRFP. The junction sequence between fluorophore proteins and CaMKII were kept the same as mRFP/GFP-Camui to see the pure effects of changing the fluorophores. This yielded mOrange/GFP-, mStrawberry/GFP-, mRFP/Venus-, mOrange/Venus-, and mStrawberry/Venus-versions of Camui (Figure 2A). The Förster distance of the pairs was calculated (Table 1).

Among the new mRFP family constructs, mOrange/Venus-Camui showed the best change upon stimulation with Ca^{2+}/calmodulin; the donor fluorescence intensity was increased by 71.6 ± 4.4% and still 37.8 ± 4.2% above the baseline after chelation (Figure 2A and B). However, the acceptor fluorescence observed may hamper the use in FLIM imaging though it may be suitable for ratiometric imaging as evidenced by a larger change in the ratio of donor and acceptor peaks (Figure 2C). mOrange/GFP-Camui has a similar calculated Förster distance compared with mOrange/Venus-Camui (Table 1) but showed a smaller response (Figure 2A-C).

Among the remaining probes, mRFP/Venus-Camui increased the donor peak by 69.3 ± 4.7% in response to the Ca^{2+} stimulation and 43.7 ± 5.0% above the baseline after the chelation of Ca^{2+} with EGTA (Figure 2A and B). mStrawberry/GFP- and mStrawberry/Venus-versions also showed significant dequenching of donor which persisted after the chelation of Ca^{2+}. Unlike mOrange, mRFP and mStrawberry peaks were negligible in these constructs. We also constructed DsRed-monomer/Venus-Camui,

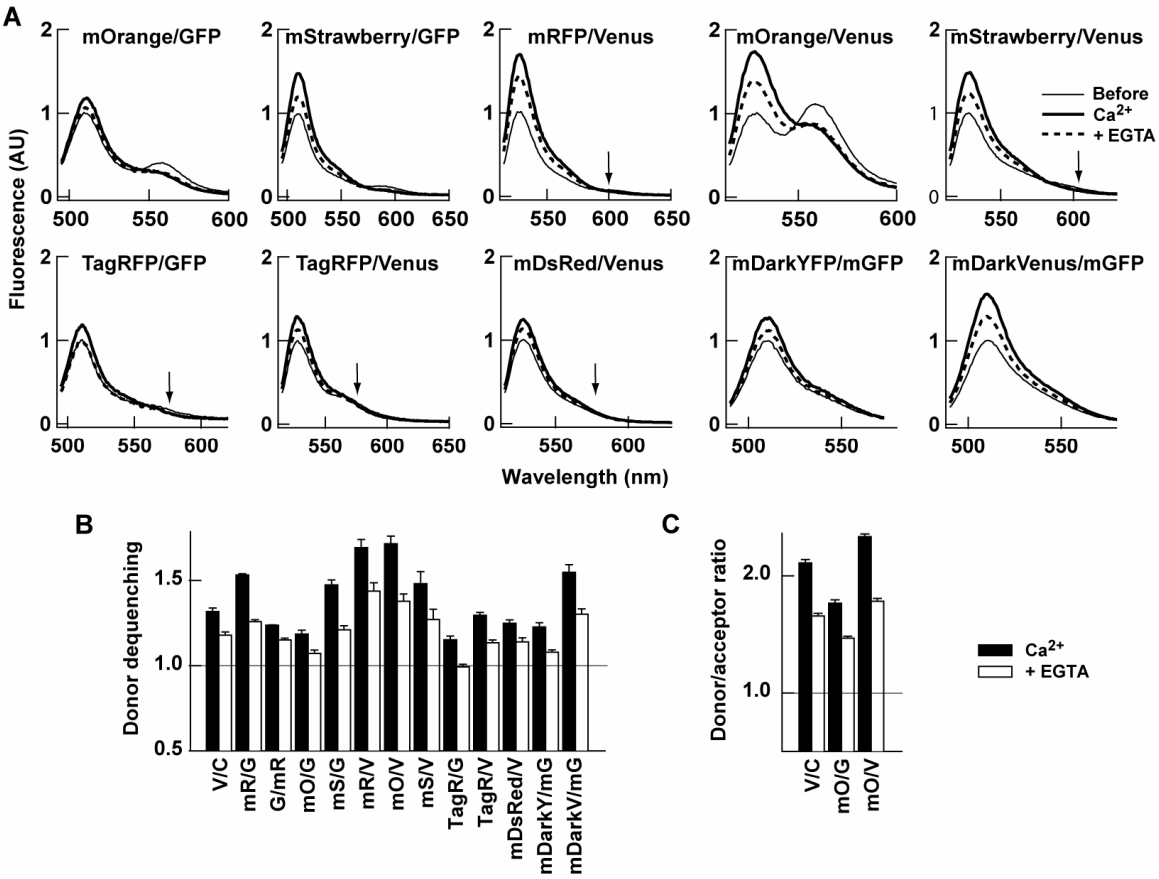

Figure 2. Comparison of various color variants of Camui. (A) The emission spectra of various color variants of Camui in response to Ca2+ and subsequent chelation with EGTA at donor specific excitation. Experiments were conducted similarly to Figure 1. (B and C) A summary of change in donor fluorescence intensity (B) and donor/acceptor ratio (C). Average ± s.e.m of 3-8 experiments.

using DsRed-monomer (Clontech) which has been monomerized in a completely different trajectory of mutagenesis as well as TagRFP, a newly reported red fluorescent protein from sea anemone [13]. Both did not show satisfactory dequenching upon Ca^{2+} stimulation (Figure 2A and B). TagRFP/GFP-Camui did not show persistent change after the addition of EGTA. We speculate this is due to the specific conFigureuration of fluorophores in this construct or simply due to overall lower efficiency of FRET.

3.4.3. Application of non-radiating YFP

As an additional effort, we employed mDarkYFP, a YFP variant with non-radiating mutations, Y145W/H148V [11], along with A206K mutation that prevents weak dimer formation [14] and mDarkVenus, a Venus variant with the same mutations, as acceptors, both with monomeric GFP (mGFP) as a donor. Among them, mDarkVenus/mGFP-Camui showed a good dequenching, 54.9 ± 4.4% above baseline upon stimulation and 30.2 ± 3.0% after chelation of Ca^{2+} (Figure 2A and B) but the extent did not exceed that of mRFP- or mStrawberry-versions.

In summary, mRFP/GFP-, mStrawberry/GFP-, mRFP/Venus-, mStrawberry/Venus-, mDarkVenus/mGFP-Camui, appeared comparably promising as FLIM probes for CaMKII activity with a robust dequenching upon stimulation and barely visible acceptor fluorescence. Different versions responded differently in a way not readily predicted by the calculated Förster distance, underscoring the importance of actually testing different fluorophore combinations (Table 1, Figure 2B). One reason for this dissociation might be the tolerance of the fluorescent protein fusing with another protein [8].

3.4.4. Fluorescence lifetime imaging of Camui activation in HEK293T cells

We chose the Camui with prototypical mRFP/GFP pair to perform FLIM imaging in living cells. We imaged mRFP/GFP-Camui in HEK293T cells (Figure 3 A-D). The averaged fluorescence lifetime was 1.82 ± 0.02 nsec (τp) and 2.62 ± 0.20 nsec (τm) (Figure 3C-D), which was significantly smaller than the GFP (2.90 ± 0.44 nsec (τp) and 2.75 ± 0.23 nsec (τm)) indicating the occurrence of FRET. Upon stimulation with Ca^{2+}-ionophore, 4-Br-A23187, the average fluorescence lifetime increased eventually to 2.13 ± 0.03 nsec (τp) and 2.83 ± 0.23 nsec (τm) after 10 min, consistent with a decrease in FRET seen in fluorospectroscopic assay (Figure 3B-D). In order to see if this change was truly induced by Ca^{2+}/calmodulin binding, we imaged mRFP/GFP-Camui with T305D/T306D mutations that abolish the binding with Ca^{2+}/calmodulin. The mRFP/GFP-Camui mutant showed a much smaller fluorescence lifetime, 1.61 ± 0.05 nsec (τp) and 2.12 ± 0.03 nsec (τm) at the basal status and was unresponsive to Ca^{2+} stimulation (Figure 4A-D), consistent with the idea that the change in time-constant seen in mRFP/GFP-Camui was indeed triggered by Ca^{2+}/calmodulin.

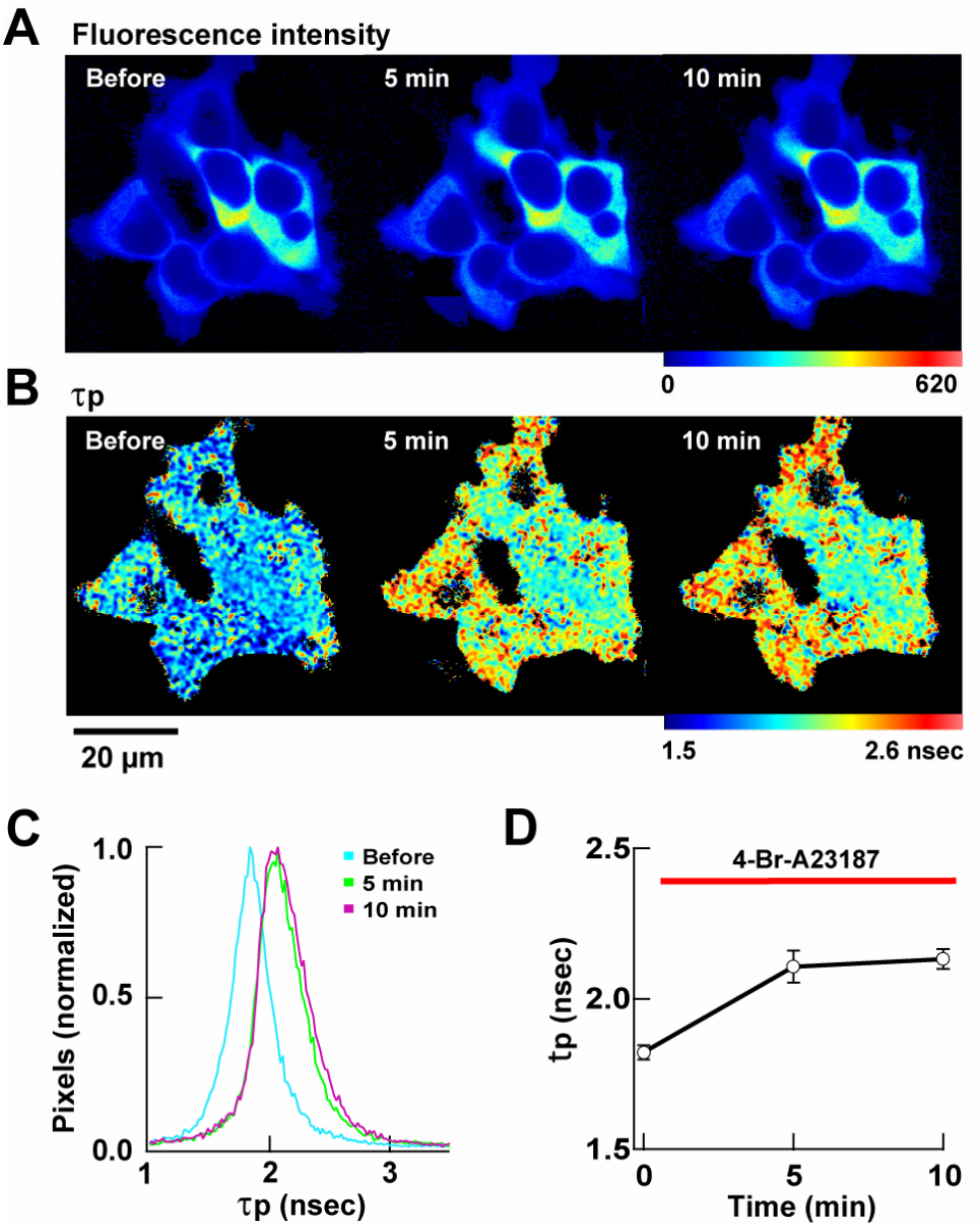

Figure 3. FLIM imaging of mRFP/GFP-Camui in HEK293T cells. (A) Pseudocolor images of fluorescence intensity. Warmer hue corresponds to higher intensity. Time stamp indicates the time elapsed after the bath application of 4-Br-A23187. When the photon count reached a set value, the acquisition was stopped to maintain a similar standard deviation in measured fluorescence lifetime values. Therefore the brightness of image can be compared only within an image. (B) Pseudocolor image of τp. The warmer hue indicates longer τp. (C) A histogram of distribution of p, before and after the application of 4-Br-A23187. (D) A plot of τp in 8 cells from 2 independent experiments. Results are average ± s.e.m.

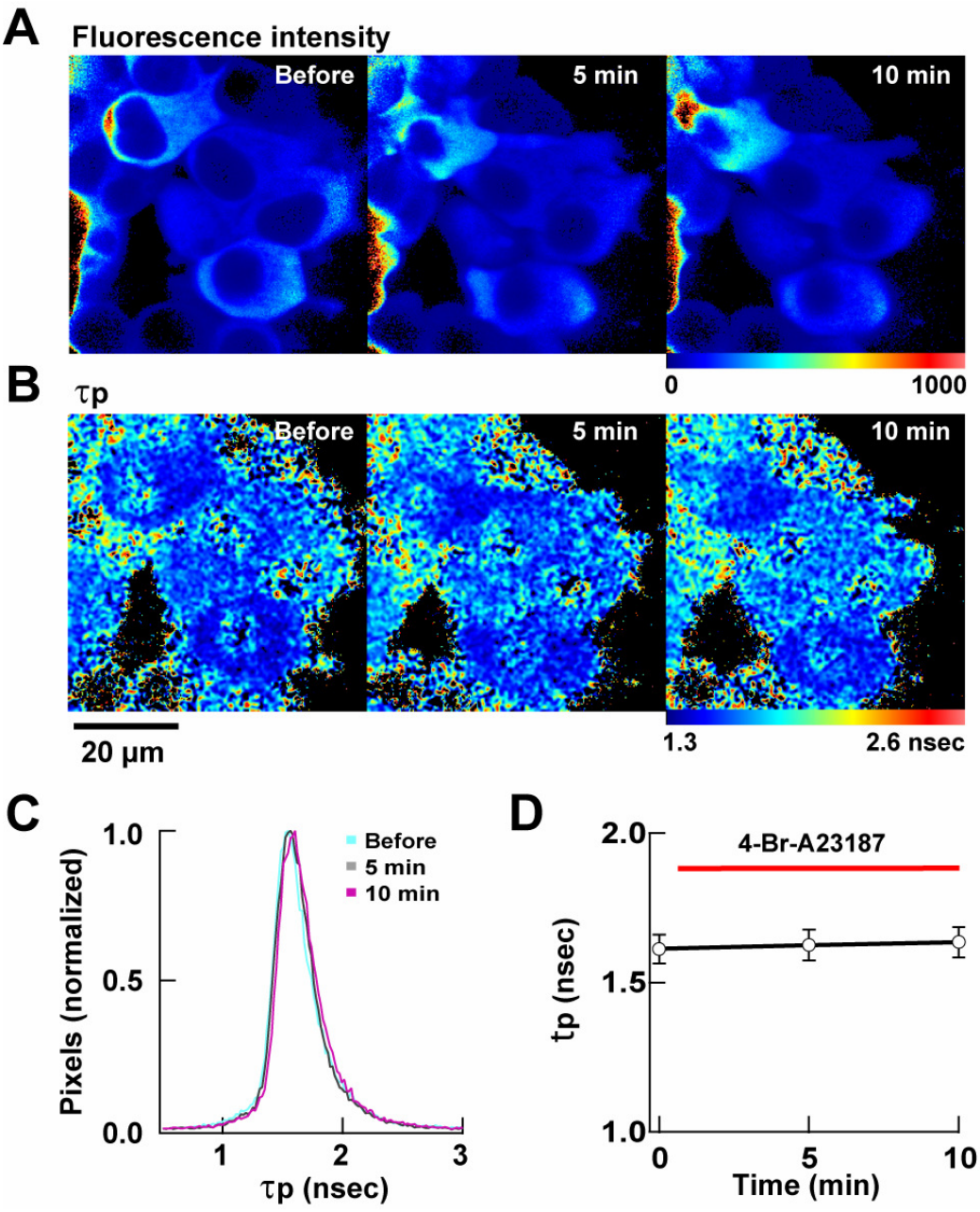

Figure 4. FLIM imaging of mRFP/GFP-Camui-T305D/T306D. FLIM images of cells expressing mRFP/GFP-Camui with T305D/T306D mutations that render CaMKII insensitive to Ca^{2+}/calmodulin. (A) Fluorescence intensity. (B) τp. (C) A histogram of distribution of τp. (D) A plot of τp in 6 cells shown in (A). See legend for Figure 3 for detail.

3.5. Discussion

FLIM has several advantages over ratiometric imaging for detecting FRET. It offers the ability to determine the absolute ratio of population showing FRET. Also, it does not depend on the fluorescence intensity or the acceptor channel. The latter feature makes FLIM ideal for *in vivo* imaging [3, 4]. In brain tissue, light is scattered significantly, depending on the depth of the tissue being imaged and the existence of local structures, such as vasculatures. Also, neuronal activity may change the scattering. If scattering affects donor and acceptor channels differently, it will give a pseudo-positive signal in the ratiometric imaging. This is no longer a concern in FLIM, however, because the scattering does not change the fluorescence lifetime. In addition, mRFP, mStrawberry, and mDarkVenus, are significantly dimmer than the donor (GFP or Venus), and therefore the emission from the acceptor is negligible (Figure 1 and 2)[8]. This allows us to use a wider band pass filter for donor channel, thereby improving the effectiveness of photon detection, unlike ratiometric imaging that requires narrow band-pass filters to separate the two channels. Furthermore, GFP and Venus are both significantly brighter than CFP, which has been the popular donor choice for ratiometric imaging.

In addition to elucidating the physiological regulation of CaMKII in living cells, the FLIM Camui probe will allow us to identify synapses undergoing synaptic potentiation, thereby empowering us in studying the functional anatomy of local synaptic circuits. Indeed, a recent study using the same FLIM probe provided important insight into the activation profile of CaMKII activity in LTP induction in a single spine [15]. Together with recent developments of two-photon imaging techniques such as imaging in freely-moving animals and of imaging deep brain structures such as hippocampus using

relay lens [16, 17], Camui will provide important information on the learning processes in unprecedented ways.

3.6. Statement of involvement

This project was initiated by Dr. Yasunori Hayashi. I carried out the majority of experiments with the help of a UROP student Ming Deng, some summer students from Japan and Dr. Yasunori Hayashi in generating certain prototype constructs. Analysis of the fluorospectrometric measurement data was greatly accelerated with Kayi Lee's Python scripts. The FLIM imaging was performed in collaboration with the Laboratory for Fluorescence Dynamics, Department of Biomedical Engineering, University of California headed by Drs. Enrico Gratton and Theodore L. Hazlett. Dr. Susana A. Sánchez helped me with the familiarization of the home-built imaging instruments and the setup of my experiment. Drs. Claudia Lee and Ryan A. Colyer helped me troubleshoot throughout my experiments, taught me how to use the analysis software and remotely assisted me with data analysis. We thank Drs. Ryohei Yasuda, Takeharu Nagai, Tomoo Ohashi, Harold P. Erickson, Mark Rizzo, Atsushi Miyawaki, Roger Tsien, and Kaoru Endo for valuable advices and sharing of resources, and Mr. John C. Howard and Ms. Marissa Stearns for editing.

Kwok S, Lee C, Sánchez SA, Hazlett TL, Gratton E, and Hayashi Y. (2008) Genetically encoded probe for fluorescence lifetime imaging of CaMKII activity. Biochemical and Biophysical Research Communications, 2008. 369(2): p. 519-525.

3.7. References

1. Lisman, J., H. Schulman, and H. Cline, *The molecular basis of CaMKII function in synaptic and behavioural memory.* Nat Rev Neurosci, 2002. **3**(3): p. 175-90.

2. Takao, K., et al., *Visualization of synaptic Ca2+ /calmodulin-dependent protein kinase II activity in living neurons.* J Neurosci, 2005. **25**(12): p. 3107-12.

3. Yasuda, R., et al., *Supersensitive Ras activation in dendrites and spines revealed by two-photon fluorescence lifetime imaging.* Nat Neurosci, 2006. **9**(2): p. 283-91.

4. Yasuda, R., *Imaging spatiotemporal dynamics of neuronal signaling using fluorescence resonance energy transfer and fluorescence lifetime imaging microscopy.* Curr Opin Neurobiol, 2006. **16**(5): p. 551-61.

5. Wallrabe, H. and A. Periasamy, *Imaging protein molecules using FRET and FLIM microscopy.* Curr Opin Biotechnol, 2005. **16**(1): p. 19-27.

6. Gratton, E., et al., *Fluorescence lifetime imaging for the two-photon microscope: time-domain and frequency-domain methods.* J Biomed Opt, 2003. **8**(3): p. 381-90.

7. Rizzo, M.A., et al., *Optimization of pairings and detection conditions for measurement of FRET between cyan and yellow fluorescent proteins.* Microsc Microanal, 2006. **12**(3): p. 238-54.

8. Shaner, N.C., P.A. Steinbach, and R.Y. Tsien, *A guide to choosing fluorescent proteins.* Nat Methods, 2005. **2**(12): p. 905-9.

9. Nagai, T., et al., *A variant of yellow fluorescent protein with fast and efficient maturation for cell-biological applications.* Nat Biotechnol, 2002. **20**(1): p. 87-90.

10. Campbell, R.E., et al., *A monomeric red fluorescent protein.* Proc Natl Acad Sci U S A, 2002. **99**(12): p. 7877-82.

11. Ganesan, S., et al., *A dark yellow fluorescent protein (YFP)-based Resonance Energy-Accepting Chromoprotein (REACh) for Förster resonance energy transfer with GFP.* Proc Natl Acad Sci U S A, 2006. **103**(11): p. 4089-94.

12. Colyer, R.A., C. Lee, and E. Gratton, *A novel fluorescence lifetime imaging system that optimizes photon efficiency.* Microsc Res Tech, In the press.

13. Merzlyak, E.M., et al., *Bright monomeric red fluorescent protein with an extended fluorescence lifetime.* Nat Methods, 2007. **4**(7): p. 555-7.

14. Zacharias, D.A., et al., *Partitioning of lipid-modified monomeric GFPs into membrane microdomains of live cells.* Science, 2002. **296**(5569): p. 913-6.

15. Lee, S.-J.R., et al., *Activation of CaMKII in single dendritic spines during long-term potentiation.* Nature, 2009. **458**(7236): p. 299.

16. Helmchen, F., et al., *A miniature head-mounted two-photon microscope. High-resolution brain imaging in freely moving animals.* Neuron, 2001. **31**(6): p. 903-12.

17. Jung, J.C. and M.J. Schnitzer, *Multiphoton endoscopy.* Opt Lett, 2003. **28**(11): p. 902-4.

CHAPTER 4: Future studies and methodological considerations

4.1. Implications

It has been clear since the work of Hubel and Wiesel in the cat visual cortex that single neurons have complex response properties [1]. The functional role of a neuron within a cortical circuit is predominantly determined by the synaptic input of that neuron. Hence, studying the synaptic input patterns of a single neuron can gain insight into the origin of its complex response properties and its role in a neural circuit. This thesis contributes to the methodology development of performing such experiments and proved that it is feasible to carry out experiments *in vivo*. Furthermore, in whole cell calcium imaging and some acute single-unit recordings, the change in response cannot be measured in the same cells before and after a manipulation and therefore one relies heavily on between-group comparisons [2]. However, we can not only measure the CaMKII activity changes in the same neuron, but also do so at a single spine level.

4.1.1. Heterogeneous population of spines

The main finding of the work detailed in Chapter 2 is that in the deprived eye domain, the spines with minimal to moderate basal CaMKII activity increased after only 4 hours of MD and those with the high basal activity decreased. Apart from the hypothesis that these spines are likely under the influence of a combination of Hebbian and homeostatic mechanisms, we also think that these layer II/III pyramidal cell spines represent a mixture of at least three different input sources. They are spines receiving input from 1) the feedforward drive of the deprived eye, 2) the local intracortical projections of the same eye and 3) the longer-range intracortical projections of the other eye. Furthermore, we speculate that spines in 1) have a high basal CaMKII activity, those in 2) and 3) have minimal to moderate basal CaMKII activity. Reductions of drive and of

CaMKII activity in the deprived eye domain after 4 hours of MD are due to the weakening of the feedfoward drive and it is Hebbian. However, the increase of CaMKII activity in about 63% of the total spines partnering 2) and 3) in the deprived eye domain is due to the feedback and homeostatic mechanisms.

4.1.2. Detecting CaMKII activity in spines with distinct input source

The three populations of spines in layer II/III pyramidal neurons are only speculations and cannot be distinguished in this study. However, it is now possible to separately label these spine pools. One can take advantage of the FLIM probes of Camui and the red shifted fluorescent protein family members [3]. To visualize the CaMKII activity changes in spines receiving input from the long horizontal projection of pyramids in the opposite eye domain, for example, one can inject HSV mDarkVenus/GFP-Camui into layer II/III of the deprived eye domain and simultaneously, injecting HSV mStrawberry into the other eye domain. We can image the fluorescence life-time of those green spines with a red presynaptic partner before and after 4 hours of MD. Similarly, HSV mStrawberry can be injected into layer IV or short distance away from the HSV mDarkVenus/GFP-Camui injection site for labeling feedforward and local intracortical horizontal projections, respectively. That way, we can understand the differential CaMKII activity changes in these spines that are innervated differently. If the homeostatic mechanisms only operate in one set of these three pools, we will be able to pinpoint which pool it is. Moreover, we can take advantage of the mice monocular eye domain, which is exclusively driven by the contralateral eye, to study the effect of MD in the CaMKII activity in these spines.

4.1.3. Detecting CaMKII activity in presynaptic boutons

During our *in vivo* imaging studies, the neurons with Camui expression showed visible spines. However, we have never observed the presynaptic boutons with this version of Camui. On the other hand, we did observe axons and boutons in the fusion protein probe which is the brightest amongst the three constructs, pointing the requirement of a bright probe to visualize the presynaptic structure. Since the quantum yield and extinction coefficient of GFP is higher than that of CFP [4], I believe that the mRFP/GFP-Camui or mDarkVenus/GFP-Camui constructs would be bright enough to be useful tools for studying the role of CaMKII activity in the presynaptic terminal when the cortex is undergoing plasticity processes.

There is evidence supporting the idea that presynaptic CaMKII is important for LTD induction and postsynaptic CaMKII is critical for LTP induction in hippocampus [5]. Stanton and Gage used extracellular bath application of the cell-permeant CaMKII inhibitor KN-62 and intracellular infusion of KN-62 into single CA1 pyramidal neurons to study the role CaMKII in LTD and LTP induction. They found that extracellular bath application of KN-62 was effective in blocking LTD induction by low-frequency Schaffer collateral stimulation while postsynaptic intracellular infusion of this inhibitor blocked LTP but not LTD. These results implied the differential role of CaMKII depending on whether it is located presynaptically or postsynaptically. One of the known substrate of presynaptic CaMKII is synapsin I, a synaptic vesicle-associated protein [6]. CaMKII is also shown to be directly associated with the outer membrane of the vesicles [7]. The presynaptic BK channel (large-conductance Ca^{2+}-activated K^+ channel) is a key negative regulator of neurotransmitter and it is regulated by CaMKII [8]. In addition, the

inactivation of $Ca_v2.1$ (P/Q-type) voltage sensitive Ca2+ channels, the primary channels that trigger neurotransmitter release at the mature synapses, is decelerated by binding to CaMKII [9]. Hinds *at el*. showed that in the conditional CA3 CaMKIIα knockout mice, the activity-dependent increase in probability of release during repetitive presynaptic stimulation was significantly enhanced [10]. Their data support the role of CaMKIIα as a negative activity-dependent regulator of neurotransmitter release at hippocampal synapses. Taken together, CaMKII is a critical player in presynaptic transmission. The FLIM Camui probe will be invaluable for studying the activity of presynaptic CaMKII in critical synaptic functions in real time *in vivo*.

4.2. Methodological considerations

4.2.1. Animals

We used critical period ferrets for this study for a number of reasons such as its relative immature visual system at birth and it has clear ocular dominance domains. However, ferrets are seasonal breeders who do not reproduce during the winter in their natural habitat. As a result, we received young ferrets that were unhealthy and did not survive well the prolonged window implant surgery during the winter. This problem retarded our progress significantly. Furthermore, we were not allowed to perform more than one survival surgery in ferrets which limited our ability to obtain the OD map and forced us to perform untargeted viral injection. In addition, there is a considerable space between the cortical surface and the skull in ferrets. This leads to the requirement of a filling material to stop the cortical movement due to the heart beat. Our filling material of

choice, agarose, prevented us from imaging more than two time points because of the increased opacity over time. Therefore, I suggest mice for the future studies.

Mouse visual cortex is emerging as the popular model for studying ocular dominance plasticity [2, 11-15]. Mice show robust OD plasticity following MD. Many imaging studies are carried out in mice [16-24]. Mice have a better resistance to infections related to cranial window implantation than ferrets. They are also genetically homogeneous and can be easily manipulated [20, 25-30]. Optical reporters in transgenic mice can promote our understanding of the detailed mechanisms in which particular genes are involved. Gene expression can be temporally and spatially restricted in transgenic mice and thereby eliminates the need for viral injection which could cause mechanical damage to the cortex [31, 32]. Moreover, behavior tests are well established in mice such that effects of genetic manipulation at the behavior level can be easily assessed to reinforce the functional analysis at a cellular or systems level. Hence, I would choose mice for future imaging studies.

4.2.2. Viral expression

I compared the expression level of three GFP expressing viruses, lentivirus with synapsin I promoter (gift from Dr. Carlos Lois), sindbis virus and herpes simplex virus (HSV). We found that HSV has a similar expression level as sindbis virus but is five times higher than that of lentivirus (unpublished data). Thus, HSV was chosen for its high expression level, in addition to its neurotropicity and rapid expression of the transgene within hours [33]. Other advantages that HSV offers are that it can accommodate a large foreign DNA on the order of 15 kb although the difficulty in molecular handling increases with the increasing size of the DNA fragment and it can be concentrated to high

titers (~ 10^8 units/ml) free of helper virus. However, its expression lasts for only about 5 days. While this transient expression could be an advantage for examining whether behavioral changes parallel changes in transgene expression and for serving as its own control after the expression levels off, for observations of CaMKII activity in a plasticity process that require days of induction manipulation, HSV system is not ideal.

Several other viruses have been improved in the past decade to serve as alternative choices for *in vivo* studies. Adeno-associated virus (AAV) has been intensively studied and improved mainly because of it promising application in gene therapy [34]. It is integrated into the genome and has a persistent transgene expression. High titer AAV (1.1×10^{12} viral genomes/ml) was effectively used for calcium imaging studies *in vivo* in Alzheimer's mice model [35]. However, a broad range of cells are infected by this virus. This could cause a concern in transgene function analysis in brain studies because transgenes expressed in non-neurons can confound the interpretation. Another often used virus for *in vivo* studies is the lentivirus [36]. Lentivirus is also integrated into the genome and has a persistent expression. Changing the promoters driving the transgene expression can control the expression level (e.g. human ubiquitin C promoter has a higher expression than synapsin I promoter) and the cell type (e.g. CaMKIIα promoter-based expression is restricted to forebrain excitatory neurons whereas synapsin I promoter also causes weaker expression in interneurons). In addition, lentivirus is often used for gene silencing through the delivery and expression of double-stranded siRNA [36]. Therefore, depending on the specific needs of a study, different viral system can be strategically utilized.

4.2.3. Imaging analysis software

In the studies included in this thesis, we used two main software tools for image processing and analysis: Metamorph (Molecular Device) for ratiometric FRET *in vivo* imaging and Globals for Images software (Laboratory for Fluorescence Dynamics, University of California, Irvine) for FLIM imaging. While Globals for Images software is custom-made by Professor Enrico Gratton, Metamorph is rather limited for easy handling of multi-channel and multi-stack images. At the beginning of image analysis, I spent much time on deciding an efficient method of converting image to a number. However, identifying spines and matching the same spine in two slightly different images (before and after 4 hrs of MD) were more complicated than what an automatic computer program could manage. Therefore, I analyzed all the spine and dendritic regions by placing regions of interest manually. This slow process was followed by data arrangement in Excel which was also time-consuming. To expedite the latter process, I recruited Kayi Lee to generate Python scripts for automatic data handling after logging the data in Metamorph. These scripts improved my productivity significantly. However, identifying the region of interest automatically remains a challenge. It is my sincere hope that a solution could be researched to significantly reduce the time spent at this step and the human errors.

4.3. References

1. Wiesel, T.N. and D.H. Hubel, *Single-cell response in striate cortex of kittens deprived of vision in one eye.* J Neurophysiol, 1963. **26**(6): p. 1003-1017.

2. Smith, G.B., A.J. Heynen, and M.F. Bear, *Bidirectional synaptic mechanisms of ocular dominance plasticity in visual cortex.* Philosophical Transactions of the Royal Society B: Biological Sciences, 2009. **364**(1515): p. 357-367.

3. Shaner, N.C., et al., *Improved monomeric red, orange and yellow fluorescent proteins derived from Discosoma sp. red fluorescent protein.* Nat Biotechnol, 2004. **22**(12): p. 1567-72.

4. Shaner, N.C., P.A. Steinbach, and R.Y. Tsien, *A guide to choosing fluorescent proteins.* Nat Meth, 2005. **2**(12): p. 905.

5. Stanton, P.K. and A.T. Gage, *Distinct synaptic loci of Ca2+/calmodulin-dependent protein kinase II necessary for long-term potentiation and depression.* J Neurophysiol, 1996. **76**(3): p. 2097-2101.

6. Kennedy, M.B., T. McGuinness, and P. Greengard, *A calcium/calmodulin-dependent protein kinase from mammalian brain that phosphorylates Synapsin I: partial purification and characterization.* J Neurosci, 1983. **3**(4): p. 818-31.

7. Benfenati, F., et al., *Biochemical and functional characterization of the synaptic vesicle-associated form of CA2+/calmodulin-dependent protein kinase II.* Brain Res Mol Brain Res, 1996. **40**(2): p. 297-309.

8. Wang, Z.W., *Regulation of synaptic transmission by presynaptic CaMKII and BK channels.* Mol Neurobiol, 2008. **38**(2): p. 153-66.

9. Jiang, X., et al., *Modulation of CaV2.1 channels by Ca2+/calmodulin-dependent protein kinase II bound to the C-terminal domain.* Proc Natl Acad Sci U S A, 2008. **105**(1): p. 341-6.

10. Hinds, H.L., et al., *Essential function of alpha-calcium/calmodulin-dependent protein kinase II in neurotransmitter release at a glutamatergic central synapse.* Proc Natl Acad Sci U S A, 2003. **100**(7): p. 4275-80.

11. Drager, U.C., *Autoradiography of tritiated proline and fucose transported transneuronally from the eye to the visual cortex in pigmented and albino mice.* Brain Res, 1974. **82**(2): p. 284-92.

12. Gordon, J.A. and M.P. Stryker, *Experience-Dependent Plasticity of Binocular Responses in the Primary Visual Cortex of the Mouse.* J. Neurosci., 1996. **16**(10): p. 3274-3286.

13. Mataga, N., N. Nagai, and T.K. Hensch, *Permissive proteolytic activity for visual cortical plasticity.* Proc Natl Acad Sci U S A, 2002. **99**(11): p. 7717-21.

14. Frenkel, M.Y. and M.F. Bear, *How Monocular Deprivation Shifts Ocular Dominance in Visual Cortex of Young Mice.* Neuron, 2004. **44**(6): p. 917.

15. Liu, C.-H., et al., *Cannabinoid Receptor Blockade Reveals Parallel Plasticity Mechanisms in Different Layers of Mouse Visual Cortex.* Neuron, 2008. **58**(3): p. 340.

16. Chow, D.K., et al., *Laminar and compartmental regulation of dendritic growth in mature cortex.* Nat Neurosci, 2009. **12**(2): p. 116.

17. Majewska, A. and M. Sur, *Motility of dendritic spines in visual cortex in vivo: changes during the critical period and effects of visual deprivation.* Proc Natl Acad Sci U S A, 2003. **100**(26): p. 16024-9.

18. Mrsic-Flogel, T.D., et al., *Homeostatic Regulation of Eye-Specific Responses in Visual Cortex during Ocular Dominance Plasticity.* Neuron, 2007. **54**(6): p. 961.

19. Mank, M., et al., *A genetically encoded calcium indicator for chronic in vivo two-photon imaging.* Nat Methods, 2008. **5**(9): p. 805-11.

20. Wang, K.H., et al., *In vivo two-photon imaging reveals a role of arc in enhancing orientation specificity in visual cortex.* Cell, 2006. **126**(2): p. 389-402.

21. Oray, S., A. Majewska, and M. Sur, *Dendritic spine dynamics are regulated by monocular deprivation and extracellular matrix degradation.* Neuron, 2004. **44**(6): p. 1021-30.

22. Majewska, A.K., J.R. Newton, and M. Sur, *Remodeling of synaptic structure in sensory cortical areas in vivo.* J Neurosci, 2006. **26**(11): p. 3021-9.

23. Holtmaat, A.J.G.D., et al., *Transient and Persistent Dendritic Spines in the Neocortex In Vivo.* Neuron, 2005. **45**(2): p. 279.

24. Lee, W.-C.A., et al., *Dynamic Remodeling of Dendritic Arbors in GABAergic Interneurons of Adult Visual Cortex.* PLoS Biology, 2006. **4**(2): p. e29.

25. Taha, S.A. and M.P. Stryker, *Ocular dominance plasticity is stably maintained in the absence of alpha calcium calmodulin kinase II (alphaCaMKII) autophosphorylation.* Proc Natl Acad Sci U S A, 2005. **102**(45): p. 16438-42.

26. Taha, S., et al., *Autophosphorylation of [alpha]CaMKII Is Required for Ocular Dominance Plasticity.* Neuron, 2002. **36**(3): p. 483-491.

27. Gordon, J.A., et al., *Deficient Plasticity in the Primary Visual Cortex of [alpha]-Calcium/Calmodulin-Dependent Protein Kinase II Mutant Mice.* Neuron, 1996. **17**(3): p. 491-499.

28. Silva AJ, S.C., Tonegawa S, Wang Y., *Deficient hippocampal long-term potentiation in alpha-calcium-calmodulin kinase II mutant mice.* Science, 1992. **257**(5067): p. 201-6.

29. Silva, A.J., et al., *Impaired spatial learning in alpha-calcium-calmodulin kinase II mutant mice.* Science, 1992. **257**: p. 206-211.

30. Glazewski, S., et al., *Requirement for alpha-CaMKII in experience-dependent plasticity of the barrel cortex.* Science, 1996. **272**: p. 421-423.

31. Kim, I.-J., et al., *Molecular identification of a retinal cell type that responds to upward motion.* Nature, 2008. **452**(7186): p. 478.

32. Nakashiba, T., et al., *Transgenic Inhibition of Synaptic Transmission Reveals Role of CA3 Output in Hippocampal Learning.* Science, 2008. **319**(5867): p. 1260-1264.

33. Carlezon, W.A., Jr., E.J. Nestler, and R.L. Neve, *Herpes simplex virus-mediated gene transfer as a tool for neuropsychiatric research.* Crit Rev Neurobiol, 2000. **14**(1): p. 47-67.

34. Goncalves, M., *Adeno-associated virus: from defective virus to effective vector.* Virology Journal, 2005. **2**(1): p. 43.

35. Kuchibhotla, K.V., et al., *A[beta] Plaques Lead to Aberrant Regulation of Calcium Homeostasis In Vivo Resulting in Structural and Functional Disruption of Neuronal Networks.* Neuron, 2008. **59**(2): p. 214.

36. Dittgen, T., et al., *Lentivirus-based genetic manipulations of cortical neurons and their optical and electrophysiological monitoring in vivo.* Proceedings of the National Academy of Sciences of the United States of America, 2004. **101**(52): p. 18206-18211.